GRANT NO.
N00014-93-1-0309

PROCEEDINGS

of the

16th ANNUAL MEETING

and the

20th DAY OF SCIENTIFIC LECTURES

of the

NATIONAL SOCIETY OF BLACK PHYSICISTS

APRIL 21-24, 1993

Florida Agricultural and Mechanical University

Tallahassee, Florida 32307

PROCEEDINGS

of the

16th ANNUAL MEETING

and the

20th DAY OF SCIENTIFIC LECTURES

of the

NATIONAL SOCIETY OF BLACK PHYSICISTS

APRIL 21-24, 1993

FLORIDA A. & M. UNIVERSITY

TALLAHASSEE, FLORIDA 32307

Edited by:

Ronald L. Williams
Charles Weatherford

The 1993 Annual Meeting was sponsored by the United States Office of Naval Research, the National Institute of Science and Technology, the FAMU NASA Center for Nonlinear & Nonequilibrium AeroScience, a grant to the FAMU Physics Department from the Packard Foundation, and the Florida Agricultural and Mechanical University.

FOREWORD

The Florida Agricultural and Mechanical University (FAMU) in Tallahassee was the site of the 16th Annual Meeting and the 20th Day of Scientific Lectures of the National Society of Black Physicists (NSBP) on April 21 to 24, 1993. The theme of the meeting was "Physics, Technology and Business". The first day of the meeting was held in the Grand Ballroom on FAMU's beautiful campus and the second day and third half-day were held at the Radisson Hotel in downtown Tallahassee. Over 20 scientific talks were given by professional and student physicists during the meeting. In addition a poster session was held on Thursday night. On Friday a panel discussion on the subject of the meeting's theme was held and had as its title "Minority Owned High Technology Businesses: Techniques for Growing a Successful One" and was led by Dr. Donald Butler of BLES Scientific. The banquet was held on Friday night at the Governor's Club and the keynote speaker was Dr. James Stith of the United States Military Academy, West Point. The Saturday morning session featured talks by undergraduate students. On Saturday afternoon a tour was held of Wakulla Springs, a nearby wildlife preserve park. Dr. Earl Shaw was elected Fellow of the National Society of Black Physicists. Dr. Cynthia McIntyre received the NSBP Outstanding Dissertation Award for 1993.

ACKNOWLEDGEMENTS

The combined efforts of many individuals resulted in the success of the 1993 Annual Meeting of the NSBP. Particular thanks go to the local planning committee for organizing and managing the meeting, which was by far the largest ever in attendance. The NSBP gratefully acknowledges the financial support of the Office of Naval Research, the National Institute of Science and Technology, the FAMU NASA Center for Nonlinear & Nonequilibrium AeroScience, a grant to the Physics Department from the Packard Foundation, and Florida A. & M. University. Special acknowledgements go to Ms. Delandrea Humose, Ms. Sonja Richardson, Ms. Katrina Jackson and Ms. Myra McNair-Gurley for their expert administrative support which made the conference and these proceedings possible.

Ronald L. Williams & Charles Weatherford, Editors
Tallahassee; April, 1994

NSBP OFFICERS FOR 1993

President	Sekazi Mtingwa
President-Elect	James Gates
Administrative Executive Officer	Barbara Williams
Treasurer	Lonzy Lewis
Technical Executive Officer	Kennedy Reed

CONFERENCE PLANNING COMMITTEE

Ronald Williams
Joseph A. Johnson, III
William Tucker
DelAndrea Humose
Sonja Richardson
Charles Weatherford
Herbert Jones
Lynette E. Johnson
Katrina Jackson
Myra McNair-Gurley

Table of Contents

Turbulent Enhancement of Second Viscosity in Nonequilibrium Flow

Jean Chabi Orou* and Joseph A. Johnson III†

CeNNAs, Florida A&M University, Tallahassee, FL 32310

Abstract

A physical model for entropy production associated with reactive flow is presented. The general form $\chi(t) \propto (1 - e^{-\frac{t}{\tau}})$ has the correct asymptotic behaviors for t->0, t->τ and t->∞ for finite τ where τ is the relaxation time. From this, a relationship between the second viscosity and the relaxation time for A+B->P is modeled from the macroscopic entropy rate equation. Finally, using a first order approximation for reaction rate distortion from reduced molecular chaos, enhanced second viscosities can be predicted for strongly turbulent fluid systems with long relaxation times and $\nabla \bullet \bar{V} \neq 0$.

Nonmenclature

S	=entropy
s	=specific entropy
Q	=quantity of heat
T	=absolute temperature
e	=specific internal energy
A	=area
ρ	=density of the fluid
$\bar{V}$	=velocity
dv	=volume element
Φ	=dissipation function
σ	=entropy generated per unit volume per unit time

τ =relaxation time

χ =entropy generated by chemical reaction

u_x =derivative of the component of the velocity vector in x direction with respect to x

Re =Reynolds number

t =time (laboratory time)

μ =viscous stress tensor

η =dynamic viscosity

ξ =second viscosity

Introduction

It is usually assumed that the second (or bulk) viscosity and the chemical relaxation time are connected. However, the second viscosity is only relevant in processes where there is a compression or an expansion and it is usually regarded as small even when it is relevant.[1] Nonetheless, it now seems appropriate to determine in general whether or not there can be circumstances where the influence of second viscosity might be important.[2] This seems especially interesting since, in some situations, effects due to turbulence are often treated as effects due to anomalous viscosity. The present paper uses the macroscopic entropy production rate equation in a reactive flow in order to approach the possibility of a connection between the second viscosity and the relaxation time. In addition, by using the qualitative implications of recent experimental results, we will speculate on a role for turbulence in these phenomena. Generally stated, this model is proposed on intuitive arguments.

Entropy and a Relaxation Process

The total change of entropy in a system is

$$S_2 - S_1 = \int_1^2 \frac{dQ_{rev}}{T}$$

where we have assumed the system is brought from state 1 to state 2 so that

$$S_2 - S_1 = \Delta S_0 + \Delta S_i.$$

The first term in the right is the entropy carried into the system over the boundaries from outside and the second term is the entropy produced in the system during the process.

In what follows, we are going to deal with a system in which the entropy carried into the system is zero and the last term in the above equation is generated by viscosity, thermal conduction and chemical reaction. Specifically, we define σ to be the entropy per unit time and Φ to be the dissipation function. Specifically, Φ can be interpreted as the irreversible dissipation of the mechanical energy into heat caused by the viscosity per unit time per unit volume.

With these definitions, the energy balance can be expressed as follows:[3]

$$\iiint \rho\left(\frac{De}{Dt} - \frac{P}{\rho^2}\frac{D\rho}{Dt}\right)dv = \iiint (\Phi - div(\bar{q}))dv$$

where

$$\Phi = div(\vec{V}\mu) - \vec{V}div\mu$$

$$\Phi = \mu_{xx}\frac{\partial u}{\partial x} + \mu_{yy}\frac{\partial v}{\partial y} + \mu_{zz}\frac{\partial w}{\partial z} + \mu_{xy}\left(\frac{\partial u}{\partial y} - \frac{\partial v}{\partial x}\right) +$$

$$+\mu_{yz}\left(\frac{\partial v}{\partial z} - \frac{\partial w}{\partial y}\right) + \mu_{xz}\left(\frac{\partial w}{\partial x} - \frac{\partial u}{\partial z}\right)$$

in which the velocity vector $\vec{V}$ has components (u, v, w), μ is the viscous stress tensor and $\bar{q}$ is the energy flow vector. The previous equation becomes:

$$\iiint \frac{\rho}{T}\left(\frac{De}{Dt} - \frac{P}{\rho^2}\frac{D\rho}{Dt}\right)dv = -\iint \frac{\vec{n}.\bar{q}}{T}dA + \iiint\left(\frac{\Phi}{T} - \frac{\bar{q}.\nabla T}{T^2}\right)dv$$

Since

$$TdS = de - \left(\frac{P}{\rho^2}\right)d\rho$$

we now have:

$$\iiint \rho \frac{Ds}{Dt} dv = \frac{D}{Dt}\iiint \rho s dv = -\iint \frac{\vec{n}.\vec{q}}{T} dA + \iiint \sigma dv$$

where $\sigma = \left(\frac{\Phi}{T} - \frac{\vec{q}\cdot\nabla T}{T^2}\right)$.

When the entropy generated by a chemical reaction is taken into account, an additional term is required in the expression of the entropy source. The new expression for the entropy becomes

$$Tds = de - \left(\frac{P}{\rho^2}\right)d\rho + \Gamma d\chi$$

where $\Gamma = T\left(\frac{\partial s}{\partial \chi}\right)_{e,\rho}$ vanishes if the gas attains an unconstrained equilibrium at all time.

In order to derive a relationship between the additional term and the entropy source, one notices that the expression for the entropy source becomes:

$$\sigma = \frac{\Phi}{T} - \frac{\vec{q}.\nabla T}{T^2} + \frac{\rho\Gamma}{T}\frac{d\chi}{dt}$$

We will limit ourselves to the case of a chemical reaction of the type A+B—>P where A, B and P are assumed to be nonmonoatomic perfect gases[4] and χ is the entropy generated by the chemical reaction during the process. Because the reaction stops after a finite time, χ must reach a limit value which is its value at equilibrium and, at that time, the derivative of χ with respect to time becomes zero .

On the other hand, the process being irreversible, the entropy must increase from zero to the limit value in a way which agrees with the active relaxation process. Assuming that χ is only a function of time and that it satisfies the above statements, the profile of χ could be a function of the form:

$$\chi(t) \propto (1 - e^{-\frac{t}{\tau}})$$

The general behavior of $\chi=\chi(t)$ during a relaxation process would be as is shown in Fig. 1 where τ is the relaxation time. We also assume that Boltzmann's equation holds.[5]

Second Viscosity and Relaxation Time

Let's consider a chemical reaction which starts at t=0 with $\chi = 0$. Elaborating the approximation above, we assume that the value of χ becomes proportional to (1-(1/e)) at $t=\tau$ and stops when t is large enough so that $e^{-\frac{t}{\tau}}$ is almost zero. Whatever value τ has, provided it is a finite one, equilibrium will eventually be reached. If the entropy at equilibrium is independent of τ, then χ_{eq} is independent of τ and the rate of change of χ is fixed. The expression of the entropy source becomes:

$$\sigma = \frac{\Phi}{T} - \frac{\vec{q}.\nabla T}{T^2} + \frac{\rho\Gamma}{T\tau}\chi_{eq}e^{-\frac{t}{\tau}}$$

The last term is the entropy generated per unit time per unit volume by the chemical reaction .

For t fixed and a small relaxation time, the equilibrium is, of course, reached more quickly than when the relaxation time is large. For one-dimensional flow, one now finds:

$$\sigma = \frac{\frac{4}{3}\eta + \xi}{T}u_x^2 - \frac{\vec{q}.\nabla T}{T^2} + \frac{\rho\Gamma}{T\tau}\chi_{eq}e^{-\frac{t}{\tau}}$$

Next we restrict the treatment to an isolated system at a constant temperature; this restriction ignores heat released (or absorbed) by the process A + B ->P. The entropy source then becomes:

$$\sigma = \frac{\frac{4}{3}\eta + \xi}{T}u_x^2 + \frac{\rho\Gamma}{T\tau}\chi_{eq}e^{-\frac{t}{\tau}}$$

Thus we achieve the previously derived energy balance equation takes the form:

$$\iiint \rho\left(\frac{De}{Dt}-\frac{P}{\rho^2}\frac{D\rho}{Dt}\right)dv=\iiint\left(\frac{\frac{4}{3}\eta+\xi}{T}u_x^2+\frac{\rho\Gamma}{T\tau}\chi_{eq}e^{-\frac{t}{\tau}}\right)dv$$

By restricting our treatment to a perfect and nonmonoatomic gas at a constant temperature in an isolated system, the integrands in the energy balance equation cannot depend on time macroscopically. This means that the derivative of σ with respect to time must be zero and, consequently, the entropy generated by the molecular process must be balanced by a change in the viscosity. Since the second viscosity alone is free to show a change with time, it is constrained by the energy balance equation above (since $d\sigma/dt = 0$) as follows:

$$\frac{d\xi}{dt}=\frac{\rho\Gamma}{u_x^2}\frac{1}{\tau^2}\chi_{eq}e^{-\frac{t}{\tau}}$$

These results are summarized in Figs. 2 and 3. Setting $b_\xi=(\rho\Gamma\chi_{eq}/u_x^2)$, we show $\frac{1}{b_\xi}\frac{d\xi}{dt}vs\frac{e^{-\frac{t}{\tau}}}{\tau^2}$ in Fig. 2. For the range in t and τ indicated, a substantial sensitivity in $d\xi/dt$ is observed; this is particularly true, for example, at low velocities u_x and high densities ρ. The relative magnitudes are indicated in Fig. 3 which is a slice through Fig. 2 at τ=30 μsec.

Notice that as the relaxation time decreases, the overall entropy change due to the chemical reaction increases. For decreasing relaxation times, there correspondingly (from the equations above) is a decreasing role for the evolution of second viscosity to play in the entropy balance.

Second Viscosity, Relaxation Time, and Turbulence

It has been observed that fully developed, as well as transitional, turbulence can be described by qualitatively predictable Orr-Sommerfeld like behav-

iors in the form I=I(Re, Re_{peak}) where I is the turbulent intensity and Re_{peak} is the Reynolds number at maximum turbulent intensity.[6] It is also observed that the reaction rate decreases with increasing turbulent intensity.[7] For $\tau = \tau(Re)$ and I = I(Re),we get $\tau = \tau(Re(I))$ implicitly where I is the turbulent intensity. Notice $\tau \underset{Re \to 0}{=} cnst$. Then the form

$$\tau = \tau_0 \exp\left(1 - \frac{(Re - Re_{peak})^2}{Re_{peak}^2}\right)$$

is a suitable intuitive first approximation.

This expression is now combined with the expression above for $d\xi/dt$ to achieve the behaviors shown in Figs. 4 and 5. In Fig. 4 one notices that the range of non-zero turbulent intensities increases as the value of Re_{peak} increases. A typical value for Re_{peak} would be roughly 10^6; using this value and a value of τ =30 μsec, one obtains the range of values for $d\xi/dt$ shown in Fig. 5. Here as in Fig. 2 the most dramatic changes are seen at very low values of laboratory time. Nonetheless, values for t (roughly 1 μsec < t < 40 μsec) are found during which a significant influence of relaxation time and turbulent intensity on the evolution of second viscosity is possible.

Conclusions

By using a physical model for entropy production associated with reactive flow, a relationship between the second viscosity and the relaxation time is determined from the macroscopic entropy production rate equation. This relationship enables us to predict the behavior of the second viscosity when turbulence evolves in a nonequilibrium flow. Taking advantage of previous studies which have concluded that the reaction rate decreases when turbulence increases, one can argue that the second coefficient of viscosity increases when turbulence increases.

It is difficult to normalize $\chi=\chi(t)$; therefore the results obtained here for the second viscosity as a function of the relaxation time and the Reynolds number give only qualitative behaviors. Nonetheless, a relationship has been established between the second viscosity and the relaxation time for a nonequilibrium process. We have shown how this relationship can lead to a dependence of the second viscosity on turbulence. For a flow where $\nabla \bullet \vec{V} \neq 0$, anomalous viscous effects can therefore be expected, under some circumstances, for turbulent nonequilibrium systems.

Acknowledgments

This work was supported in part by NASA Grant NAGW-2930.

References

* Research Assistant. Also Graduate Student, IMSP/Université Nationale du Benin, Cotonou, Benin.

† Distinguished Professor of Science and Engineering, Professor of Physics and Mechanical Engineering. Associate Fellow AIAA.

[1]Landau, L and Lifshitz, E., Fluid Mechanics, Pergamon Press, New York, 1987, pp 44-94 and pp 308-312.

[2]Emanuel, G., "Effect of Bulk Viscosity on a Hypersonic Boundary Layer," Physics of Fluids A, Vol. 4 , No. 3, 1992, pp. 491-495

[3]Becker, E.. Gas Dynamics, Academic Press, New York, 1968, pp 1-70.

[4]Clarke, J. F. and McChesney, M. The Dynamics of Real Gases, Butterworths, London, 1964, pp. 100-274.

[5]Vincenti, W. and Kruger, C., Introduction to Gas Dynamics, John Wiley & Sons, Inc., New York, 1965, pp. 328-333.

[6]Johnson, J. A. III, Lin I and Ramaiah, R., "Reduced Molecular Chaos and Flow Instability, in "Stability in the Mechanics of Continua (F. H. Schroeder, ed.), Springer-Verlag, Berlin, 1982 pp 318-329.

[7]Johnson, J. A. III, Johnson, L. E., and Lu, X.-N., "Turbulence in a Reacting Contact Surface," Physics of Fluids A, Vol. 2, No. 11, 1990, pp. 2002-2010.

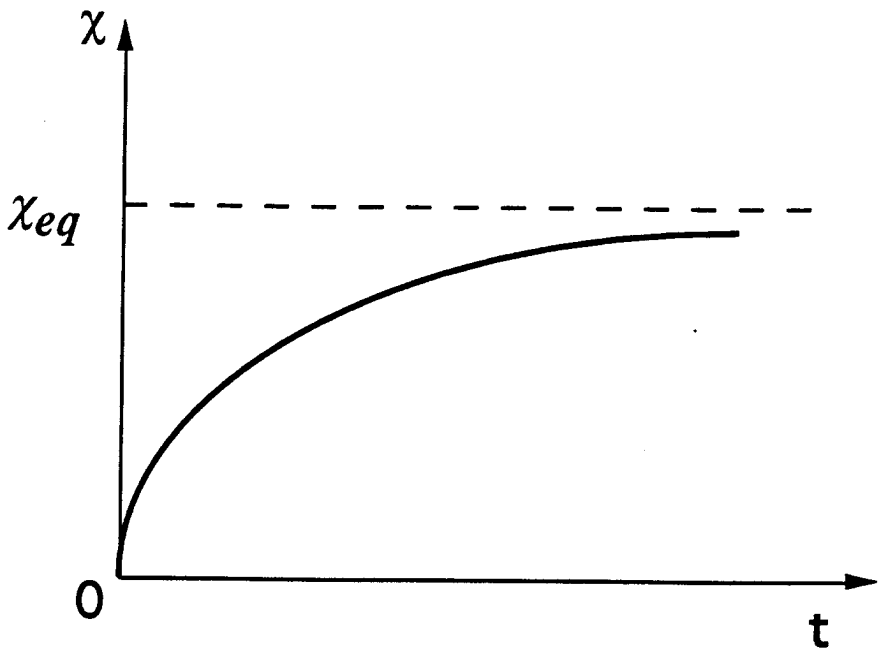

Figure 1. A Model for the Entropy Generation Term Resulting from a Chemical Process.

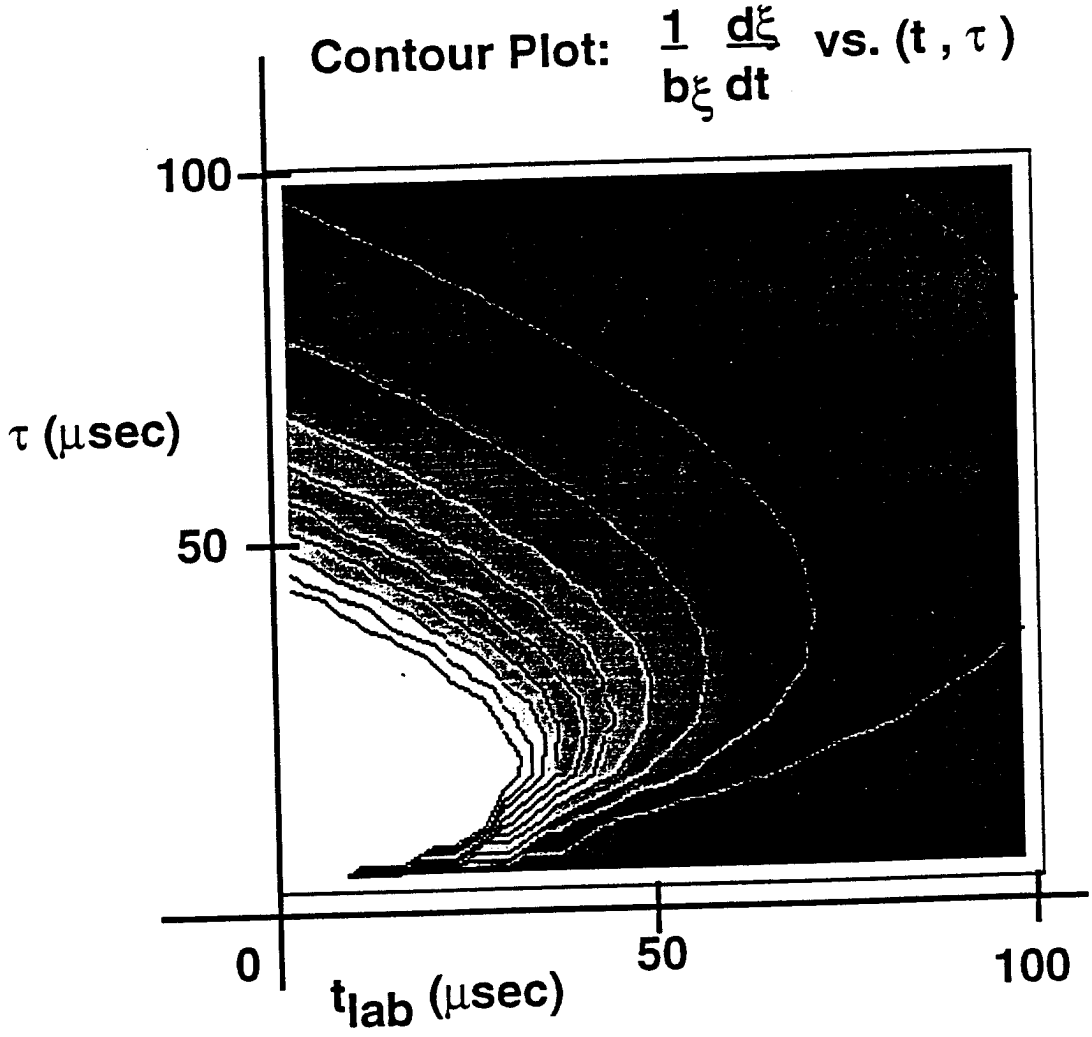

Figure 2. The Sensitivity of the Rate of Change in Second Viscosity ($d\xi/dt$) to Changes in Laboratory Time (t) and Chemical Relaxation Time (τ).

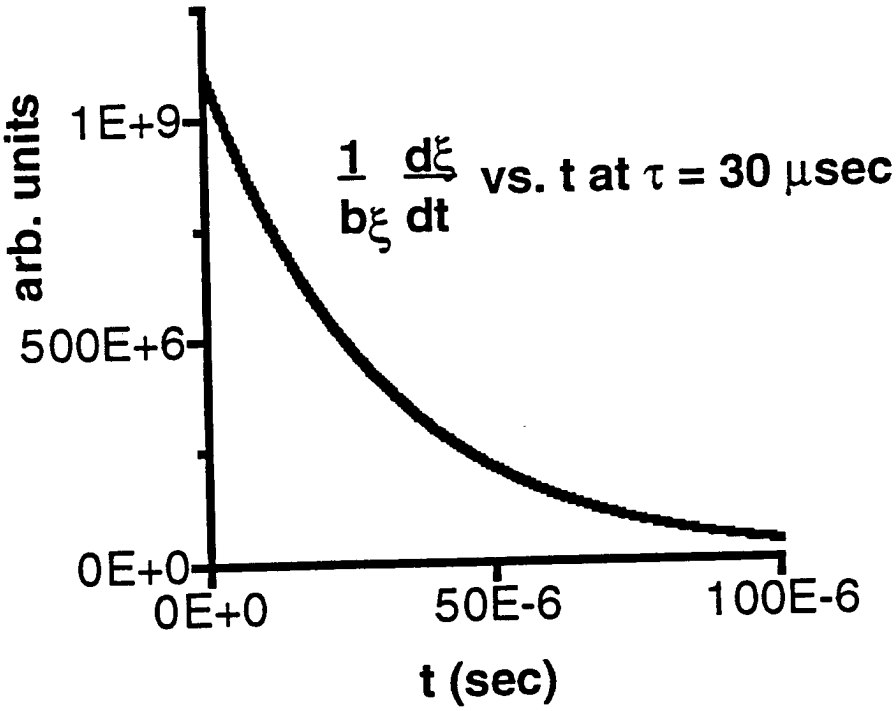

Figure 3. A Slice through the Contour Plot in Fig. 2 at $\tau = 30$ μsec.

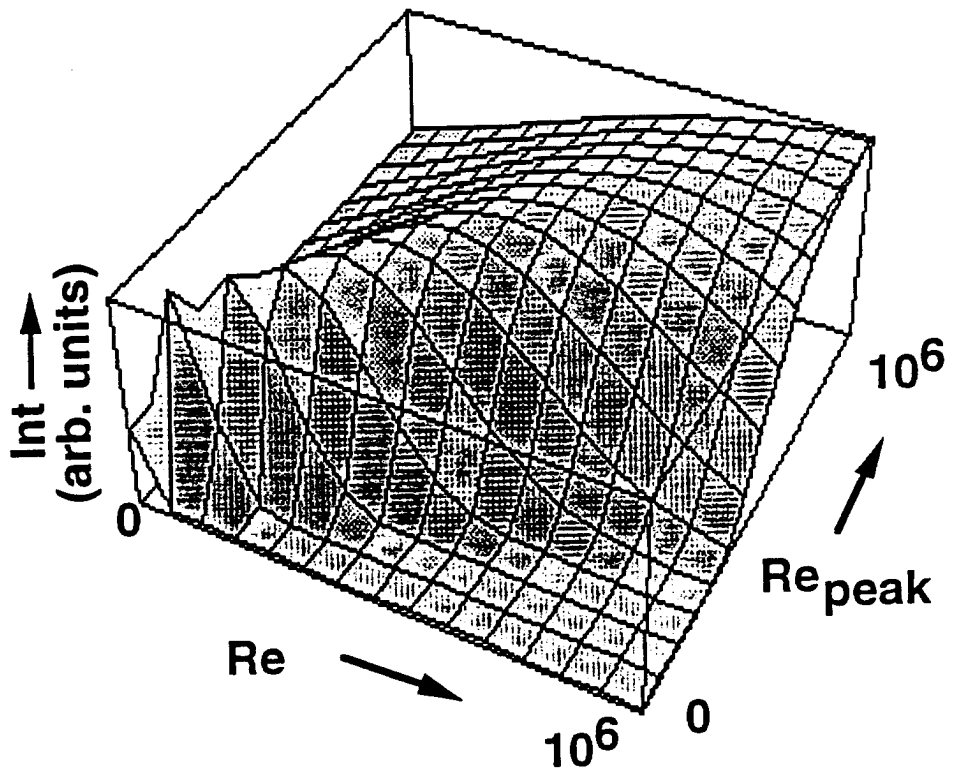

Figure 4. The Sensitivity of Turbulent Intensity to Changes in Reynolds Number. Turbulent Intensity is indicated by Int and Re_{peak} is the value of the Reynolds number at peak turbulent intensity as discussed in Ref. 6.

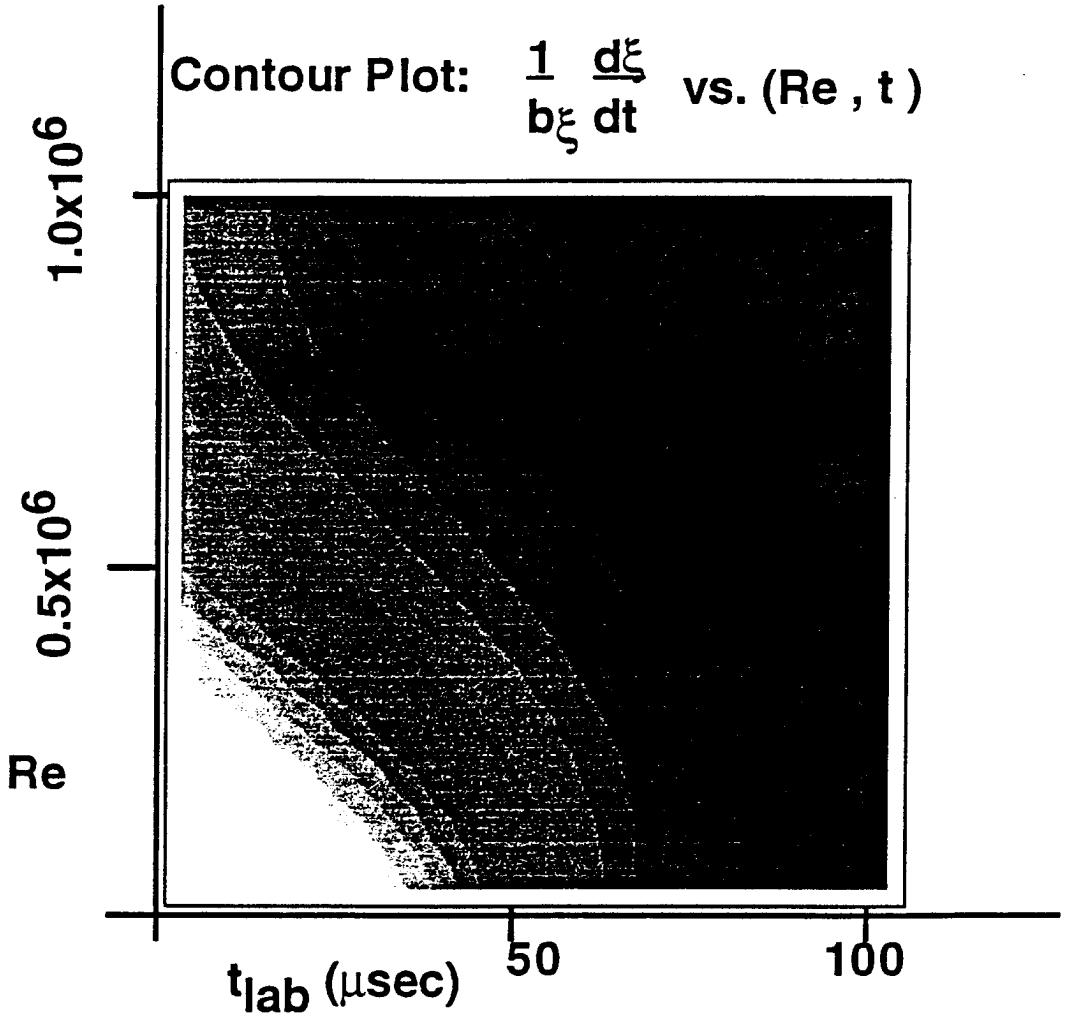

Figure 5. The Sensitivity of the Rate of Change in Second Viscosity ($d\xi/dt$) to Changes in Laboratory Time (t_{lab}) and Reynolds Number. A value of $Re_{peak} = 1.0 \times 10^6$ is used for this contour plot.

ADDITION THEOREMS FOR COULOMB STURMIANS IN COORDINATE AND MOMENTUM SPACE

by

Charles A. Weatherford
Physics Department
and
Center for Nonlinear & Nonequilibrium Aeroscience
Florida A&M University
Tallahassee, FL 32307
U.S.A.

ABSTRACT

Addition theorems are derived for Coulomb Sturmian functions and reduced Coloumb Sturmian functions in coordinate and momentum space. The Coulomb Sturmians and their Fourier Transforms, are complete in the sense of distributions in Sobolev space $W_2^{(1)}(\mathbf{R}^3)$, which is a proper subset of Hilbert space $L^2(\mathbf{R}^3)$. The derivations involve the use of the relationship between Coulomb Sturmians and four dimensional spherical harmonics (Fock hyperspherical projection) and proceeds by representing the translation operator in coordinate and momentum space, on a basis of Coulomb Sturmians and their Fourier Transforms respectively. The resulting matrix representations of the translation operator in coordinate and momentum space are respectively, finite linear combinations of Coulomb Sturmians and their Fourier Transforms, and are both unitary. The addition theorems are useful for application to problems which involve the evaluation of multicenter integrals over exponentially decaying orbitals.

I. INTRODUCTION

The problem of performing multicenter integrals is endemic to the solution of many problems of functional analysis. The solution may be approached by the method of numerical quadrature or by analytical analysis. The present paper is concerned with the method of analytical analysis. Given this delimitation, two further possible approaches are generally available: either a transformation of variables is sought or an addition theorem is used. However, it is fequently the case that numerical quadratures are combined with variable transformations and/or addition theorems. The literature on these techniques is large and diverse and no attempt will be made here to review or contrast these methods. The proceedings of a conference on multicenter integrals[1] and a recent review paper[2] provide a prospective on the literature.

The present work is concerned with the derivation of addition theorems. Such addition theorems may be generally defined by

$$F(\vec{r}_1,\vec{r}_2)=\sum_i\sum_j C_{ij}f_i(\vec{r}_1)g_j(\vec{r}_2) \tag{1}$$

If no integration over one of the vectors (say $\vec{r}_2$) is to be performed, Eq. (1) is sometimes rewritten as

$$F(\vec{r}_1,\vec{r}_2)=\sum_i B_i(\vec{r}_2)f_i(\vec{r}_1) \tag{2}$$

where

$$B_i(\vec{r}_2)=\sum_j C_{ij}g_j(\vec{r}_2) \tag{3}$$

Thus, an addition theorem explicitly separates the variables $\vec{r}_1$ and $\vec{r}_2$ so that integrations may be performed over one or both of them.

The addition theorems indicated schematically in Eqs. (1) and (2) are to be distinguished from the Löwdin α-function (or α-function) technique,[3] which is defined by

$$F(\vec{r}_1,\vec{r}_2)=\sum_i\sum_j \alpha_{ij}(r_1,r_2)Y_{l_i}^{m_i}(\hat{r}_1)Y_{l_j}^{m_j}(\hat{r}_2) \tag{4}$$

The characteristic which distinguishes the α-function method (Eq. (4)) from the present method (Eq. (1)) is that the addition theorem in the α-function method has an assumed angular behavior (spherical harmonics $Y_l^m(\hat{r})$) and the radial behavior is then worked out exactly (α-function). The α-function has assumed many forms which vary in detail (see for example Refs. 3 - 6), but which are very similar. Some of these methods are not called α-function methods, but they share the fundamental form of Eq. (4). One key characteristic is the two-range nature of the α-function and the slowly convergent infinite series which obtain.[7-9]

The problem of performing multicenter integrals is especially important in quantum chemistry when the LCAO (linear combination of atomic orbitals) method is used.[10] In the LCAO method, wavefunctions for molecules are constructed as a solution of the Schrödinger equation by taking linear combinations of atomic orbitals with coordinate centers at various locations in space. In particular, the atomic orbitals are frequently placed at the origin of the atomic nuclei that compose the molecule. It is known that the convergence of basis set expansions is critically controlled by how well the basis functions satisfy the boundary conditions which the wavefunction is required to satisfy. There are fundamentally three such requirements: (1) long-range exponential decay;[11] (2) electron-nuclear cusp;[12] and electron-electron cusp.[13] The basis functions used by most quantum chemists (Gaussians) satisfy none of the three requirements. They are chosen because of the relative simplicity of the multicenter integrals which result.

The proper atomic orbitals Φ are well known to be composed of linear combinations of Slater Type Orbitals (STOs)

$$\Phi_i(\alpha,\vec{r}) = \sum_{(nlm)_j} a_{ij} S^{m_j}_{(nl)_j}(\alpha,\vec{r}) \tag{5}$$

where

$$S^{m_j}_{(nl)_j}(\alpha,\vec{r}) = N_{n_j}(\alpha) r^{(n_j-1)} e^{-\alpha r} Y^{m_j}_{l_j}(\hat{r}) \tag{6}$$

and

$$N_{n_j}(\alpha) = \frac{(2\alpha)^{n_j+\frac{1}{2}}}{[(2n_j)!]^{\frac{1}{2}}} \tag{7}$$

The function represented by S is a normalized STO. The STOs satisfy requirements one and two.

The difficulty of performing multicenter integrals when the STOs are used as the atomic orbitals is well known[9] and led to the use of Gaussian Type Orbitals (GTOs).[10] The GTOs have a dependence on r that involves a form $exp(-\alpha r^2)$, as opposed to the STO form $exp(-\alpha r)$. Although the multicenter integrals are easier to perform than the corresponding integrals are for STOs, they suffer from the fact that the cusp at the nuclei and the proper exponential long-range behavior, are difficult to represent when the wavefunction is calculated from linear combinations of GTOs.[11]

It is the intent of the present work, to suggest another set of exponentially decaying functions (Coulomb Sturmians[12]), related to the STOs, which have a number of properties which aid in the evaluation of multicenter integrals, when the integrand is composed of them. Further, an addition theorem is derived which facilitates the derivation of explicit analytic formulas for the evaluation of the multicenter integrals. In section II, some properties of the Coloumb Sturmians (CSs), which are useful for the derivation of the addition theorem, for evaluating special cases of the addition theorem, or for evaluating multicenter integrals over CSs, are presented. In section III, the addition theorem is derived for the CSs. In section V, procedures useful for evaluating certain multicenter over CSs are

discussed. In section V, certain special cases of the addition theorem and multicenter integrals are discussed. Finally, section V gives the summary and conclusions.

II. SOME PROPERTIES OF COULOMB STURMIANS

An important set of exponentially decaying functions was first formally introduced by Rotenberg,[12] in 1962, which he called Sturmians. These functions are more commonly called Coulomb Sturmians now[13] to distinguish them from other types of Sturmian functions with different potentials. An important feature of the CSs is that they are a complete set in Sobolev space[14,15] $W_2^{(1)}(\mathbf{R}^3)$, which is a proper subset of Hilbert space $L^2(\mathbf{R}^3)$. Thus completeness in $W_2^{(1)}(\mathbf{R}^3)$ implies completeness in $L^2(\mathbf{R}^3)$ as explicited pointed out by Weniger.[16] The CSs are defined by[16]

$$\Psi_{nl}^m(\alpha,\vec{r}) \equiv N_{nl}(\alpha)e^{-\alpha r}L_{n-l-1}^{(2l+1)}(2\alpha r)\mathcal{Y}_l^m(2\alpha\vec{r}\,) \tag{8}$$

where

$$N_{nl}(\alpha) = (2\alpha)^{3/2}\left[\frac{(n-l-1)!}{2n(n+l)!}\right]^{1/2} \tag{9}$$

is the normalization constant, L is a Laguerre polynomial (same definition as given in Arfken[17]) given by

$$L_n^{(\beta)}(x) = \binom{n+\beta}{n}\,{}_1F_1(-n;\beta+1;x) \tag{10}$$

where ${}_1F_1$ is a confluent hypergeometric function[18] and $\mathcal{Y}$ is a solid spherical harmonic given by

$$\mathcal{Y}_l^m(\vec{r}) = r^l Y_l^m(\hat{r}) \tag{11}$$

and Y is a regular spherical harmonic.[16] The series for L terminates in the present case and gives

$$L_{n-l-1}^{(2l+1)}(2\alpha r) = \sum_{\tau=0}^{n-l-1} B_{\tau nl}(2\alpha r)^\tau \tag{12}$$

$$B_{\tau nl} = \frac{(-1)^\tau(n+l)!}{(n-l-1-\tau)!(2l+1+\tau)!\tau!} \tag{13}$$

In particular, the Coulomb Sturmians are complete with a purely discrete spectrum. It is easy to show that a normalized STO (S) can be expanded in a terminating series of CSs (Ψ)[19]

$$S^{m_i}_{(nl)_i}(\alpha,\vec{r}\,) = \sum_{n_f=l_i+1}^{n_i} b^{(nl)_i}_{n_f}(\alpha)\Psi^{m_i}_{n_f l_i}(\alpha,\vec{r}\,) \tag{14}$$

with

$$\begin{aligned} b^{(nl)_i}_{n_f}(\alpha) = &\left[\frac{2\alpha n_f(l_i+1)(n_f-l_i-1)!(n_f+l_i)!}{(2n_i)!}\right]^{\frac{1}{2}} \\ &\times \sum_{\sigma=0}^{n_f-l_i-1} \frac{(-1)^\sigma(n_i+l_i+\sigma)!}{(n_f-l_i-1-\sigma)!(2l_i+1+\sigma)!\sigma!} \end{aligned} \tag{15}$$

and *vice versa*

$$\Psi^{m_i}_{(nl)_i}(\alpha,\vec{r}\,) = \sum_{n_f=l_i+1}^{n_i} c^{(nl)_i}_{n_f}(\alpha)S^{m_i}_{n_f l_i}(\alpha,\vec{r}\,) \tag{16}$$

$$\begin{aligned} c^{(nl)_i}_{n_f}(\alpha) = &\left[\frac{(n_i-l_i-1)!(n_i+l_i)!}{\alpha n_i}\right]^{\frac{1}{2}} \\ &\times (-1)^{n_f-l_i-1}\frac{[(n_f)!]^{\frac{1}{2}}}{(n_i-n_f)!(n_f+l_i)!(n_f-l_i-1)!} \end{aligned} \tag{17}$$

For reasons that will be discussed in section IV below, it is useful to "equalize" the screening parameters in one electron, single center densities, composed of CSs basis functions. To accomplish this, it is first useful to equalize the screening parameters for densities composed of STOs. Some trivial algebra produces

$$\Upsilon^{m_1 m_2}_{(nl)_1(nl)_2}(\alpha,\beta,\vec{r}) = \frac{N_{n_1}(\alpha)N_{n_2}(\beta)}{N_{n_1}(\gamma)N_{n_2}(\gamma)}\Upsilon^{m_1 m_2}_{(nl)_1(nl)_2}(\gamma,\gamma,\vec{r}) \tag{18}$$

where $\gamma = \frac{\alpha+\beta}{2}$ and Υ is the STO one electron density defined by

$$\Upsilon^{m_1 m_2}_{(nl)_1(nl)_2}(\alpha,\beta,\vec{r}) \equiv S^{*m_1}_{(nl)_1}(\alpha,\vec{r}\,)S^{m_2}_{(nl)_2}(\beta,\vec{r}\,) \tag{19}$$

Then, defining the one electron, single center, CS density by

$$\Omega^{m_1 m_2}_{(nl)_1(nl)_2}(\alpha,\beta,\vec{r}) \equiv \Psi^{*m_1}_{(nl)_1}(\alpha,\vec{r}\,)\Psi^{m_2}_{(nl)_2}(\beta,\vec{r}\,) \tag{20}$$

the required expression (which equalizes the CS screening parameters for the density Ω), is obtained by first using Eq. (16) for each CS in Ω, then using Eq. (18) to equalize the screening parameters in Υ, and then using Eq. (14) to recover the required Ω with equalized screening parameters. The result is

$$\Omega^{m_1 m_2}_{(nl)_1(nl)_2}(\alpha,\beta,\vec{r}) = \sum_{n_3=l_1+1}^{n_1} c^{(nl)_1}_{n_3}(\alpha)\frac{N_{n_3}(\alpha)}{N_{n_3}(\gamma)} \sum_{n_5=l_1+1}^{n_3} b^{n_3 l_1}_{n_5}(\gamma)$$
$$\times \sum_{n_4=l_2+1}^{n_2} c^{(nl)_2}_{n_4}(\beta)\frac{N_{n_4}(\beta)}{N_{n_4}(\gamma)} \sum_{n_6=l_2+1}^{n_4} b^{n_4 l_1}_{n_6}(\gamma) \tag{21}$$
$$\times \Omega^{m_1 m_2}_{(n_5 l_1)(n_6 l_2)}(\gamma,\gamma,\vec{r})$$

It is important to note that all of the sums in Eq. (21) represent terminating series. The b coefficients are given by Eq. (15) and the c coefficients are given by Eq. (17).

The CSs satisfy a partial differential equation[17] given by

$$[\nabla^2_{\vec{r}} - \alpha^2]\Psi^m_{nl}(\alpha,\vec{r}) = -\frac{2\alpha n}{r}\Psi^m_{nl}(\alpha,\vec{r}) \tag{22}$$

This can be contrasted with the partial differential equation satisfied by the STOs

$$[\nabla^2_{\vec{r}} - \alpha^2]S^m_{nl}(\alpha,\vec{r}) = V_{nl}(\alpha,r)S^m_{nl}(\alpha,\vec{r}) \tag{23}$$

where

$$V_{nl}(\alpha,r) = -\frac{2\alpha n}{r} - \frac{[l(l+1) - n(n-1)]}{r^2} \tag{24}$$

It can be easily demonstrated that the CSs satisfy a homogeneous Fredholm integral equation of the second kind[17]

$$\Psi^m_{nl}(\alpha,\vec{r}) = \int d\vec{x} G(\alpha,|\vec{r}-\vec{x}|)\frac{2\alpha n}{x}\Psi^m_{nl}(\alpha,\vec{x}) \tag{25}$$

where G is the Green's function (same as for the modified Helmholtz equation) and is given by

$$G(\alpha,|\vec{r}-\vec{x}|) = \frac{e^{-\alpha|\vec{r}-\vec{x}|}}{4\pi|\vec{r}-\vec{x}|} \tag{26}$$

The Green's function satisfies the partial differential equation

$$[\nabla^2_{\vec{r}} - \alpha^2]G(\alpha,|\vec{r}-\vec{x}|) = -\delta(\vec{r}-\vec{x}) \tag{27}$$

The translation operator $\hat{T}_{\vec{A}} = e^{\vec{\nabla}_{\vec{A}}}$ (note that $\vec{\nabla}_{\vec{A}}$ has to be expressed in Cartesian coordinates for this expression to be valid) is defined by

$$\hat{T}_{\vec{A}}F(\vec{r}) = F(\vec{r}+\vec{A}) = F(\vec{r}_A) \tag{28}$$

where $\vec{r}_A = \vec{r}+\vec{A}$. Now an important characteristic of the Laplacian, which is well known, is its invariance with respect to translations

$$\nabla^2_{\vec{r}+\vec{A}} = \nabla^2_{\vec{r}} \tag{29}$$

Applying the translation operator to both sides of Eq. (22) and using Eq. (29) yields

$$[\nabla^2_{\vec{r}} - \alpha^2]\Psi^m_{nl}(\alpha, \vec{r} + \vec{A}) = -\frac{2\alpha n}{|\vec{r} + \vec{A}|}\Psi^m_{nl}(\alpha, \vec{r} + \vec{A}) \tag{30}$$

It may be noted, in passing, that Eq. (30) can be used to generate an algebraic eigenvalue equation by expanding $\Psi^m_{nl}(\alpha, \vec{r} + \vec{A})$ in terms of $\Psi^m_{nl}(\alpha, \vec{r})$ and letting $\nabla^2_{\vec{r}}$ operate. Then premultiplication by $\Psi^{*m}_{nl}(\alpha, \vec{r})$ is used and finally, integration over $d\vec{r}$. The result is an eigenvalue equation in which the exact eigenvalues are known. However, the coefficients (eigenvectors) in the aforementioned expansion, which result from the diagonalization of the coefficient matrix, are the desired quantities and unfortunately, these components have first order errors in them, as opposed to second order errors in the approximate eigenvalues. Thus this procedure proves too slowly convergent[20] to be useful, without some systematic way of correcting the eigenvectors.

The integral equation solution to Eq. (30) can, nevertheless, be written

$$\Psi^m_{nl}(\alpha, \vec{r} + \vec{A}) = \int d\vec{x}\; G(\alpha, |\vec{r} - \vec{x}|)\frac{2\alpha n}{|\vec{x} + \vec{A}|}\Psi^m_{nl}(\alpha, \vec{x} + \vec{A}) \tag{31}$$

This can be contrasted with the result of applying the translation operator directly to both sides of Eq. (25) to give

$$\Psi^m_{nl}(\alpha, \vec{r} + \vec{A}) = \int d\vec{x}\; G(\alpha, |\vec{r} + \vec{A} - \vec{x}|)\frac{2\alpha n}{x}\Psi^m_{nl}(\alpha, \vec{x}) \tag{32}$$

Finally, the CSs satisfy the orthonormality condition[16]

$$\int d\vec{r}\; \Psi^{*m_1}_{(nl)_1}(\alpha, \vec{r}\,)\frac{1}{r}\Psi^{m_2}_{(nl)_2}(\alpha, \vec{r}\,) = \frac{\alpha}{n_1}\delta_{(nlm)_1(nlm)_2} \tag{33}$$

and the closure condition[21]

$$\hat{1} = \sum_{nlm} |\Psi^m_{nl}\rangle\langle\Psi^m_{nl}\;\omega_n| \tag{34}$$

where $\omega_n(\alpha, r) \equiv \frac{n}{\alpha r}$ and the overlap of two CSs is given by[16,20]

$$\int d\vec{r}\; \Psi^{*m_1}_{(nl)_1}(\alpha, \vec{r}\,)\Psi^{m_2}_{(nl)_2}(\alpha, \vec{r}\,) = \delta_{(lm)_1(lm)_2}\left[\gamma^+_{n_2 l_2}\delta_{n_1, n_2+1} + \delta_{n_1, n_2} + \gamma^-_{n_2 l_2}\delta_{n_1, n_2 - 1}\right] \tag{35}$$

where

$$\gamma^{\pm}_{nl} = -\left[\frac{(n \mp l)(n \pm l \pm 1)}{4n(n \pm 1)}\right]^{1/2} \tag{36}$$

Note that the integrands of Eqs. (33) and (35) are composed of CSs with the same screening parameters. The expression given in Eq. (35) is derived from Eq. (33) using the following recursion relation:

$$\alpha r\ \Psi^m_{nl}(\alpha,\vec{r}) = \frac{\gamma^+_{nl}}{(n+1)}\ \Psi^m_{n+1,l}(\alpha,\vec{r}) \times n\ \Psi^m_{nl}(\alpha,\vec{r}) + \frac{\gamma^-_{nl}}{(n-1)}\ \Psi^m_{n-1,l}(\alpha,\vec{r}) \tag{37}$$

These equations will prove useful in the discussions given below.

III. COULOMB STURMIAN ADDITION THEOREM

Filter and Steinborn[23] have given an addition theorem for orthonormalized Slaters (ONSs, orthonormalized functions built up from the STOs by analytical Gram-Schmidt orthonormalization) by using the translation operator explicitly and deriving a formula for the matrix elements of the translation operator. These results have been applied to the calculation of the ground state wavefunction of H_2^+ with somewhat disappointing results.[24] The results were disappointing because of the slowness of the convergence of the series expressions that resulted from the use of the addition theorem.

The present work derives an addition theorem for the CSs, similar in structure, to the addition theorem of Filter and Steinborn for the ONSs. The present derivation, however, is quite different in approach. As is presented below, the present work exploits the Fourier transform of a CS[16] and the relationship of the Fourier transform to four-dimensional spherical harmonics[25] using the Fock hyperspherical projection.[26] The method is similar in many respects to techiniques of Shibuya and Wulfman[27] and to the work of Alper[28] and Novosadov.[29] The differences between these techniques and the present technique will be implicit in the derivation presented, and in the approach by which the addition theorem is used to evaluate the multicenter integrals. The work of Alper[28] is perhaps most closely related to the present methods. The differences and improvements, compared to the work of Alper, will be explicitly discussed below.

The symmetric definition of the three-dimensional Fourier transform is first applied to a CS so that

$$\Psi^m_{nl}(\alpha,\vec{r}) = (2\pi)^{-3/2}\int d\vec{p}\ e^{i\vec{r}\cdot\vec{p}}\ \overline{\Psi}^{\ m}_{nl}(\alpha,\vec{p}) \tag{38}$$

$$\overline{\Psi}^{\ m}_{nl}(\alpha,\vec{p}) = (2\pi)^{-3/2}\int d\vec{r}\ e^{-i\vec{p}\cdot\vec{r}}\ \Psi^m_{nl}(\alpha,\vec{r}) \tag{39}$$

where $\overline{\Psi}^{\ m}_{nl}$ is the Fourier transform of the CS (CSFT). Weniger[16] demonstrated the relationship between a CSFT and a four-dimensional spherical harmonic (the FDSH is the one used by Shibuya and Wulfman, Ref. 27 and Alper, Ref. 28) given by

$$X^m_{nl}(\tau,\theta,\phi) = (-1)^{n-1}(-i)^l\pi_{nl}2\pi\frac{(\tau^2+p^2)^2}{(2\tau)^{5/2}}\overline{\Psi}^{\ m}_{nl}(\alpha,\vec{p}) \tag{40}$$

where the relationship between τ (hyperangle) and α (screening parameter) is defined by

$$\xi = \frac{2\alpha p_x}{\alpha^2 + p^2} = sin(\tau)sin(\theta)cos(\phi) \tag{41a}$$

$$\eta = \frac{2\alpha p_y}{\alpha^2 + p^2} = sin(\tau)sin(\theta)sin(\phi) \tag{41b}$$

$$\zeta = \frac{2\alpha p_z}{\alpha^2 + p^2} = sin(\tau)cos(\theta) \tag{41c}$$

$$\chi = \frac{\alpha^2 - p^2}{\alpha^2 + p^2} = cos(\tau) \tag{41d}$$

Thus α is a scaling parameter and

$$\xi^2 + \eta^2 + \zeta^2 + \chi^2 = 1 \tag{42}$$

It is clear then that a point $\vec{p}$ of three-dimensional space is mapped (one-to-one) onto a surface of a four-dimensional unit sphere described by the angular variables ξ, η, ζ, χ. The following relationships are then determined.

$$sin^l(\tau) = [\frac{2\alpha p}{\alpha^2 + p^2}]^l \tag{43}$$

$$d\Omega \equiv sin^2(\tau)sin(\theta)d\tau d\theta d\phi = [\frac{2\alpha}{\alpha^2 + p^2}]^3 d\vec{p} \tag{44}$$

Do not confuse the four-dimensional spherical differential surface element $d\Omega$ with the single center charge density of Eq. (20). The quantity π_{nl} has been defined in various ways (as pointed out by Weniger[16]). For example, Biedenharn[25] uses $\pi_{nl} = (-i)^l$ and Shibuya and Wulfman[27] and Alper[28] use $\pi_{nl} = 1$. In any event, $|\pi_{nl}| = 1$. The orthonormality conditions for the CSFTs and FDSHs are given by

$$\begin{aligned} &\int_0^\pi d\tau\ sin^2(\tau) \int_0^\pi d\theta\ sin(\theta) \int_0^{2\pi} d\phi\ X^{*\ m_1}_{(nl)_1}(\tau,\theta,\phi) X^{m_2}_{(nl)_2}(\tau,\theta,\phi) \\ &\quad = 2\pi^2 \int d\vec{p}\ \overline{\Psi}^{*\ m_1}_{(nl)_1}(\alpha,\vec{p}\,) \frac{\alpha^2 + p^2}{2\alpha^2} \overline{\Psi}^{\ m_2}_{(nl)_2}(\alpha,\vec{p}\,) \\ &\quad = 2\pi^2 \delta_{(nlm)_1 (nlm)_2} \end{aligned} \tag{45}$$

The convention of $\pi_{nl} = 1$ will be used from this point on. The Shibuya and Wulfman[27] expansion of a plane wave in terms of CSs is used and is given by

$$e^{i\vec{p}\cdot\vec{r}} = 4(\pi\alpha)^{1/2} \sum_{nlm} (-1)^{n-l-1} i^l \frac{1}{(\alpha^2 + p^2)} \Psi^m_{nl}(\alpha,\vec{r}) X^{*\ m}_{nl}(\tau,\theta,\phi) \tag{46}$$

Eq. (44) may be compared with the expansion of a plane wave in terms of CSs and CSFTs given by Weniger[16]

$$e^{i\vec{p}\cdot\vec{r}} = (2\pi)^{3/2} \sum_{nlm} \overline{\Psi}_{nl}^{*\ m}(\alpha, \vec{p}\,) \frac{\alpha^2 + p^2}{2\alpha^2} \Psi_{nl}^{m}(\alpha, \vec{r}\,) \tag{47}$$

For later use, the Fourier transform representation of a three-dimensional Dirac delta function and the Coulomb potential may be written as

$$\delta(\vec{p}_2 - \vec{p}_1) = \frac{1}{(2\pi)^3} \int d\vec{r}\ e^{i\vec{r}\cdot(\vec{p}_2 - \vec{p}_1)} \tag{48}$$

$$\frac{1}{|\vec{r}_1 - \vec{r}_2|} = \frac{1}{2\pi^2} \int d\vec{p}\ \frac{e^{i\vec{p}\cdot(\vec{r}_1 - \vec{r}_2)}}{p^2} \tag{49}$$

The derivation of the addition theorem begins by applying the translation operator defined by Eq. (28) to both sides of Eq. (38). The result is

$$\Psi_{nl}^{m}(\alpha, \vec{r} + \vec{A}\,) = (2\pi)^{-3/2} \int d\vec{p}\ e^{i\vec{r}\cdot\vec{p}}\ e^{i\vec{A}\cdot\vec{p}}\ \overline{\Psi}_{nl}^{\ m}(\alpha, \vec{p}) \tag{50}$$

The Shibuya and Wulfman plane wave expansion of Eq. (46), is used for both plane wave terms (separately expanded) in the integrand of Eq. (50). Then Eq. (44) is used to transform the volume integral over $\vec{p}$ to an integral over the surface of a four-dimensional unit sphere with the result

$$\begin{aligned} \Psi_{nl}^{m}(\alpha, \vec{r} + \vec{A}\,) = & \sum_{(nlm)_1} \sum_{(nlm)_2} [2(-1)^{n_1+n_2-n-l_1-l_2-l-1} i^{l_1+l_2-l} \pi^{-3/2}] \\ & \times\ \Psi_{(nl)_1}^{m_1}(\alpha, \vec{r}\,) \Psi_{(nl)_2}^{m_2}(\alpha, \vec{A}\,) \\ & \times \int d\Omega\ \frac{\alpha^{1/2}}{\alpha^2 + p^2} X_{(nl)_1}^{*\ m_1}(\Omega) X_{(nl)_2}^{*\ m_2}(\Omega) X_{nl}^{m}(\Omega) \end{aligned} \tag{51}$$

At the stage of Eq. (51), there are six infinite sums. Unless some of the sums can be terminated, the results that derive from Eq. (51) would seem to of limited use. This problem will be alleviated below. Then, a critical step is to use the result[27,28]

$$\frac{1}{\alpha^2 + p^2} = 4\alpha^2 \left[2X_{10}^{0}(\Omega) + X_{20}^{0}(\Omega)\right] \tag{52}$$

where $X_{10}^{0}(\Omega) = 1$ and $X_{20}^{0}(\Omega) = cos(\tau)$. Thus, using Eq. (50) in Eq. (49) produces

$$\Psi_{nl}^{m}(\alpha, \vec{r} + \vec{A}\,) = \alpha^{5/2} \sum_{(nlm)_1} \sum_{(nlm)_2} C_{(nl)_1(nl)_2}^{(nl)} J_{(nlm)_1(nlm)_2}^{(nlm)} \Psi_{(nl)_1}^{m_1}(\alpha, \vec{r}\,) \Psi_{(nl)_2}^{m_2}(\alpha, \vec{A}\,) \tag{53}$$

where

$$C_{(nl)_1(nl)_2}^{(nl)} = 8(-1)^{n_1+n_2-n-l_1-l_2-l-1} i^{l_1+l_2-l} \pi^{-3/2} \tag{54}$$

$$J^{(nlm)}_{(nlm)_1(nlm)_2} = \int d\Omega\ [2 + X^0_{20}(\Omega)] X^{*\,m_1}_{(nl)_1}(\Omega) X^{*\,m_2}_{(nl)_2}(\Omega) X^m_{nl}(\Omega) \tag{55}$$

where $X^0_{10}(\Omega) = 1$ has explicitly been used. It should be noticed that C and J in Eq. (53) are explicitly independent of the screening constant α and the translation vector $\vec{A}$. The relation

$$X^{*\,m}_{nl}(\Omega) = (-1)^m X^m_{nl}(\Omega) \tag{56}$$

is also of use. The property of the FDSHs which allows the product of two FDSHs on the same hypersurface, to be written as a finite linear combination of a single FDSH on the same surface, is central to the present strategy. This expression was given by Shibuya and Wulfman[27] and used to great advantage by Alper.[28] It may be expressed as

$$X^{m_1}_{(nl)_1}(\Omega) X^{m_2}_{(nl)_2}(\Omega) =$$

$$\times \sum_{n_3=|n_1-n_2|+1,2}^{n_1+n_2-1} \sum_{l_3=|l_1-l_2|,2}^{l_1+l_2} C(n_1 l_1 m_1, n_2 l_2 m_2; n_3 l_3, m_1+m_2)\ X^{m_1+m_2}_{n_3 l_3}(\Omega) \tag{57}$$

The ', 2' on the sum indicates every other term is used. The C is defined by

$$C(n_1 l_1 m_1, n_2 l_2 m_2; n_3 l_3 m_3) = i^{l_1+l_2-l_3}[n_2 n_3 (2l_1+1)(2l_2+1)]^{1/2}$$
$$\times \langle l_2 l_1 m_2 m_1 | l_2 l_1 l_3 m_3 \rangle \begin{Bmatrix} \frac{(n_2-1)}{2} & \frac{(n_1-1)}{2} & \frac{(n_3-1)}{2} \\ \frac{(n_2-1)}{2} & \frac{(n_1-1)}{2} & \frac{(n_3-1)}{2} \\ l_2 & l_1 & l_3 \end{Bmatrix} \tag{58}$$

The $\langle \cdots \rangle$ term is a $3j$ symbol[30] and

$$\begin{Bmatrix} \cdots \\ \cdots \\ \cdots \end{Bmatrix}$$

is a Wigner $9j$ coefficient.[30] The efficient evaluation of the $9j$ symbol is critical to the ultimate computational success of the present program. However, present and projected computer technology offers great encouragement in this regard. Even now, textbooks have reasonably adequate computer codes included in the appendices.[31]

The evaluation of the J coefficient proceeds by using Eqs. (56) and (57) in Eq. (55) and then using the orthogonality condition expressed by Eq. (45), to give

$$J^{(nlm)}_{(nlm)_1(nlm)_2} = (-1)^{m_1} 2\pi^2 \sum_{n_3=|n_1-n_2|+1,2}^{n_1+n_2-1} \sum_{l_3=|l_1-l|,2}^{l_1+l} C(n_1 l_1 - m_1, nlm; n_3 l_3, m-m_1)$$
$$\times \delta_{l_2 l_3} \left[2\delta_{n_2 n_3} + \sum_{n_4=|n_3-2|+1,2}^{n_3+1} C(200, n_3 l_3, m-m_1; n_4 l_3, m-m_1) \delta_{n_2 n_4} \right] \tag{59}$$

Then, analyzing the limits of the integrals in Eq. (53) resulting from Eq. (59), produces a result which is a specfic form of Eq. (1) of the present paper (and analogous to Eq. (5.11a) of Ref. (23))

$$\Psi^m_{nl}(\alpha,\vec{r}+\vec{A}\,) = \alpha^{5/2}\sum_{l_1=0}^{\infty}\sum_{l_2=|l_1-l|}^{l_1+l}\sum_{n_1=l_1+1}^{\infty}\sum_{n_2=n_2^{min}}^{n_2^{max}} C^{(nl)}_{(nl)_1(nl)_2}$$

$$\times \sum_{m_1=-l_1}^{+l_1} J^{(nlm)}_{(nlm)_1(n_2l_2,m-m_1)}\ \Psi^{m_1}_{(nl)_1}(\alpha,\vec{r}\,)\ \Psi^{m-m_1}_{(nl)_2}(\alpha,\vec{A}\,) \tag{60}$$

where the limits on the n_2 sum are defined by

$$n_2^{min} = max(l_2+1, |n_1-n|-1);\ n_2^{max} = n_1+n+1 \tag{61}$$

Note that C is defined by Eq. (58) and J is defined by Eq. (59). The expression in Eq. (60) is very similar to the expression given in Eq. (5.11a) of Ref. (23). The summation structure is exactly the same and the limits of the summations are exactly the same. Most of the comments concerning the character of the convergence follow also with the exception that Eq. (5.11a) of Ref. (23) is an expansion which is valid in Hilbert space $L^2(\mathbf{R}^3)$, while Eq. (61) above, is an expansion which is valid in Sobolev space $W_2^{(1)}(\mathbf{R}^3)$, a proper subset of Hilbert space. Thus, the right hand side of Eq. (61) converges pointwise for all $\vec{r}$ and $\vec{R}$. Also, as pointed in Ref. (23), "The number of terms in the summations over l_2 and n_2 is completely determined by the fixed indices n and l. It is given by $(2l+1)(2n+2)$ for arbitrary order l_1 and n_1, and, therefore, the number of terms in the series does not increase with the order of terms." Note that I have substituted l for L and n for N in the quotation.

Actually, an addition theorem for CSs can be obtained from the addition theorem for the orthonormalized Slaters (ONSs) of Ref. (23) by using the terminating expansion of CSs in ONSs which can be developed easily from the expressions given in ref. (19). However, that expression would not be as compact as Eq. (60). One of the central points of the present derivation is to emphasize the use of the FDSHs and the integration over the surface of the four-dimensional Fock hypersphere. The utility of this technique, using the work of Alper[28] as a guide with the present appropriate extensions, will be demonstrated in the next section.

IV. MULTICENTER INTEGRALS OVER COULOMB STURMIANS

The work of Alper,[28] which applied the Fock hyperspherical projection[26], with the developments of Shibuya and Wulfman,[27] to the problem of performing multicenter integrals over exponential type orbitals, was very nearly successful in terminating in finite series expressions, all of the integrals which are required in the LCAO approach to *abinitio* quantum

chemistry. However, two problems plagued his developments. The first problem was that the basis set for which he developed his expressions, namely hydrogenic energy eigenstates, are not complete without inclusion of the continuum.[32] Thus, his formulas were of limited utility because they only applied for discrete eigenstates. The second problem was that the allowed screening parameters were restricted so as to allow the Fock projection only onto the same hypersphere. That is, the screening parameter determines the hypersphere onto the surface of which the projection is being made. Thus all hydrogenic orbitals occuring in a particular integral had to have the same screening parameter. In order to accomplish this with an expansion of finite length, the nuclear charge of the hydrogenic orbitals had to be related to the principal quantum number by $Z = nk_0$ where n is the principal quantum number and k_0 is a fixed constant, common to all of the hydrogenic orbitals used in the expansion.

The present analysis relaxes both of these retrictions. Firstly, the CSs are complete in Sobolev space with a purely discrete spectrum. Secondly, as will be demonstrated, since the translations are made in $\mathbf{R}^3$, using Eq. (59), to the final coordinate centers before projecting onto the Fock hypersphere, Eq. (21) may be used to transform the integrals, with a finite length expansion, to integrals over CSs with the same screening parameters before projecting onto the same Fock hypersphere. It should be noted that the initial projection onto the Fock hypersphere to determine J of Eqs. (56) and (59) is distinct from the second Fock projection made to perform the final multicenter integrals.

ACKNOWLEGEMENTS

This work was supported by the Air Force Office of Scientific Research under Contract No. F49620-89-C-007 and by NASA RTOP 432-36-58-01, NASA grant NAG-5307 and NASA contract NAGW-2930.

REFERENCES

1. *Proceedings of the First International Conference on ETO Multicenter Molecular Integrals* , edited by C.A. Weatherford and H.W. Jones, (D. Reidel, Holland, 1982).
2. E.O. Steinborn, in *Methods of Computational Molecular Physics*, edited by G.H.F. Diercksen, (D. Reidel, Holland, 1983), p. 37.
3. P.O. Löwdin, Adv. Phys. **5**, 1 (1956).
4. M.P. Barnett and C.A. Coulson, Philos. Trans. R. Soc. London Ser. A **243**, 221 (1951); M.P. Barnett, in *Methods in Computational Physics*, V. 3, edited by B. Alder, S. Fernbach, and M. Rotenberg, (Academic Press, New York, 1963), p. 95; and

references therein.
5. F.E. Harris and H.H. Michels, J. Chem. Phys. **43**, S165 (1965).
6. H.W. Jones and C.A. Weatherford, Int. J. Quant. Chem. **S12**, 483 (1978).
7. H.J. Silverstone, J. Chem. Phys. **48**, 4098 (1986); and references therein.
8. C.A. Weatherford, Int. J. Quant. Chem. **33**, 19 (1988).
9. E.J. Weniger and E.O. Steinborn, in *Numerical Determination of the Electronic Structure of Atoms, Diatomic and Polyatomic Molecules*, edited by M. Defranceschi and J. Delhalle (Kluwer, Dordrecht, 1989), p. 341.
10. H.H.H. Homeier and E.O. Steinborn, J. Comp. Phys. **87**, 61 (1990).
11. S. Agmon *Lectures on Exponential Decay of Solutions of Second – Order Elliptic Equations : Bounds on Eigenfunctions of N – body Schrödinger Operators*, (Princeton University Press, Princeton, New Jersey, 1982).
12. T. Kato, Commun. Pure and Appl. Math. **10**, 151 (1951).
13. R.N. Hill, J. Chem. Phys. **83**, 1173 (1985).
14. I. Shavitt, Ref. 2, p. 1; and references therein.
15. F.E. Harris and H.H. Michels, J. Chem. Phys. **45**, 116 (1966); F.E. Harris and H.H. Michels, Adv. Chem. Phys. **13**, 205 (1967).
16. M. Rotenberg, Ann. Phys. (NY) **19**, 262 (1962).
17. A. Maquet, P. Martin, and V. Véniard, Ref. 7, p. 295.
18. S. L. Sobolev, *Applications of Functional Analysis in Mathematical Physics*, (American Mathematical Society, Providence, RI, 1963).
19. B. Klahn and W. Bingel, Theoret. Chim. **44**, 9 (1977); **44**, 27 (1977).
20. E. J. Weniger, J. Math. Phys. **26**, 276 (1985).
21. G. Arfken, *Mathematical Methods For Physicists*, Third Edition, (Academic Press, New York, 1985).
22. I.N. Sneddon, *Special Functions of Mathematical Physics and Chemistry*, (Oliver and Boyd, Edinburgh, 1966).
23. C.A. Weatherford, Ref. 1, p. 29.
24. C.A. Weatherford, unpublished.
25. R. Shakeshaft, Phys. Rev. **A34**, 244 (1986).
26. R. Shakeshaft, J. Phys. **B8**, 1114 (1975).
27. E. Filter and E.O. Steinborn, J. Math. Phys. **21**, 2725 (1980).
28. H.H. Kranz and E.O. Steinborn, Phys. Rev. **A25**, 66 (1982).
29. L.C. Biedenharn, J. Math. Phys. **2**, 433 (1961).
30. V. Fock, Z. Phys. **98**, 145 (1935).
31. T-I. Shibuya and C. Wulfman, Proc. R. Soc. London Ser. A **286**, 376 (1965).
32. J.S. Alper, J. Chem. Phys. **55**, 3770 (1971); **55**, 3780 (1971).
33. B.K. Novosadov, Int. J. Quant. Chem. **24**, 1 (1983).
34. A.R. Edmunds, *Angular Momentum in Quantum Mechanics*, (Princeton U.P., Princeton, New Jersey, 1957).
35. R.N. Zare, *Angular Momentum*, (Wiley, Princeton, New York, 1988).
36. H.A. Bethe and E.E. Salpeter, *Quantum Mechanics of One – and Two – Electron Atoms*, (Plenum, New York, 1977).

A Calculation of the Magnetic Moment of the Δ^{++}

Milton Dean Slaughter*

Department of Physics, University of New Orleans, New Orleans, LA 70148

A fully relativistic, gauge invariant, and nonperturbative calculation of the Δ^{++} magnetic moment, $\mu_{\Delta^{++}}$, is made using equal-time commutation relations (ETCRs) and the dynamical concepts of asymptotic $SU_F(2)$ flavor symmetry and realization. Physical masses of the Δ and nucleon are used in this broken symmetry calculation. It is found that $\mu_{\Delta^{++}} = 2.04\mu_p$, where μ_p is the proton magnetic moment. This result is very similar to that obtained by using static $SU_F(6)$ symmetry or the broken $SU_F(6)$ quark model.

I. INTRODUCTION

Why should one study the Δ^{++} magnetic moment?

The answer is that such a study can yield information on hadronic structure. This information is important to the development of a correct quantitative description of hadrons. By comparing experimental and theoretical determinations of the Δ^{++} magnetic moment, one can obtain constraints on QCD, quark models, Bag models, etc..

In this talk results are presented which are applicable to pion-proton bremsstralung experiments at energies near the Δ resonance.

II. ASYMPTOTIC LEVEL REALIZATION

We first consider the well-known chiral $SU(2) \otimes SU(2)$ charge algebra

$$[A_{\pi^+}, A_{\pi^-}] = 2\, V_3. \tag{1}$$

Sandwich the above commutator between the identical baryon $SU_F(N)$ states $\left\langle B(\alpha, \overrightarrow{p}, \lambda\right|$ and $\left|B(\alpha, \overrightarrow{p'}, \lambda\right\rangle$ with momentum $\overrightarrow{p}$, $\overrightarrow{p'}$ ($\left|\overrightarrow{p}\right| \to \infty, \left|\overrightarrow{p'}\right| \to \infty$), helicity λ, and physical $SU_F(N)$ index α. Then

*Supported in part by NSF Grant No. PHYS-9012374

$$\sum_{n_L} \{\langle B(\alpha,\lambda)|\, A_{\pi+}\, |n_L\rangle \langle n_L|\, A_{\pi-}\, |B(\alpha,\lambda)\rangle - \langle B(\alpha,\lambda)|\, A_{\pi-}\, |n_L\rangle \langle n_L|\, A_{\pi+}\, |B(\alpha,\lambda)\rangle\} = C(\alpha,\lambda), \tag{2}$$

where $C(\alpha,\lambda) = 2\langle B(\alpha,\lambda)|\, V_3\, |B(\alpha,\lambda)\rangle$ is a pure number. Among the sum over single particle hadronic intermediate states, we distinguish (for given α and λ) the fractional contribution $f^L(\alpha,\lambda)$ coming from *all* the states n_L belonging to a level $L(L = 0, 1, 2, \ldots)$, where L connotes angular momentum. Note that upon varying the $SU_F(N)$ index α which produces non-vanishing values of $C(\alpha,\lambda)$, the intermediate states n_L also undergo corresponding $SU_F(N)$ rotations.

The algebraic level realization hypothesis then states that $f^L(\alpha,\lambda)$ for a given level L will depend on λ but *not* on α.

Thus, the fractional contribution from each level L is universal and invariant under $SU_F(N)$ rotation.

We next define relevant axial-vector matrix elements as follows:

$$\begin{aligned} \langle p, 1/2|\, A_{\pi+}\, |n, 1/2\rangle &\equiv f \quad , \\ \langle \Delta^{++}, 1/2|\, A_{\pi+}\, |\Delta^{+}, 1/2\rangle &\equiv -\sqrt{\tfrac{3}{2}}\, g \quad , \\ \langle \Delta^{++}, 1/2|\, A_{\pi+}\, |p, 1/2\rangle &\equiv -\sqrt{6}\, h \quad . \end{aligned} \tag{3}$$

Using the commutator Eq. (1) and asymptotic level realization for the $L = 0$ ground state baryons ($J^{PC} = \frac{1}{2}^+, \frac{3}{2}^+$), it can be shown easily that

$$h^2 = \frac{4}{25} f^2, g = -\frac{\sqrt{2}}{5} f \quad . \tag{4}$$

III. COMMUTATORS USED TO CALCULATE THE Δ^{++} MAGNETIC MOMENT

$$[\,[J^{\mu}_{em}(0),\, A_{\pi+}]\,, A_{\pi-}] = 2\, J^{\mu}_3(0) \tag{5}$$

$$[\,[J^{\mu}_3(0),\, A_{\pi+}]\,, A_{\pi-}] = 2\, J^{\mu}_3(0) \tag{6}$$

Here, $J^{\mu}_{em}(0)$ is the the electromagnetic current, and $A_{\pi+}$ and $A_{\pi-}$ are axial-vector charge operators (generators). $J^{\mu}_{em}(0)$ can be written as $J^{\mu}_{em} = V^{\mu}_3 + V^{\mu}_S$, where $V^{\mu}_3 \equiv J^{\mu}_3$ is the isovector part of the electromagnetic current and V^{μ}_S is the isoscalar part.

Insert the algebra, Eq. (6), between the ground states, $\left\langle B(\alpha, \overrightarrow{s}, \lambda = -1/2\right|$ and $\left|B'(\beta, \overrightarrow{t'}, \lambda = +1/2\right\rangle$ with $\overrightarrow{s} \to \infty$ and $\overrightarrow{t} \to \infty$. Then the following 10 equations are generated:

$$\left\langle \Delta^{++}\right| \left[J_3^\mu,\, A_{\pi+}\right] A_{\pi-} \left|\Delta^{++}\right\rangle - \left\langle \Delta^{++}\right| A_{\pi-} \left[J_3^\mu,\, A_{\pi+}\right] \left|\Delta^{++}\right\rangle = 2 \left\langle \Delta^{++}\right| J_3^\mu \left|\Delta^{++}\right\rangle \tag{7}$$

$$\left\langle \Delta^{+}\right| \left[J_3^\mu,\, A_{\pi+}\right] A_{\pi-} \left|\Delta^{+}\right\rangle - \left\langle \Delta^{+}\right| A_{\pi-} \left[J_3^\mu,\, A_{\pi+}\right] \left|\Delta^{+}\right\rangle = 2 \left\langle \Delta^{+}\right| J_3^\mu \left|\Delta^{+}\right\rangle \tag{8}$$

$$\left\langle \Delta^{0}\right| \left[J_3^\mu,\, A_{\pi+}\right] A_{\pi-} \left|\Delta^{0}\right\rangle - \left\langle \Delta^{0}\right| A_{\pi-} \left[J_3^\mu,\, A_{\pi+}\right] \left|\Delta^{0}\right\rangle = 2 \left\langle \Delta^{0}\right| J_3^\mu \left|\Delta^{0}\right\rangle \tag{9}$$

$$\left\langle \Delta^{-}\right| \left[J_3^\mu,\, A_{\pi+}\right] A_{\pi-} \left|\Delta^{-}\right\rangle - \left\langle \Delta^{-}\right| A_{\pi-} \left[J_3^\mu,\, A_{\pi+}\right] \left|\Delta^{-}\right\rangle = 2 \left\langle \Delta^{-}\right| J_3^\mu \left|\Delta^{-}\right\rangle \tag{10}$$

$$\langle p| \left[J_3^\mu,\, A_{\pi+}\right] A_{\pi-} |p\rangle - \langle p| A_{\pi-} \left[J_3^\mu,\, A_{\pi+}\right] |p\rangle = 2 \langle p| J_3^\mu |p\rangle \tag{11}$$

$$\langle n| \left[J_3^\mu,\, A_{\pi+}\right] A_{\pi-} |n\rangle - \langle n| A_{\pi-} \left[J_3^\mu,\, A_{\pi+}\right] |n\rangle = 2 \langle n| J_3^\mu |n\rangle \tag{12}$$

$$\left\langle \Delta^{+}\right| \left[J_3^\mu,\, A_{\pi+}\right] A_{\pi-} |p\rangle - \left\langle \Delta^{+}\right| A_{\pi-} \left[J_3^\mu,\, A_{\pi+}\right] |p\rangle = 2 \left\langle \Delta^{+}\right| J_3^\mu |p\rangle \tag{13}$$

$$\langle p| \left[J_3^\mu,\, A_{\pi+}\right] A_{\pi-} \left|\Delta^{+}\right\rangle - \langle p| A_{\pi-} \left[J_3^\mu,\, A_{\pi+}\right] \left|\Delta^{+}\right\rangle = 2 \langle p| J_3^\mu \left|\Delta^{+}\right\rangle \tag{14}$$

$$\left\langle \Delta^{0}\right| \left[J_3^\mu,\, A_{\pi+}\right] A_{\pi-} |n\rangle - \left\langle \Delta^{0}\right| A_{\pi-} \left[J_3^\mu,\, A_{\pi+}\right] |n\rangle = 2 \left\langle \Delta^{0}\right| J_3^\mu |n\rangle \tag{15}$$

$$\langle n| \left[J_3^\mu,\, A_{\pi+}\right] A_{\pi-} \left|\Delta^{0}\right\rangle - \langle n| A_{\pi-} \left[J_3^\mu,\, A_{\pi+}\right] \left|\Delta^{0}\right\rangle = 2 \langle n| J_3^\mu \left|\Delta^{0}\right\rangle \tag{16}$$

Define:

$$\begin{aligned}
< p, -1/2, \vec{s}\,|\, J_3 |\, p, 1/2, \vec{t}\,> \;&\equiv\; b \;=\; - < n, -1/2, \vec{s}\,|J_3|\, n, 1/2, \vec{t}\,>, \\
< n, -1/2, \vec{s}\,|\, J_3 |\, \Delta^0, 1/2, \vec{t}\,> \;&\equiv\; c \;=\; + < p, -1/2, \vec{s}\,|J_3|\, \Delta^+, 1/2, \vec{t}\,>, \\
< \Delta^0, -1/2, \vec{s}\,|\, J_3 |\, n, 1/2, \vec{t}\,> \;&\equiv\; d \;=\; + < \Delta^+, -1/2, \vec{s}\,|J_3|\, p, 1/2, \vec{t}\,> \\
< \Delta^+, -1/2, \vec{s}\,|\, J_3 |\, \Delta^+, 1/2, \vec{t}\,> \;&\equiv\; a \;=\; - < \Delta^0, -1/2, \vec{s}\,|\, J_3 |\, \Delta^0, 1/2, \vec{t}\,>, \\
< \Delta^{++}, -1/2, \vec{s}\,|\, J_3 |\, \Delta^{++}, 1/2, \vec{t}\,> \;&\equiv\; 3a \;=\; - < \Delta^-, -1/2, \vec{s}\,|J_3|\, \Delta^-, 1/2, \vec{t}\,>.
\end{aligned} \tag{17}$$

Thus, with the definitions given in Eqs. (17), Eq.(7), for instance, becomes explicitly:

$$6ag^2 + 18ah^2 + 3dgh^2 - 3cgh - 6bh^2 = 6a \tag{18}$$

One can solve this system of 10 simultaneous non-linear algebraic equations and finds that (physical solution):

$$a : b : c : d = 1 : -2 : \pm 2\sqrt{2}/5 : \mp 2\sqrt{2}/5, \tag{19}$$

corresponding to $h = \pm\frac{2}{5} f$.

(Note that the Lorentz index μ has been dropped for convenience).

Clearly then, we have the result:

$$< \Delta^+, -1/2, \vec{s}\,|\, J_3^\mu |\, \Delta^+, 1/2, \vec{t}\,> = -(1/2) < p, -1/2, \vec{s}\,|\, J_3^\mu |\, p, 1/2, \vec{t}\,>, \quad \vec{s}, \vec{t} \to \infty. \tag{20}$$

What about the matrix element $< \Delta^+, -1/2, \vec{s}\,|V_S^\mu|\, \Delta^+, 1/2, \vec{t}\,>$?

To obtain it, we first write all matrix elements in terms of their isovector and isoscalar parts, i.e.

$$\begin{array}{rcl}
\langle p|\, J_{em}\, |p\rangle & \equiv & i + \delta, \\
\langle n|\, J_{em}\, |n\rangle & = & -i + \delta, \\
\langle \Delta^{++}|\, J_{em}\, |\Delta^{++}\rangle & \equiv & 3j + \beta, \\
\langle \Delta^{+}|\, J_{em}\, |\Delta^{+}\rangle & = & j + \beta, \\
\langle \Delta^{0}|\, J_{em}\, |\Delta^{0}\rangle & = & -j + \beta, \\
\langle \Delta^{-}|\, J_{em}\, |\Delta^{-}\rangle & = & -3j + \beta, \\
\langle n|\, J_{em}\, |\Delta^{0}\rangle & = & \langle p|\, J_{em}\, |\Delta^{+}\rangle \equiv k, \\
\langle \Delta^{0}|\, J_{em}\, |n\rangle & = & \langle \Delta^{+}|\, J_{em}\, |p\rangle \equiv l.
\end{array} \tag{21}$$

In Eq.(21) i, j, k and l denote the isovector matrix elements whereas β and δ denote the isoscalar matrix elements.

Next insert the algebra, Eq. (6), between the ground states, $\left\langle B(\alpha, \overrightarrow{s}, \lambda = -1/2\right|$ and $\left|B'(\beta, \overrightarrow{t'}, \lambda = +1/2\right\rangle$ with $\vec{s} \to \infty$ and $\vec{t} \to \infty$.

We find that $\beta = \alpha = 0$, i.e.

$$< \Delta, -1/2, \vec{s}\,|\, V_S^\mu |\, \Delta, 1/2, \vec{t}\,> = 0 \tag{22}$$

for all charge states of the Δ. Therefore, we have as our main result:

$$< \Delta^+, -1/2, \vec{s}\,|J_{em}^\mu|\, \Delta^+, 1/2, \vec{t}\,> = -(1/2) < p, -1/2, \vec{s}\,|\, J_3^\mu |\, p, 1/2, \vec{t}\,>, \quad \vec{s}, \vec{t} \to \infty. \tag{23}$$

We explore the consequences of Eq. (22):

First:

$$\begin{aligned}
\left\langle p(\vec{s},\lambda)\,|J^{\mu}_{em}(0)|\,p(\vec{t},\lambda')\right\rangle &= \sqrt{\tfrac{m^2}{E_{\vec{s}}E_{\vec{t}}}}\,\bar{u}_P(\vec{s},\lambda)\,[\Gamma^{\mu}]\,u_P(\vec{t},\lambda'),\\
\Gamma^{\mu} &= F_1(q^2)\gamma^{\mu}+\tfrac{i\sigma^{\mu\nu}q_\nu F_2(q^2)}{2m},\\
F_1(0)=1 \quad , &\quad F_2(0)=\kappa_p \text{ (proton anomalous magnetic moment)},\\
\mu_p &= (F_1(0)+F_2(0))(\tfrac{e}{2m}) = \text{ proton magnetic moment}
\end{aligned} \tag{24}$$

$$\begin{aligned}
\left\langle \Delta(\vec{s},\lambda)\,|J^{\mu}_{em}(0)|\,\Delta(\vec{t},\lambda')\right\rangle &= \sqrt{\tfrac{m^{*2}}{E^{\Delta}_{\vec{s}}E^{\Delta}_{\vec{t}}}}\,\bar{u}^{\alpha}_{\Delta}(\vec{s},\lambda)\left[\Gamma^{\mu}_{\alpha\beta}\right]u^{\beta}_{\Delta}(\vec{t},\lambda'),\\
\Gamma^{\mu}_{\alpha\beta} &= g_{\alpha\beta}\left\{F^{*}_1(q^2)\gamma^{\mu}+\tfrac{i\sigma^{\mu\nu}q_\nu F^{*}_2(q^2)}{2m^{*}}\right\}+\tfrac{q_\alpha q_\beta}{2m^{*2}}\left\{F^{*}_3(q^2)\gamma^{\mu}+\tfrac{i\sigma^{\mu\nu}q_\nu F^{*}_4(q^2)}{2m^{*}}\right\},\\
F^{*}_1(0)=Q_{\Delta} \quad , &\quad F^{*}_2(0)\equiv\kappa_{\Delta} \text{ (Δ anomalous magnetic moment)},\\
\mu_{\Delta} &= (F^{*}_1(0)+F^{*}_2(0))(\tfrac{m}{m^{*}})(\tfrac{e}{2m}) = \ \Delta \text{ magnetic moment}\ .
\end{aligned} \tag{25}$$

Here, $q \equiv p' - p$.

IV. Kinematics

We take $\overrightarrow{t}$ to lie along the z-axis and $\overrightarrow{s}$ in the $x-z$ plane such that

$$\left|\vec{t}\right| = t_z \to \infty\ , \quad s_z = rt_z \to \infty\ , \quad 0 < r \leq 1\ , \quad r \text{ held constant.}$$

We find that

$$q^2|_{p\to p+\gamma} = -\frac{(1-r^2)}{r}m^2 - \frac{s_x^2}{r}\ ,\ \text{and}\ q^2|_{\Delta\to\Delta+\gamma} = -\frac{(1-r^2)}{r}m^{*2} - \frac{s_x^2}{r}\ .$$

Note that in the limit where $r \to 1$, that $q^2 \to 0$ *independently* of m or m^* as $s_x \to 0$.

Now choose $\mu = 0$, evaluate Eq. (23), and use the fact that $F_2^V(0) = \frac{1}{2}(k_p - k_n)$. We then find that:

$$\mu_{\Delta^+} = \left\{[1+\frac{3}{8}(k_p-k_n)](\frac{m^*}{m})\right\}\left\{\frac{m}{m^*}\right\}\left[\frac{e}{2m}\right] \quad . \tag{26}$$

From Eqs. (21) and (22), we also find that:

$$\begin{aligned}
F_2^{\Delta^{++}}(0) &= 3F_2^{\Delta^{+}}(0)\\
\mu_{\Delta^{++}} &= \left\{2+F_2^{\Delta^{++}}(0)\right\}\left\{\tfrac{m}{m^*}\right\}\left[\tfrac{e}{2m}\right],\\
F_2^{\Delta^{++}}(0) &= \tfrac{9}{8}\,\tfrac{m^*}{m}(k_p-k_n)\quad .
\end{aligned} \tag{27}$$

Numerically, we obtain (when $m^* = 1.232$ GeV/c):

$$\left.\frac{\mu_{\Delta++}}{\mu_p}\right|_{\text{Theory}} = 2.04 \quad , \quad \mu_{\Delta++}|_{\text{Theory}} = 5.69\,\frac{e}{2m}. \tag{28}$$

OTHER THEORETICAL CALCULATIONS

	$\mu_{\Delta++}$ $[e/2m]$
$SU(6)$[1]	5.58
$SU(6)$ Mass Corrected[2]	4.25
Bag Model Corrections to Quark Model[3]	$4.41 - 4.89$
Lattice Gauge[4]	4.91 ± 0.61
QCD Sum Rule[5]	2.7 ± 0.4

"EXPERIMENTAL" VALUES

	$\mu_{\Delta++}$ $[e/2m]$
UCLA[6]	$3.7 - 4.2$
SIN[7]	$4.6 - 4.9$
Musakhanov[8]	3.6 ± 2.0
Pascual and Tarrach[9]	5.6 ± 2.1
Heller *et al.*[10]	$7.0 - 9.8$
Wittman[11]	$5.58 - 7.53$
Bossard *et al.*[12]	4.58 ± 0.33

V. CONCLUSIONS

The Δ^{++} magnetic moment, $\mu_{\Delta++}$, can be calculated in a fully relativistic, gauge invariant manner *without* assuming $SU(6)$ symmetry.

Estimated theoretical error is $\approx 7\%$ since radial configuration mixing of excited Δ states is neglected.

Results are in good agreement with experiment.

References

[1] M. A. Beg, B. W. Lee, and A. Pais, Phys. Rev. Lett. **13**, 514 (1964).

[2] M. A. Beg and A. Pais, Phys. Rev. **137**, B1514 (1965)

[3] G. E. Brown, M. Rho, and V. Vento, Phys. Lett. **97B**, 423, (1980)

[4] Derek B. Leinweber, Terrence Draper, and R. M. Woloshyn, Phys. Rev. D**46**, 3067 (1992).

[5] B. L. Ioffe and A. V. Smilga, Nucl. Phys. B**232**, 109 (1984).

[6] B. M. K. Nefkens et al., Phys. Rev. D**18**, 3911 (1978). Extracted value by Dahang Lin, M. K. Liou, and Z. M. Ding, Phys. Rev. C**44**, 1819 (1991).

[7] C. A. Meyer et al., Phys. Rev. D**38**, 754 (1988). Extracted value by Dahang Lin, M. K. Liou, and Z. M. Ding, Phys. Rev. C**44**, 1819 (1991).

[8] N. M. Musakhanov, Yad. Fiz. **19**, 630 (1974)[Sov. J. Nucl. Phys. **19**, 319 (1974).

[9] P. Pascual and R. Tarrach, Nucl. Phys. B**134**, 133 (1978).

[10] L. Heller, S. Kumano, J. C. Martinez, and E. J. Moniz, Phys. Rev. C**35**, 718 (1987).

[11] R. Wittman, Phys. Rev. C**37**, 2075 (1988).

[12] A. Bossard et al., Phys. Rev. Lett. **64**, 2619 (1990).

Spectra of Heliumlike Krypton form TFTR Plasmas; A Potential T_i Diagnostic for ITER

A. J. Smith
Lock Haven University
Lock Haven, PA 17745

M. Bitter, H. Hsuan,K. W. Hill, K. M. Young
and M. Zarnstorff

Princeton University
Plasma Physics Laboratory
Princeton, NJ 08543

Peter Beiersdorfer

University of California
Lawrence Livermore National Laboratory
Livermore, CA 94550

B. Fraenkel

Hebrew University
Jerusalem, Israel

Presented at the XX Day of Scientific Lectures and the 16th Annual Meeting of the National Society of Black Physicists. Tallahassee, Florida, April 21-24, 1993

Abstract

Spectra of He-like Krypton from TFTR Plasmas; a potential T_i diagnostic for ITER.* A. J. Smith[+], M. Bitter, H. Hsuan, P. Beiersdorfer[++], B Fraenkel[+++], K. W. Hill, K. M. Young, and M. Zarnstorff, *Princeton University, Plasma Physics Laboratory, Princeton, NJ 08543.* We have obtained spectra of heliumlike Krypton from TFTR plasmas. Since the wavelength of the Kα line of He-like krypton is .95 Å, the spectra were observed in second order Bragg reflection so as to utilize Bragg angles $\theta > 40^0$ and thus having sufficient resolution. It was also necessary to use Xe as a detector gas to enhance the efficiency of the position sensitive detectors for detection of the 13 keV photons. These measurements are important because Doppler broadening measurements on the KrXXXV spectrum have been proposed for T_i diagnostic on the International Thermonuclear Experimental Reactor. In this study we also look at the effect of highly ionized krypton on plasma performance.

*Supported by DoE Contract No. DE-AC02-76-CHO-3073

[+]Lock Haven University, Lock Haven PA 17745;

[++]Lawrence Livermore National Laboratory, Ca 94550;

[+++]Hebrew University Jerusalem, Israel.

INTRODUCTION

The conceptual design of the International Thermonuclear Experimental Reactor (ITER)[1] indicates that this next generation tokamak will have a stored energy of 600 MJ, a plasma volume of 550 m^3, and pulse lengths of 400-2500 sec. In comparison present generation tokamaks such as TFTR (Tokamak Fusion Test Reactor) have the stored energy of 1-5 MJ, a volume of 50 m^3 and pulse lengths of 5 sec. Two of the main issues of concern with ITER operation will be, a) controlled release of stored energy, and b) measurement of the central ion temperature $T_i(0)$. It has been suggested that both of these problems be solved by the injection of high-Z elements into the plasma. In this regard krypton (Z=36) appears to be the natural choice; it is an inert gas and therefore easy to inject into the plasma, and heliumlike krypton, KrXXXV is the dominant ionization state at ITER operating temperatures ~7-30 keV. Doppler broadening measurements of the resonance line of He-like Kr could be used as a $T_i(0)$ diagnostic, while the lower charge states could release through the emission of line radiation from the plasma edges.

It is therefore important to study the effects of Kr on plasmas and to investigate the conditions under which heliumlike Kr is produced. In this paper we present results for the injection of krypton into ohmically heated TFTR plasmas, and also spectra of heliumlike krypton obtained from tokamak discharges.

EXPERIMENTAL

An important aspect of this study has been the construction of a high resolution crystal spectrometer suitable for the observation of the satellite spectrum of KrXXXV. The wavelength of the resonance Kα line of heliumlike Kr is 0.95 Å, which is less than the 2d spacing of natural crystals, the Kr spectrum must therefore be observed in second-order Bragg reflection at the expense of a significant reduction in crystal reflectivity. The 13 keV x-ray photons of He-like krypton were recorded with one arm of the TFTR Vertical (high resolution) spectrometer[2] using a 2023 - quartz crystal (2d = 2.7497 Å; with a radius of curvature 11.43 m) in second-order Bragg reflection. This arrangement leads to a large Bragg angle of 43.7° and a therefore a high resolving power $\lambda/\Delta\lambda$ = 12,000. The spectrometer also reflects 6.5 keV photons in first-order Bragg reflection, i.e. with much higher efficiency. It was thus necessary to include an 8 mil Al foil absorber in front of the detector; this has a 1.5% transmission at 6.5 keV and a 48% transmission at 13 keV and hence a significant improvement in the signal-to-noise ratio. Furthermore, xenon was used as detector gas in the position

sensitive multi-wire proportional counter, this increases the detection efficiency for 13 keV photons by 40%.

RESULTS AND DISCUSSION

Krypton was injected at a rate of 0.2-0.35 Torr-liter/sec for 0.2-0.3 sec into ohmically heated helium discharges at three different plasma currents of 1.4, 1.6 and 1.8 MA. These discharges had electron temperatures in the range 5-6 keV and electron densities $1.5 - 2.5 \times 10^{19}$ m^{-3}. Fig. 1 shows the radial electron temperature profiles for these discharges; peaked for 1.4 and 1.6 MA discharges, wide for the 1.8 MA discharge.

A survey spectrum of the emitted line radiation for the 1.8 MA discharge, obtained by the TFTR X-ray Pulse Height Analysis (PHA) system[3], is shown in Fig. 2a. The spectrum shows the Kα-line from Kr and various metal impurities Cr, Fe and Ni, superimposed on a bremsstrahlung continuum. Since the energy resolution of the PHA system is 230 eV, the peak at 13 keV includes radiation from all the krypton charge states present.

Figure 2b shows the time history of the Kr peak at 13 keV for the three discharge currents. The intensity of the Kα peak represents a chord integrated measurement along the horizontal sight-line of the PHA system through the plasma center; it is expected to increase with the electron temperature profile. Further analysis shows that at the peak in Fig. 2b the krypton density is 0.1% of the total electron density.

The total radiated power (see Fig. 3) as measured by the TFTR bolometer array[4] increased from 40% to 100% of the ohmic power input, for the 1.4 and 1.6 MA discharges and from 40 % to 70% of the ohmic power input for the 1.8 MA discharge. The fact that at 1.8 MA the intensity of the Kα radiation increased while the radiated power decreased, indicates that at broader electron temperature profiles the ionization equilibrium was shifted to higher charge states which emit significantly less line radiation than lower charge states.

This conclusion is confirmed by Fig. 4, which shows high resolution spectra of KrXXXV obtained for plasma currents of 1.4 MA (Fig. 4a) and 1.8 MA (Fig. 4b). The data were accumulated for 6 and 18 discharges respectively. For a peaked electron temperature profile, Fig. 4a, only berylliumlike and boronlike features are present, whereas for the wide electron temperature profile, all the features, including

heliumlike lines **w, x, y, and z** and their associated lithiumlike, berylliumlike and boronlike satellites (Fig 4b). The features have been identified using the instrumental dispersion and theoretical wavelengths from Vainshtein and Safronova[5]; they are listed in Table 1.

A noticeable difference between the KrXXXV spectrum and high resolution satellite spectra of TiXXI, CrXXIII , FeXXVand NiXXVII is that the heliumlike features **w, x, y, and z**, are well separated from each other, and that the lithiumlike and beryllium features are now much closer to the resonance line **w**. An important aspect of the results is that the forbidden line **z** seems to be isolated from lithiumlike and boronlike features, its intensity is comparable to that of the line **w**, but unlike **w**, **z** is uncontaminated by $n \geq 3$ satellites. It would therefore appear that the **z** line is a better candidate for Doppler broadening measurements, and preliminary analysis gives $T_i = 2.5 \pm 0.4$ keV, in agreement with $T_i(0) = 2.3$ keV from FeXXV which was simultaneously observed on another arm of the TFTR vertical spectrometer. In contrast the measurement from the KrXXXV resonance line yielded the higher value $T_i(0) = 6.3 \pm 0.5$ keV.

CONCLUSIONS

We have injected krypton into ohmically heated TFTR plasmas in order to study the emitted line x-ray radiation, both for the purpose of measurement of the central ion temperature and the controlled release of plasma energy for future tokamaks such as ITER. We have observed that the ionization equilibrium and the loss of power via radiation depend on the electron temperature profile. High resolution spectra have been obtained showing heliumlike KrXXXV lines and the associated lithiumlike, berylliumlike and boronlike satellites. Preliminary measurements of T_i appear to be in agreement with established methods. Further studies, both theoretical and experimental atomic physics, and with large tokamaks are needed in order to better understand the effects that krypton injection will have on ITER.

References

(1) K. Tomabechi et al., Nuclear Fusion **31**, 1135 (1991); ITER Documentation Series, No 23: *"ITER Operations and Research Programme", International Atomic Energy Agency, Vienna, 1991.*

(2) M. Bitter, K. W. Hill, S. Cohen, S. von Goeler, H. Hsuan, L. C. Johnson, S. Raftopoulos, M. Reale, N. Schechtman, S. Sesnic, F. Spinos, J. Timberlake, S. Weicher, N. Young, Rev. Sci Instrum. **57**, 2145 (1986).

(3) K. W. Hill, M. Bitter, M. Diesso, L. Dudek, S. von Goeler, s. Hayes, L. C. Johnson, J. Kiraly, E. Moshey, G. Renda, S. Sesnic, N. R. Sauthoff, F. Tenney and K. M. Young, Rev. Sci. Instrum. **56**, 840 (1985).

(4) J. Schivell, G. Renda, J. Lawrence, and H. Hsuan, Rev. Sci. Instrum. **53**, 1527 (1982); J. Schivell, Rev. Sci. Instrum. **56**, 972 (1985)

(5) L. A. Vainshtein and U. I. Safronova, [Acad. Sci. USSR] P. N. Lebedev Institute of Spectroscopy, Rep 2, 1985.

TABLE I: Theoretical wavelengths for the transitions in heliumlike krypton, KrXXXV, and the main n = 2 satellites from Vainshtein and Safronova (Ref. 14)

Key	Transition	Wavelength (Å)
w	$\mathbf{1s^2\ {}^1S_0 - 1s2p\ {}^1P_1}$	0.94538
x	$\mathbf{1s^2\ {}^1S_0 - 1s2p\ {}^3P_2}$	0.94708
s	$1s^2 2s\ {}^2S_{1/2} - 1s2p2s({}^3P){}^2P_{3/2}$	0.94746
t	$1s^2 2s\ {}^2S_{1/2} - 1s2p2s({}^3P){}^2P_{1/2}$	0.94804
q	$1s^2 2s\ {}^2S_{1/2} - 1s2p2s({}^1P){}^2P_{3/2}$	0.94961
k	$1s^2 2p\ {}^2P_{1/2} - 1s2p^2\ {}^2D_{3/2}$	0.94995
j	$1s^2 2p\ {}^2P_{3/2} - 1s2p^2\ {}^2D_{5/2}$	0.95137
y	$\mathbf{1s^2\ {}^1S_0 - 1s2p\ {}^3P_1}$	0.95156
r	$1s^2 2s\ {}^2S_{1/2} - 1s2p2s\ ({}^1P)\ {}^2P_{1/2}$	0.95288
β	$1s^2 2s^2\ {}^1S_0 - 1s2p2s^2\ {}^1P_1$	0.9529*
z	$\mathbf{1s^2\ {}^1S_0 - 1s2s\ {}^3S_1}$	0.95525
e	$1s^2 2p\ {}^2P_{3/2} - 1s2p^2\ {}^4P_{5/2}$	0.95615
u	$1s^2 2s\ {}^2S_{1/2} - 1s2s2p({}^3P){}^4P_{3/2}$	0.95652

*from present calculations

Figure Captions

Fig. 1 Radial profiles of the electron temperature of ohmically heated TFTR plasmas with different plasma currents: (a) I_p = 1.4 MA, (b) I_p = 1.6 MA and (c) I_p = 1.8 MA . The data were obtained from Laser Thomson scattering measurements.

Fig. 2 Results from the TFTR X-ray Pulse Height Analysis system: (a) X-ray spectrum consisting of the bremsstrahlung continuum and Kα line radiation from Cr, Fe, Ni and Kr; (b) time evolution of the krypton Kα peak, where t = 0 corresponds to the starting time of the krypton injection.

Fig. 3 Total radiated power as measured by a bolometer array for (a) I_p = 1.4 MA, (b) I_p = 1.6 MA amd (c) I_p = 1.8 MA. The dotted lines represent data from comparison discharges without krypton injection.

Fig. 4 Krypton Kα spectra as measured from one channel of the TFTR Vertical Crystal Spectrometer with a vertical sightline through the center of the vacuum vessel at R_0 = 2.65 m. The data were accumulated (a) for 6 nearly identical ohmic discharges with Ip = 1.4 MA, and (b) for 18 nearly identical ohmic discharges with Ip = 1.8 MA.

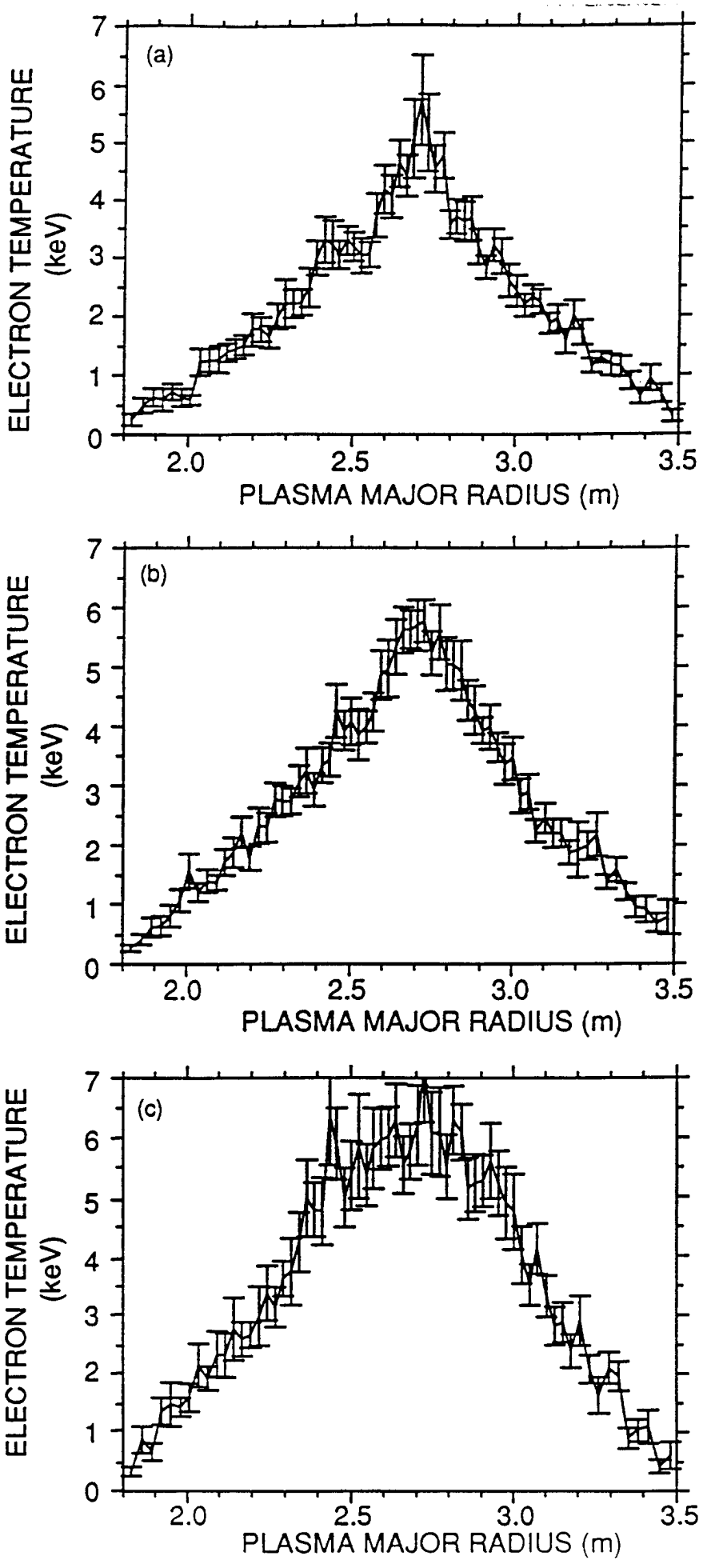
(a)
ELECTRON TEMPERATURE (keV)
PLASMA MAJOR RADIUS (m)
(b)
ELECTRON TEMPERATURE (keV)
PLASMA MAJOR RADIUS (m)
(c)
ELECTRON TEMPERATURE (keV)
PLASMA MAJOR RADIUS (m)

Figure 1

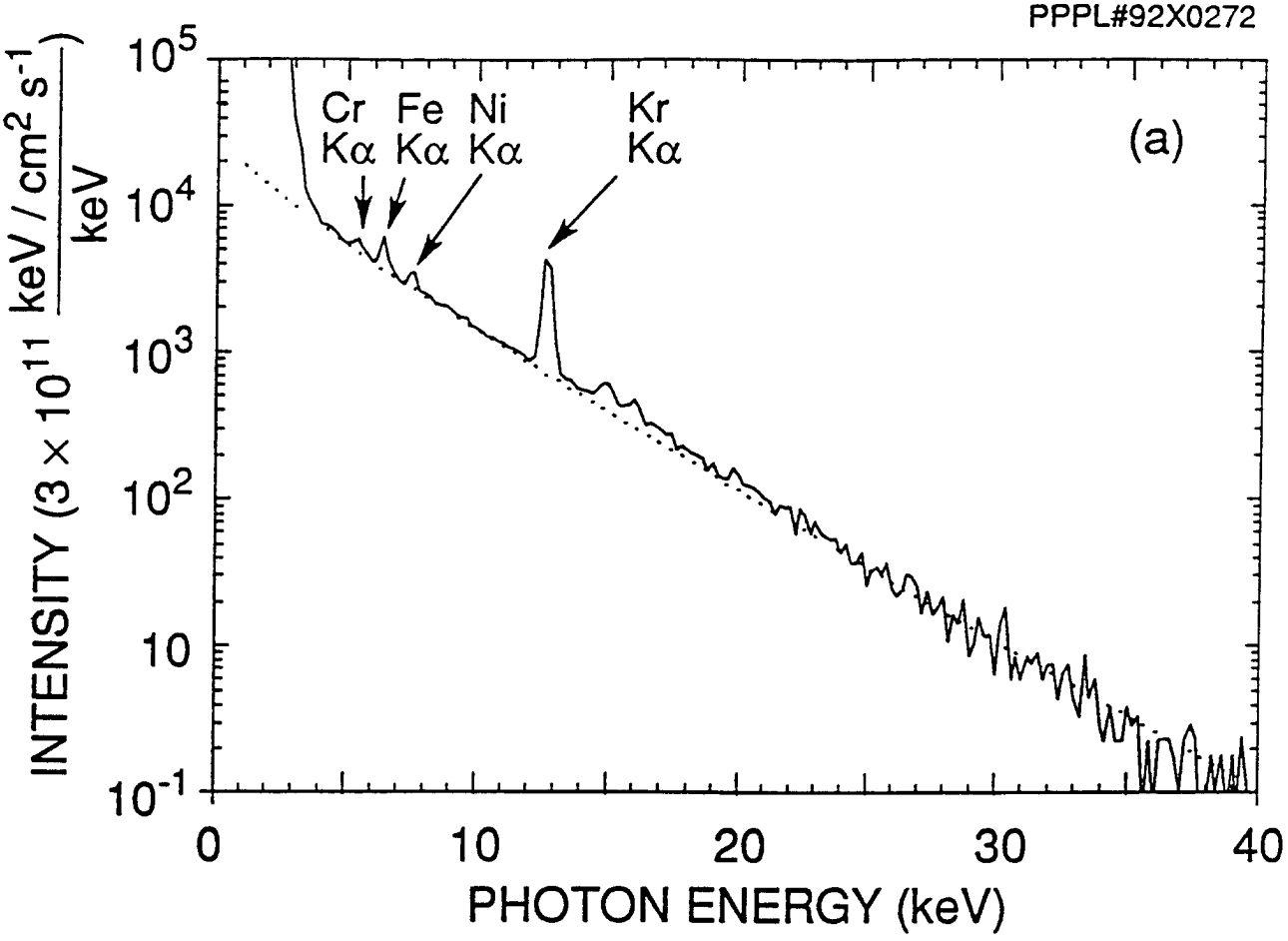
INTENSITY (3 × 10^11 keV / cm^2 s^-1 / keV)
10^5
10^4
10^3
10^2
10
10^-1
Cr Kα
Fe Kα
Ni Kα
Kr Kα
(a)
0
10
20
30
40
PHOTON ENERGY (keV)

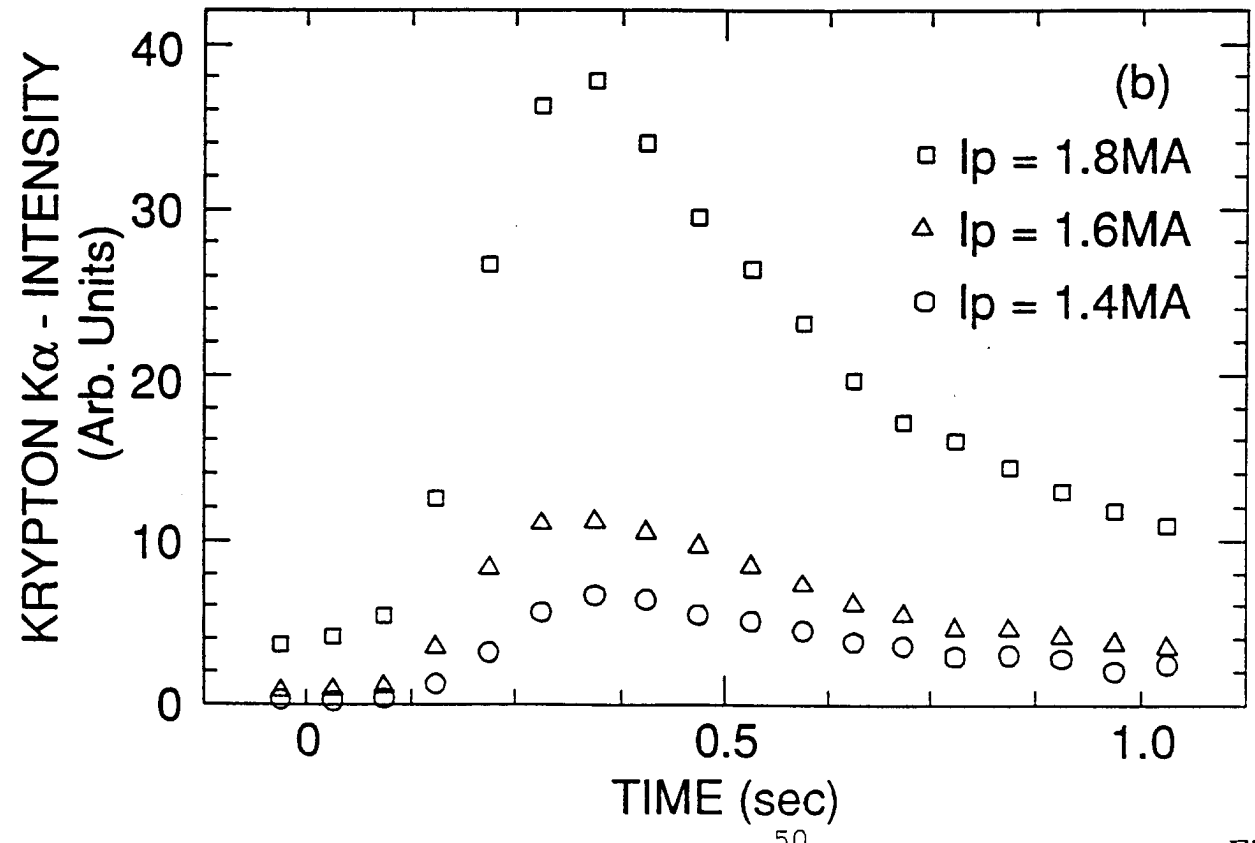
KRYPTON Kα - INTENSITY (Arb. Units)
40
30
20
10
0
(b)
Ip = 1.8MA
Ip = 1.6MA
Ip = 1.4MA
0
0.5
1.0
TIME (sec)

Figure 2

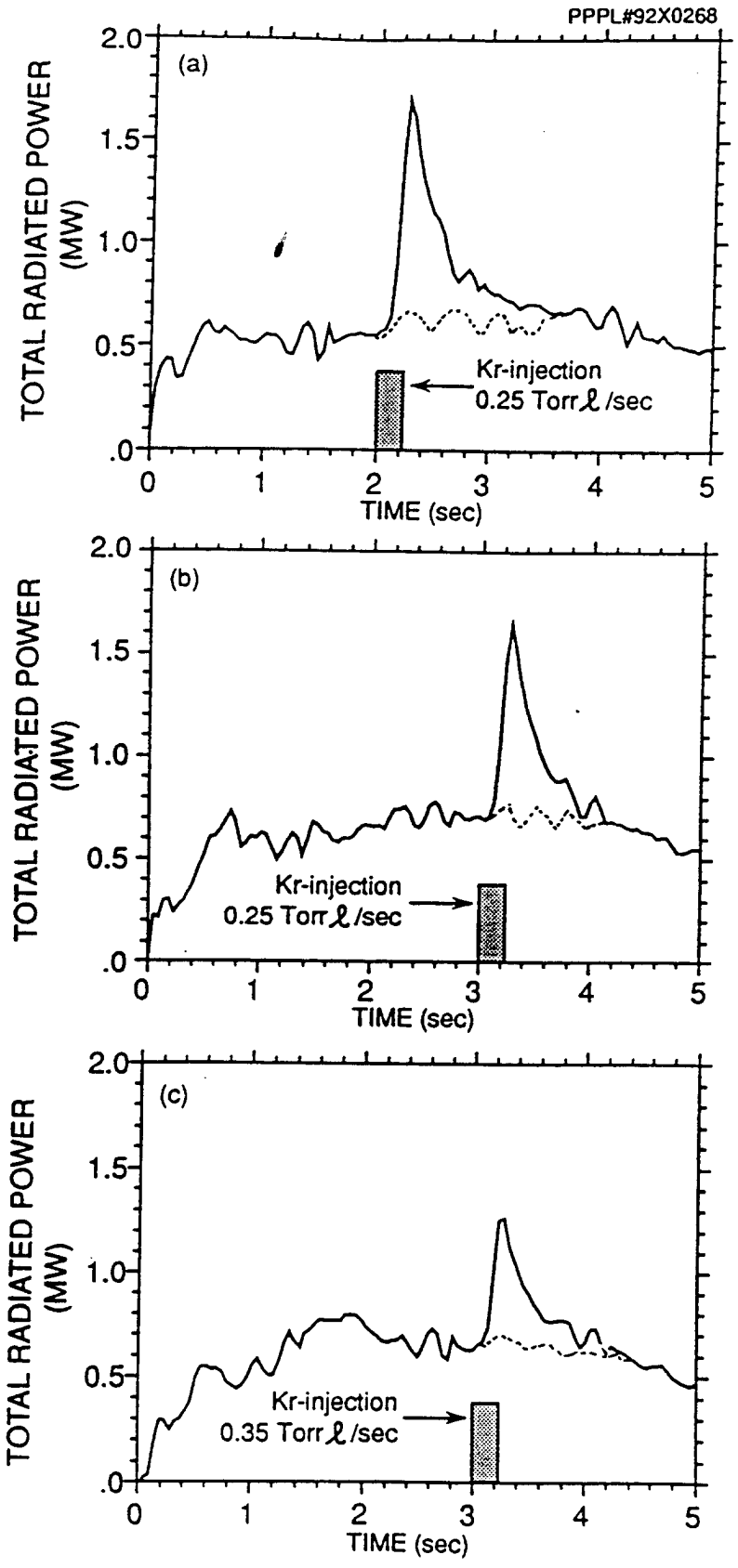
PPPL#92X0268
(a)
TOTAL RADIATED POWER (MW)
2.0
1.5
1.0
0.5
.0
Kr-injection
0.25 Torr ℓ /sec
0
1
2
3
4
5
TIME (sec)
(b)
TOTAL RADIATED POWER (MW)
Kr-injection
0.25 Torr ℓ /sec
TIME (sec)
(c)
TOTAL RADIATED POWER (MW)
Kr-injection
0.35 Torr ℓ /sec
TIME (sec)

Figure 3

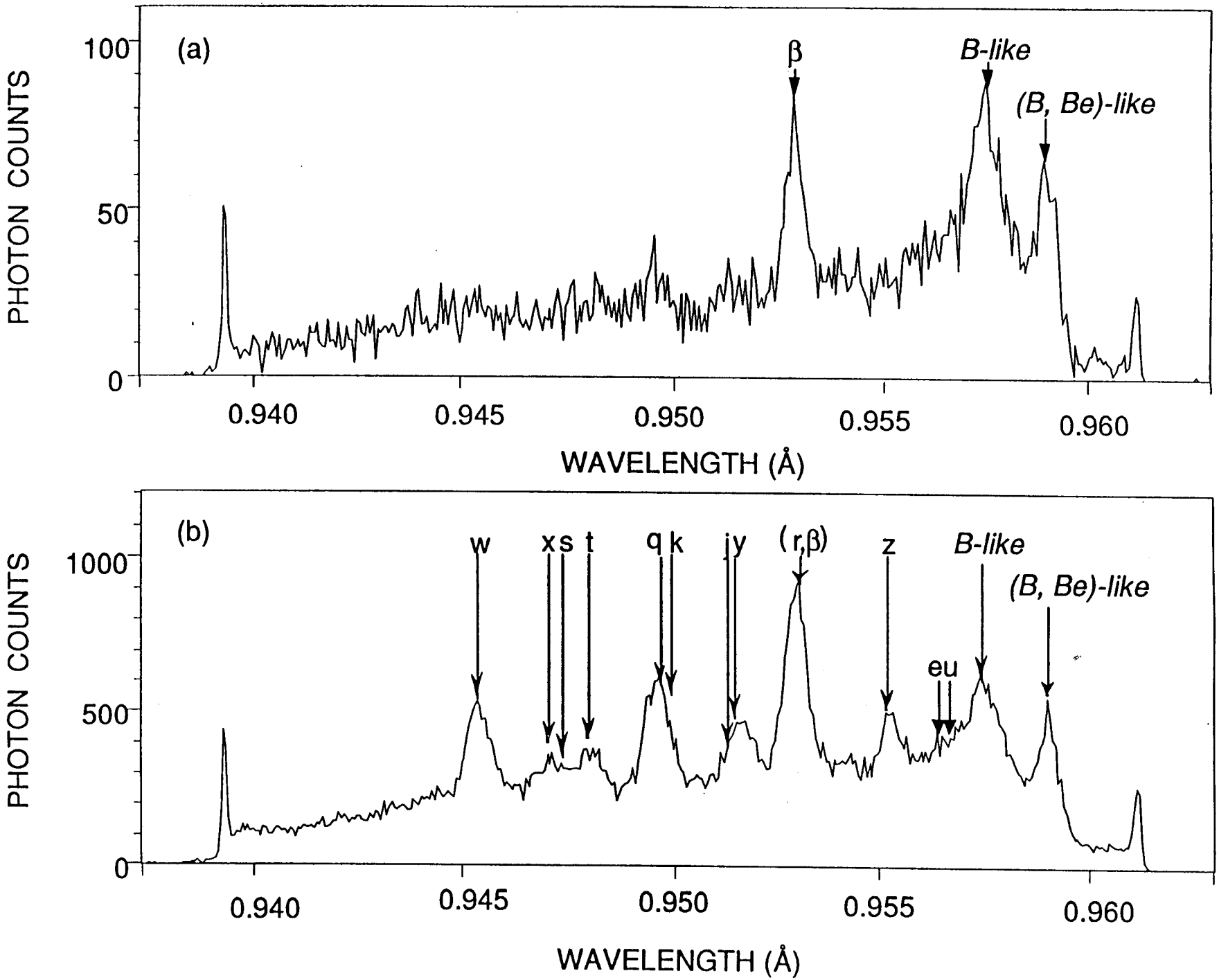
(a)
β
B-like
(B, Be)-like
PHOTON COUNTS
100
50
0
0.940
0.945
0.950
0.955
0.960
WAVELENGTH (Å)
(b)
w
x
s
t
q
k
j
y
(r,β)
z
eu
B-like
(B, Be)-like
PHOTON COUNTS
1000
500
0
0.940
0.945
0.950
0.955
0.960
WAVELENGTH (Å)

Figure 4

Progress in Multicenter Molecular Integrals Over Slater-Type Orbitals

Herbert W. Jones
Department of Physics
Florida A&M University
Tallahasee, FL 32307

Introduction

Quantum Mechanics was first applied to the hydrogen molecule in 1927 by Heitler and London [1]. They used a trial solution consisting of a linear combination of atomic orbitals (LCAO) of the hydrogen atom type which were solutions to the Schrodinger wave equation and applied the variational principle. This method evolved and was generalized to the use of combinations of Slater-type orbitals as basis sets and applications to more complicated molecules. At most we must deal with four-center and two-electron integrals. During the 1950's and 1960's, the University of Chicago under the leadership of Mulliken and Roothaan systematized the molecular orbital method and developed formulas [2] for molecular integrals over Slater-type orbitals (STOs). Difficulties with the formulas were encounted when they were programmed on computers with finite word lengths. More formidable difficulties developed when calculating integrals needed for three and four-atom molecules. These overwhelming difficulties gave STOs the reputation of being "intractable".

This "bottleneck" in molecular integrals was broken by Boys [3] with the introduction of Gaussian-type orbitals (GTOs), characterized by the functional form $\exp(-x^2)$ rather than $\exp(-x)$ as characterized by STOs. Mathematically, any function can be represented by a complete set of STOs or GTOs. But in the case of molecules, generally speaking, STOs are three times more efficient than GTOs because they represent the basic physical characteristics of electron clouds near nuclei and at large distances from nuclei. And in specialized situations, such as

NMR, Mossbauer effect, and collisions of particles, STOs are very much more efficient than GTOs.

In 1976 Sharma [4] showed that Lowdin α-functions could be represented by a finite number of terms of exponentials and powers. At Florida A&M University, Jones and Weatherford [5] used this knowledge to reformulate this development using computer algebra to generate a "C matrix" with integer elements for expressing the α-function. The basic ideal of expanding a displaced STO in spherical harmonics with functional coefficients originated with Coolidge [6], but was formalized and used extensively by Lowdin [7]. We were able to demonstrate the power of a computer algebra approach to molecular integrals in a series of papers that generated formulas for two-center overlap, Coulomb, hybrid, exchange, and three-center and four-center [8] integrals. The cancellation problem was solved by using computer algebra that could produce numbers of arbitrary precision. Our success and the support of Dr. William A. Lester, Jr., made it possible to organized the first international conference on molecular integrals in Tallahassee in August, 1981. The publication [9] of the proceedings gave a boost to the field.

Progress continues to be made on the multicenter molecular integral problem. (Our latest innovation is in the use of *Mathematica*). Computer programs continue to be developed for speed in Fortran. Much work remains to be done and the issue of a competitive program with GTOs remains in doubt. But the challenge has been taken up by groups in Germany [10], Spain [11], Russia [12], France [13], and of course, at FAMU.

Lowdin Alpha -Function

A review of the α-function method together with computer algebra generation of formulas has been given before [14]. In essence, a displaced STO in its coordinate system (R,Θ,ϕ) can be written as an infinite series of spherical harmonics with α-

NMR, Massbauer effect, and collisions of particles, STOs are very much more efficient than GTOs.

In 1976 Sharma [4] showed that Lowdin α-functions could be represented by a finite number of terms of exponentials and powers. At Florida A&M University, Jones and Weatherford [5] used this knowledge to reformulate this development using computer algebra to generate a "C matrix" with integer elements for expressing the α-function. The basic ideal of expanding a displaced STO in spherical harmonics with functional coefficients originated with Coolidge [6], but was formalized and used extensively by Lowdin [7]. We were able to demonstrate the power of a computer algebra approach to molecular integrals in a series of papers that generated formulas for two-center overlap, Coulomb, hybrid, exchange, and three-center and four-center [8] integrals. The cancellation problem was solved by using computer algebra that could produce numbers of arbitrary precision. Our success and the support of Dr. William A. Lester, Jr., made it possible to organized the first international conference on molecular integrals in Tallahassee in August, 1981. The publication [9] of the proceedings gave a boost to the field.

Progress continues to be made on the multicenter molecular integral problem. (Our latest innovation is in the use of *Mathematica*). Computer programs continue to be developed for speed in Fortran. Much work remains to be done and the issue of a competitive program with GTOs remains in doubt. But the challenge has been taken up by groups in Germany [10], Spain [11], Russia [12], France [13], and of course, at FAMU.

Lowdin Alpha -Function

A review of the α-function method together with computer algebra generation of formulas has been given before [14]. In essence, a displaced STO in its coordinate system (R,Θ, ϕ) can be written as an infinite series of spherical harmonics with α-

function coefficients when viewed from a distance a in the coordinate system (r, θ, ϕ) displaced in the z - direction:

$$\chi = A\, R^{N-1}\, e^{-\zeta R}\, Y_L^M(\Theta,\phi)$$

$$\chi = \frac{A}{\zeta^{N-1}}\left[\frac{(2L+1)(L+M)!}{4\pi(L-M)!}\right]^{1/2} \sum_{\ell-M}^{\infty}\left[\frac{4\pi(\ell+M)!}{(2\ell+1)(\ell-M)!}\right]^{1/2}(-1)^M$$

$$\times\quad \alpha_\ell^{NLM}(\zeta a,\zeta r)Y_\ell^M(\theta,\phi)$$

where

$$\alpha_\ell^{NLM}(\zeta a,\zeta r) = \frac{(2\ell+1)(\ell-M)!}{2(\ell+M)!}\sum_{i=0}^{N+L+\ell}\sum_{j=0}^{N+\ell} C_\ell^{NLM}(i,j)$$

$$\times\qquad H_{ij}(\zeta a)^{i-L-\ell-1}(\zeta r)^{j-\ell-1}$$

and

$$H_{ij} = \begin{cases} e^{-\zeta a}\left[(-1)^j\, e^{\zeta r}\cdot e^{-\zeta r}\right], & r < a \\ e^{-\zeta r}\left[(-1)^i\, e^{\zeta a} - e^{-\zeta a}\right], & r > a \end{cases}$$

A $(2\zeta)^{N+1/2}\,[(2N)!]^{-1/2}$ is normalization factor; N, L, and M are the quantum numbers of the orbital, and ζ is the screening constant or orbital exponent.

It leads to greater efficiency to first simplify the α-function by summing over the constant values to obtain T and X one-dimensional matrices:

$$T_\ell(j) = \frac{(2\ell+1)(\ell-M)!}{2(\ell+M)}\, e^{-\zeta a}\;\zeta^{j-\ell-1}\sum_{i=0}^{N+L+\ell} C_\ell^{NLM}(i,j)(\zeta a)^{i-L-\ell-1},\ r < a$$

$$X_\ell(j) = \frac{(2\ell+1)(\ell-M)!}{2(\ell+M)!}\,\zeta^{j-\ell-1}\sum_{i=0}^{NLM} C_\ell^{NLM}(i,j)\left[(-1)^i e^{\zeta a} - e^{-\zeta a}\right](\zeta a)^{i-L-\ell-1},\ r > a.$$

Hence,

$$\alpha_\ell^{NLM}(r)=\begin{cases}\sum_{j=0}^{N+\ell} T_\ell(j)\left[(-1)^j e^{\zeta r} - e^{-\zeta r}\right] r^{j-\ell-1}, & r < a \\ e^{-\zeta r}\sum_{j=0}^{N+\ell} X_\ell(j)\, r^{j-\ell-1}, & r > a\end{cases}$$

Overlap Integral

As an example of our methods, the overlap integral will be worked out. The simplest non-trivial example is the two-center overlap integral, i.e., the integral of the product of two orbitals located at (0,0,0) and (0,0,a). Thus

$$S = \int \chi_a \chi_b dv$$

If we take 1s orbitals (N=1, L=0, M=0,$\zeta_a=\zeta_b=\zeta$) the C matrix is

$$C_0^{100} = \begin{pmatrix} 1 & 1 \\ 1 & 0 \end{pmatrix}$$

$$\chi_a = A\, r^{N-1} e^{-\zeta r} Y_L^M(\theta,\phi) = A\, e^{-\zeta r} Y_0^0(\theta,\phi).$$

$$\chi_b = A\, R^{N-1} e^{-\zeta R} Y_L^M(\Theta,\phi) = \sum_{\ell=0}^{\infty} \alpha_\ell\, Y_\ell^0(\theta,\phi).$$

$$S = A^2 \sum_{\ell=0}^{\infty} \int r^2\, dr \quad e^{-\zeta r}\, \alpha_\ell \quad \int d\theta\, \sin\theta\, d\phi\; Y_0^0(\theta,\phi)\, Y_\ell^0(\theta,\phi).$$

The orthogonal conditions for spherical harmonics are

$$\int d\theta\, \sin\theta\, d\phi\; Y_L^M(\theta,\phi)\, Y_{\ell'}^{M'}(\theta,\phi) = \delta_{\ell\ell'}\, \delta_{MM'}$$

Hence, only one term (ℓ=o) survives in the infinite summation.

$$S = A^2 \int r^2\, dr\, e^{-\zeta r}\, \alpha_o, \qquad \text{with } A = 2.$$

$$\alpha_{\circ} = \frac{1}{2} \sum_{l=0}^{1} \sum_{j=0}^{1} C_0^{100}(i,j)\, e^{-\zeta a}\left[(-1)^j\, e^{\zeta r} - e^{-\zeta r}\right](\zeta a)^{i-1}(\zeta r)^{j-1},\ r < a$$

$$\alpha_{\circ} = \frac{1}{2} \sum_{l=0}^{1} \sum_{j=0}^{1} C_0^{100}(i,j)\, e^{-\zeta r}\left[(-1)^j\, e^{\zeta a} - e^{-\zeta a}\right](\zeta a)^{i-1}(\zeta r)^{j-1},\ r > a.$$

By use of computer algebra one may arrive at the well known formula

$$S = e^{-\zeta a}\left[1 + \zeta a + (\zeta a)^2/3\right].$$

On the other hand, the integral may be done by numerical integration. This approach is under current investigation.

One disturbing aspect of the C matrix is the explosive growth of the values of the C matrix elements with high quantum numbers. But this is just a reflection of the ever present danger of cancellation errors, i.e., the subraction of nearly identical numbers with a resulting loss of significant figures. We have succeeded in writing a computer algebra program to expand the a-function for small r values in terms of an E and F matrix [15], which avoids large numbers. A definitive and simple program for C,E, and F matrices together with an overlap program has been written in terms of *Mathematica* [16]. This program has been used to find numerous errors in Tai's recent article on overlap integrals [17]. Although *Mathematica* always gives correct answers, it is far too slow to compete against FORTRAN in a production mode.

Current Research

FAMU has gained recognition as one of the main world centers for the study of STO molecular integrals. The first center that produces a complete computer package for evaluating STO integrals will be in a position to do work of unprecedented accuracy over the entire range of molecular phenomena. Some groups are working with transforms into momentum space, but we continue to make progress in coordinate space. Jones and Etemadi [18] have just obtained the most accuracy calculations to date for the ground state of H_2^+ using LCAO methods with orbitals up to principal quantum number 6 and angular momentum number 5.

For our LCAO we used a very systematic sequence of orbitals:

$$\psi = \sum_{N=1}^{6} \sum_{L=0}^{N-1} C_{NL} A_N r^{N-1} e^{-\zeta a} Y_L^0(\theta,\phi)$$

Note that only one screening constant was used. Surpisingly, only one screening constant was needed for HeH^{2+}. Our program was written in FORTRAN and run on a CRAY-YMP. However, it was checked using *Mathematica*. The strategy of using *Mathematica* to check FORTRAN is the key to our current research,. In order to insure accuracy, we are installing an interface program so that a program running in FORTRAN may occassional obtain crucial evaluations in *Mathematica*. This is what we must be prepared to do in order to break through, if we meet a road block.

Two of our students, Andrew Jackson and Jay Jackson, are assisting in implementing a semianalytic approach [20] to molecular integrals. All - analytic methods can be slow and may require arbitrary precision. For the important two-electron integrals, we plan to evaluate α-functions along a grid and do the second integral for energy by using Gauss-Legendre and Gauss-Laguerre quadratures.

Our numerical integrals should be trouble-free, since the α-functions and potential do not have singularities. (It is singularities and function pathologies that plague investigators using transform methods).

Our mood remains optimistic; we believe that the strategies developed here for dealing with problems that "do not compute" will be generally useful.

Acknowledgments

Support for this work was provided by the Air Force Office of Scientific Research under Contract No. F49620-92-J-0063, and NASA (CeNNAs). The authors thank the Florida State University Supercomputer Computations Research Institute for computer time.

REFERENCES

[1] W. Heitler and F. London, Z. Physik **44**, 455 (1927).

[2] R. Mulliken, C. Rieke, D. Orloff, and H. Orloff, J. Chem. Phys. **17**, 1278 (1949); C.C. J. Roothaan, J. Chem. Phys. **19**, 1450 (1951)

[3] S.F. Boys, Proc. R. Soc. London **200**, 542 (1950).

[4] R.R. Sharma, Phys. Rev. A **13**, 517 (1976).

[5] H.W. Jones and C.A. Weatherford, Int. J. Quantum Chem. Symp **12**, 483 (1978).

[6] A.S. Coolidge, Phys. Rev. **42**, 189 (1932).

[7] P.O. Lowdin, Adv. Phys. **5**, 1 (1956).

[8] H.W. Jones, Int. J. Quantum Chem. **18**, 709 (1980); **19**, 567 (1981); **20**, 1217 (1981); **515**, 287 (1981); **21**, 1079 (1982); **23**, 453 (1983); **18**, 61 (1984); **519**, 157 (1986); **29**, 177 (1986); Phys. Rev. A **33**, 2081 (1986).

[9] International Conference on ETO Multicenter Molecular Integrals, Tallahassee, 1981, edited by C.A. Weatherford and H.W. Jones (Reidel, Dordrecht, 1982).

[10] J. Grotendorst and E.O. Steinborn, Phys. Rev. A **38**, 3857 (1988).

[11] J.F. Rico, R. Lopez, and G. Ramirez, J. Chem. Phys. **91**, 4202 (1989).

[12] I.I. Guseinov, Phys. Rev. A **31**, 2851 (1985).

[13] A. Bouferguene, M. Fares, and D. Rinaldi (Private communication).

[14] H.W. Jones and C.A. Weatherford, J. Mol. Struct. (Theochem) **199**, 233 (1989).

[15] H.W. Jones, B. Bussery, and C.A. Weatherford, Int. J. Quantum Chem. Symp. **21**, 693 (1988).

[16] H.W. Jones, Int. J. Quantum Chem. **41**, 749 (1992).

[17] H. Tai, Phys. Rev. A **45**, 1464 (1992).

[18] H.W. Jones and B. Etemadi, Phys. Rev. A **47**, 3430 (1993).

[19] B. Etemadi and H.W. Jones, Int. J. Quantum Chem. Symp. (Submitted).

[20] H.W. Jones, Int. J. Quantum Chem **42**, 779 (1992).

Results from the Galileo Laser Uplink; A JPL demonstration of Deep-space Optical communications

K. E. Wilson, J. R. Lesh

Jet Propulsion Laboratory, California Institute of Technology
Pasadena, California 91109

ABSTRACT

The successful completion of the Galileo Optical Experiment (GOPEX), represented the accomplishment of a significant milestone in JPL's optical communication plan. The experiment demonstrated the first transmission of a narrow laser beams to a deep-space vehicle. Laser pulses were beamed to the Galileo spacecraft by Earth-based transmitters at the Table Mountain Facility (TMF), California, and Starfire Optical Range (SOR), New Mexico. The experiment took place over an eight-day period (December 9 through December 16, 1992) as Galileo receded from Earth on its way to Jupiter, and covered ranges from 1 - 6 million km. At 6 million km (15 times the Earth-Moon distance), the laser uplink from TMF covered the longest known range for laser beam transmission and detection. This demonstration is the latest in a series of accomplishments by JPL in the development of deep-space optical communications technology.

I. INTRODUCTION

JPL's Deep Space Network is singular in its ability to track and communicate with deep-space probes. As we continue to explore and better understand our solar system, there will be demands to return increasing volumes of data from deep-space probes to Earth. Existing 70 meter DSN systems will be unable to support this increased demand, and communication systems at optical and microwave (32 GHz, Ka band) frequencies are considered the most viable emerging technologies for the missions of the twenty-first century. With NASA's directive of faster, better and cheaper, the mini and micro spacecraft are expected to play an ever increasing role in the future. Weight and size are the primary driving considerations for subsystems on mini and micro spacecraft and small light weight optical telescopes coupled to miniature laser transmitters are being favorably considered as an attractive alternative to the large microwave antennae.

Although there has been significant progress in the component technologies for deep-space optical communications, it was becoming apparent that a systems-level demonstration to show the viability of optical communications was needed. The Galileo spacecraft's second flyby of Earth, part of the Venus-Earth-Earth Gravity Assist (VEEGA) trajectory [1], afforded a unique opportunity to perform a deep-space optical uplink with the spacecraft as it receded from Earth on its way to Jupiter. The Galileo Optical Experiment (GOPEX) was conducted over the period December 9 through December 16 from transmitter sites at Table Mountain Facility (TMF), California, see figure 1, and at the Starfire Optical Range (SOR), New Mexico; see figure 2. The spacecraft's Solid State Imaging (SSI) camera was used as the optical communications uplink receiver. The experiment had three principal objectives, namely:

- Demonstrate laser beam transmission to a spacecraft at deep-space distances

- Verify laser-beam pointing strategies applicable to an optical uplink based solely on spacecraft ephemeris predicts

- Validate the models developed to predict the performance of the optical link

Galileo's phase angle after its second Earth flyby was approximately 90°. Thus as the spacecraft receded from Earth, it looked back at a half-illuminated Earth image. This geometry allowed laser beam transmission against a dark-Earth background, and the experiment was conducted between 3:00 a.m. and 6:00 a.m. Pacific Standard Time. The nighttime transmission had two distinct advantages:

- It allowed the uplink to be performed at the frequency-doubled Nd:YAG laser wavelength of 532 nm, where the responsivity of the solid-state imaging (SSI) camera is high.

- Long-exposure camera frames could be taken. This facilitated the identification of the detected laser transmissions. Analysis of the stray-light intensity in the focal plane of the camera showed that the camera shutter could remain open for up to 800 milliseconds before the scattered light from the bright Earth saturated the pixels that detected the laser uplink.

The camera was scanned across the Earth, parallel to the Earth's terminator, during each exposure to facilitate the identification of the laser uplink from spurious noise counts in the camera frame. Using this strategy, the laser uplink appeared as a series of evenly spaced bright dots within the camera frame, and was quite distinct from other features in the frame. Laser uplink data were received on each of the seven days of the experiment with detections on 50 of the 159 GOPEX frames taken. The demonstration covered a period of eight days, but other spacecraft activities precluded laser transmission on Day 5. Because of an unanticipated bias in the scan platform pointing , pulses were detected on only two of the frames with exposure times less than 400 milliseconds. Inclement weather, aborted transmissions, and restrictions imposed by regulatory agencies and by the Project Galileo team accounted for the loss of data on the remaining frames.

The two GOPEX laser/telescope transmitters and SSI camera receiver are discussed in Section II and III of this paper. Section IV describes the telescope pointing strategy which used bright stars in the vicinity of Galileo as references, and the GOPEX results are presented in Section V. Conclusions are discussed in Section VI.

II. GOPEX Laser Transmitters

The laser transmitters at both sites consisted of a frequency-doubled Nd:YAG laser operating at 532 nm coupled to an optical telescope through a coudé mount arrangement. The transmitter characteristics are given in Table 1.

A 0.6-meter equatorial-mount astronomical telescope was used for the TMF transmitter. This is the same telescope that was used in 1968 to perform the laser transmission to the Surveyor 7 spacecraft on the Moon. The telescope is f/36 at the coudé focus, and the appropriate beam-forming lens set was inserted into the optical train, figure 3, to achieve the required laser beam divergence. See Table 1. The optical train was designed so that the transmitted laser beam illuminated a 15 cm sub-aperture of the primary mirror. The principal benefit of this technique over full aperture illumination was that it eliminated the large loss in transmitted energy that would have been caused by occultation from the 0.2-meter secondary.

Table 1. GOPEX laser transmitter characteristics.

Characteristic	Table Mountain Facility	Starfire Optical Range
Wavelength, nm	532	532
Pulse energy, mJ	250	350
Repetition rate, Hz	15–30	10
Pulse width, ns	12	15
Beam divergence, μrad		
Days 1–4	110	80
Days 6–8	60	40
Telescope mirror diameter		
Primary, m	0.6	1.5
Secondary, m	0.2	0.1
Optical train transmission	60%	43%

The two beam-forming lens sets, one for the 110-microradian divergence and a second for the 60-microradian divergence, were designed so that the laser beam was brought to a focus at a distance of 1.3 kilometers when the telescope was focused at infinity. Light from the reference stars used to point the telescope to Galileo was collected across the instrument's full 0.6-meter aperture.

SOR's telescope was the 1.5-meter system that is used for adaptive-optics experiments at this facility. A thin-film-plate polarizer served as the aperture-sharing element, and it coupled the laser output to the telescope optical train while allowing reference stars to be observed by the charge-coupled device (CCD) camera positioned in the orthogonal leg of the optical train. The required laser beam divergence was achieved by focusing the outgoing laser beam at ranges of 40 kilometers and 20 kilometers, corresponding to 40-microradian and 80-microradian beam divergence, respectively.

The SOR laser output was transmitted through the full 1.5-meter aperture of the telescope, and the effects of occultation by the 10-centimeter secondary were mitigated by reconfiguring the laser resonator so that it generated a flat-top intensity profile across the beam. This design resulted in less than 10% loss in energy of the outgoing beam due to occultation by the secondary.

III. GOPEX Receiver

The Galileo SSI camera was used to detect the GOPEX uplink. The camera is mounted on the spacecraft scan platform located on the despun section of the spacecraft. It consists of a CCD array of 800 X 800 silicon pixels located at the focal plane of a 1500 mm focal length f/8.5 Cassegrain telescope [2]. The angular resolution per pixel was 10.6 μrad with a full well capacity of 100,000 electrons. The dark current was less than 10 electrons per pixel with readout noise of 8 electrons. Four SSI gain states scale the video analog data to the 8 bit analog-to-digital converter. Over the eight-day experiment window two gain states were used for GOPEX; gain state 2 which has 400 detected photoelectrons per data number (dn) was used on the first two

days, and the more sensitive gain state 3 with 160 detected photoelectrons per dn was used on subsequent days.

Field correction elements, an eight position filter wheel, and a two blade shutter are positioned along the optical train between the telescope primary and the focal plane of the SSI camera. The latter two elements were inherited from the Voyager program. The filter wheel contained one clear filter, one infrared transmitting filter and six 20 nm bandpass color-filters. These were rotated into the optical train, as required, to enable the color reconstruction of an imaged scene. The green color-filter with 50 % transmission at 532 nm (the peak transmission was 90% at 560 nm) was used for GOPEX.

The SSI shutter is operable in any one of 28 exposure times ranging from 4.16 milliseconds to 51.2 seconds. Exposure time selection was based on the estimate of the best balance between the conflicting requirements of short duration to reduce stray light effects, and long duration to ensure that enough pulses were detected to confirm the laser uplink. Improved estimates of the scattered light intensity were made using data taken at the Gaspra encounter. Final estimates of the scattered light rates due to Earth-shine ranged from a high of 110 e^-/msec on the end of the first day for the SOR location to 32 e^-/msec on day 8 for both sites. On the basis of these estimates, the GOPEX imaging sequence was designed with shutter times ranging from 133 msec to 800 msec. Actual scattered light rates measured during GOPEX ranged from 8 to 10 e^-/msec. The low actual scatter levels would have allowed longer camera exposure times and the accumulation of more data.

IV. GOPEX telescope-pointing strategy

Telescope-pointing files for TMF and SOR were generated from updates of the spacecraft ephemeris files that were provided to the GOPEX team on December 8 and December 11. The strategy was to off-point the telescope from reference stars located within 0.5° of the spacecraft position. Over the eight-day period, six guide stars of magnitudes 6 to 10 were used to point the TMF telescope at Galileo.

Transmission to Galileo was accomplished by using a "point and shoot" approach. Here, the telescope was set to track the reference star in the intervals between the three-second bursts of laser transmissions. Two and one-half minutes before laser transmission, the reference star was positioned in the center of the field of view of the focal plane aperture at coudé and the telescope was calibrated. Ten seconds prior to transmission, the telescope was pointed to Galileo's predicted location and set to track the spacecraft for the next thirteen seconds. This procedure was repeated during the three-minute to six-minute intervals between the laser transmissions. Because the telescope calibration was performed just before transmission, the pointing errors introduced by mount sag were reduced significantly. In addition, the high elevation of the spacecraft during the uplink—the experiment was conducted when the spacecraft's elevation from TMF was greater than 30° —and the proximity of the reference stars to Galileo's position obviated the need to implement atmospheric refraction compensation techniques while pointing to the spacecraft.

The beam width of the rf beam to Galileo was approximately forty times that of the laser beam, 2 millirad versus 60 microrad. To verify the accuracy of the pointing predicts SOR dithered the laser beam in a 85 microrad radius circle about the spacecraft's predicted position while the TMF transmitter pointed directly to Galileo's predicted position. This strategy was implemented for several of the long-duration frames (frames with exposure times greater than 400 milliseconds) on the first day. The results from one of the dithered uplinks are shown in Figure 4. Nine pulses can be clearly discerned in the figure; seven are from the 15-hertz TMF transmitter, and two are from the 10-hertz SOR transmitter. Without beam scanning, a total of four pulses would have been detected from the SOR transmitter. The presence of only two

pulses from SOR and of seven from TMF clearly demonstrates that the error in the telescope pointing predicts was significantly less than 85 microradians. This was further confirmed by the successful use of a 60-microradian beam from TMF for laser transmissions on the last three days of GOPEX.

V. GOPEX RESULTS

Table 2 gives a summary of the detected GOPEX laser transmissions over the duration of the experiment.

Table 2. Summary of detected laser signals.

Day	Shutter speed (ms)	Frames received	Frames with detections
1	133	9 of 10	0
	200	24 of 25	0
	400	19 of 20	6
	800	5 of 5	4
2	200	5 of 5	0
	267	15 of 15	0
	533	15 of 15	11
	800	5 of 5	5
3	200	5 of 5	0
	267	10 of 10	0
	533	5 of 5	5
4	200	3 of 3	1[b]
	267	4 of 4	0
	533	3 of 3	2[b]
5		No activity planned	
6[a]	133	3 of 3	0
	267	6 of 6	0
	533	3 of 3	3
7[a]	200	3 of 3	1
	400	3 of 4	3
	800	3 of 3	3
8[a]	267	2 of 2	0
	533	4 of 4	4
	800	2 of 2	2

a Adverse weather at Starfire Optical Range precluded laser transmission on this day.

b Adverse weather at Table Mountain Observatory precluded laser transmission on this day, and it was cloudy at Starfire Optical Range.

Over the eight-day period, transmissions to the spacecraft were made over a range beginning at 600,000 kilometers on the morning of December 9 and ending at 6,000,000 kilometers on the morning of December 16. Signals were successfully detected on each of the experiment days, although not on all frames within a given day. Unfavorable weather (which caused outages), regulatory agency restrictions on transmissions, temporary signal-to-noise anomalies on the downlink, and an unexpected camera-pointing bias error resulted in the lack of detection on several frames. Final results show that the laser uplink was successfully detected on 50 camera images during the experiment window. Figures 4 and 5 show two representative images of the detected laser pulses.

Adverse weather at the sites and not telescope pointing was the most severe impediment to successful detection of the laser transmissions. Winter storms at TMF and SOR brought snow, heavy clouds, and ground fog to these facilities. Transmission from TMF was most affected on the first and fourth days of the experiment. The last seven frames obtained on the first day were taken with TMF completely overcast and SOR in daylight. On the fourth day, falling snow at TMF precluded transmission from this facility; also on that day, during only one of the ten transmissions was there clear sky between the SOR transmitter and the spacecraft. Falling snow and heavy cloud cover prevented transmission from SOR on the last three days.

Restrictions from regulatory agencies also caused data outages. Transmission of the GOPEX laser beam into space required the concurrence of the US. Space Defense Operations Center (SPADOC). On the first day, SPADOC restrictions prevented TMF from transmitting during four frames. An additional frame was lost because the ground receiving station (at Goldstone, California) momentarily lost lock on the Galileo spacecraft downlink signal. Owing to the loss of downlink signal, the orientation of the spacecraft could not be confirmed, and since one of the GOPEX concurrence conditions was that laser uplink would proceed only if the spacecraft orientation was known, no laser transmissions were sent during this data outage.

During the first two days of GOPEX, the spacecraft orientation resulted in the low-gain antenna being pointed away from Earth. This resulted in a low signal-to-noise ratio (SNR) of the spacecraft downlink and was evidenced by the numerous burst errors in the data files. The GOPEX images for these days showed numerous streaks across the frames and made it difficult to discern successful laser transmissions on the images. On the second day, just after the GOPEX uplink, a planned spacecraft maneuver that increased the SNR of the radio frequency downlink was executed. This resulted in clearer GOPEX images for the remainder of the demonstration.

The GOPEX demonstration required that the SSI camera be operated in a mode for which it was not designed (that is, slewing the camera during imaging). To get the GOPEX transmitter sites in the field of view during the slew, the camera was initially pointed to a position above or below the targeted direction and the shutter was opened at a prescribed time after the start of the slew. Uncertainties in the stray-light intensity in the focal plane of the SSI camera dictated the shutter times used for GOPEX. The times chosen ranged from 133 milliseconds to 800 milliseconds, and these were loaded into the spacecraft sequence of events prior to GOPEX. As the experiment progressed, it was observed that laser transmissions were consistently detected only on frames with greater than 400-millisecond exposure times; laser pulses were detected in one 200 msec exposure frame taken on day 4 and again on day 7. The consistent absence of detections on the shorter duration frames was traced to a pointing error caused by the scan platform acceleration being slower than predicted. As a result, no clear evidence of laser transmission was observed on 88 of the 90 frames taken with exposure times less than 400 milliseconds.

After determining the reasons for the missing pulse detections on selected frames, the remaining frames were analyzed to calculate the detected pulse energy statistics and to compare those statistics with theoretical predictions. Figure 6 shows a typical comparison. The histogram of the detected pulse energies was constructed from a total of 51 pulses received on this day, and it is plotted along with the theoretical distribution using atmospheric turbulence data and the appropriate turbulence model. The error bars in the histogram heights are large because of the small data set. They show the expected range of the relative frequency of detections for the GOPEX demonstration performed again under the similar atmospheric conditions. The poor fit near the lower laser energies is due to the difficulty in estimating low detected laser energies. The log-normal intensity distribution, based on statistics of the measured data, is also shown. The data show good agreement between the measured and theoretically predicted distributions.

VI. CONCLUSION

GOPEX represents the achievement of a significant milestone in deep-space optical communications. The laser transmission was performed from transmitters located at TMF, California, and SOR, New Mexico. The laser uplink was detected on every day of the experiment—out to a range of 6,000,000 kilometers for the TMF transmission. The camera images returned from Galileo and the analysis of the data show that all the experiment objectives were achieved.

VII. ACKNOWLEDGMENTS

The authors would like to recognize the invaluable contributions of other members of the GOPEX team. These were at TMF, Dr. T. Yan, test director, Dr. W. Owen, Mr. K. Masters, Dr. J. Yu, Dr. M. Shao, Mr. J. Young, Mr. R. Dotson, Mr. G. Okamoto, and Mr. W. Hornaday, and at SOR Dr. R. Fugate, site test director, Dr. H. Hemmati, Mr. R. Cleis, Dr. J. Spinhirne, and Mr. B. Boeke.

The work described in this paper was carried out by the Jet Propulsion Laboratory, California Institute of Technology, under a contract with the National Aeronautics and Space Administration.

VIII. REFERENCES

1. K. E. Wilson, J. Schwartz, and J. R. Lesh, "GOPEX: A deep space optical communications experiment with the Galileo spacecraft," *SPIE Proceedings,* Vol. 1417, pp. 22–26, January 1991.

2. K. P. Klaasen, M. C. Clary. J. R. Janesick, "Charge -coupled Device Television Camera for NASA's Galileo Mission to Jupiter", Optical Engineering Vol. 23 No. 3 pp. 334-342 May/June 1984.

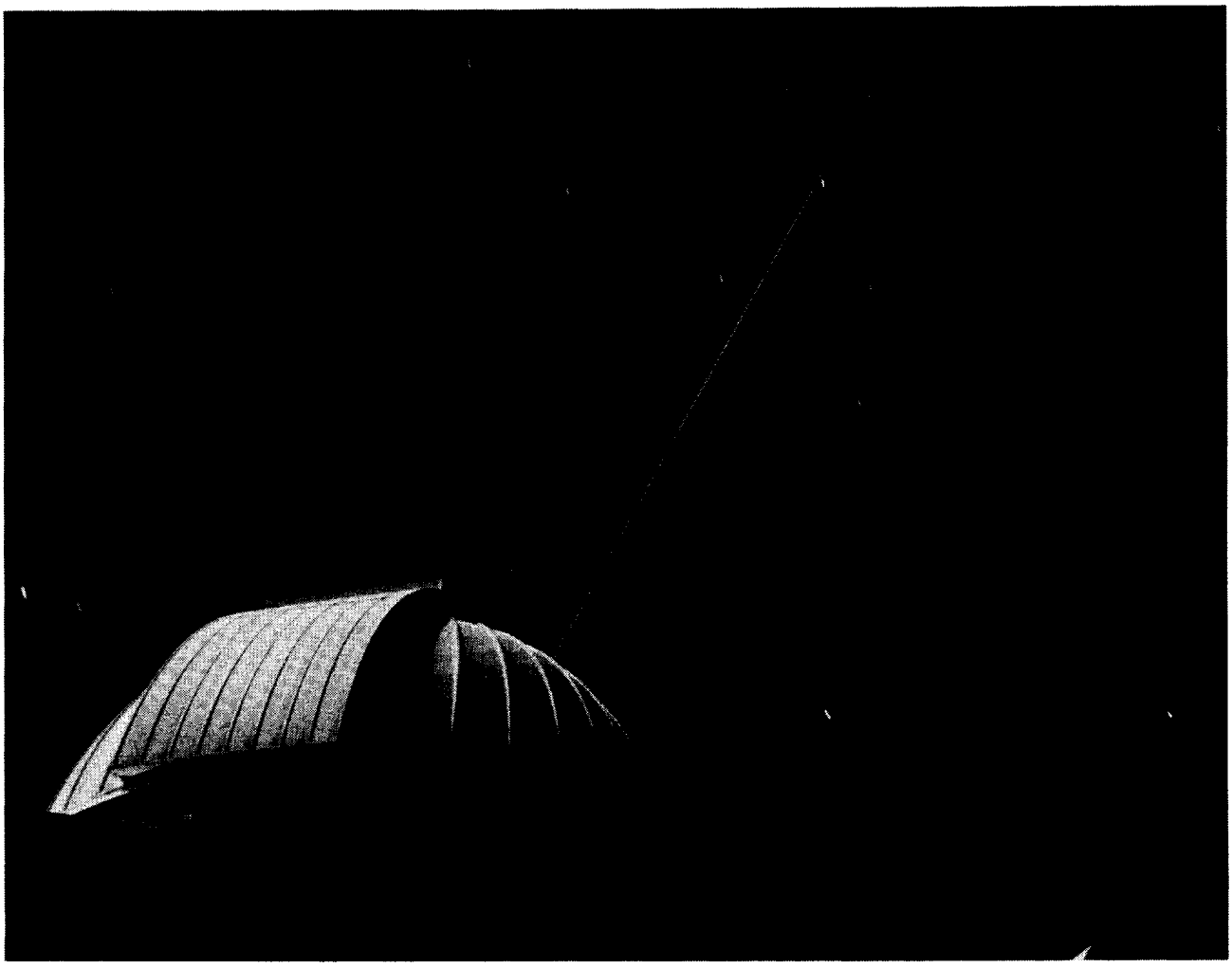

Figure 1. Laser transmission from 0.6-meter telescope at TMF, Wrightwood, CA.

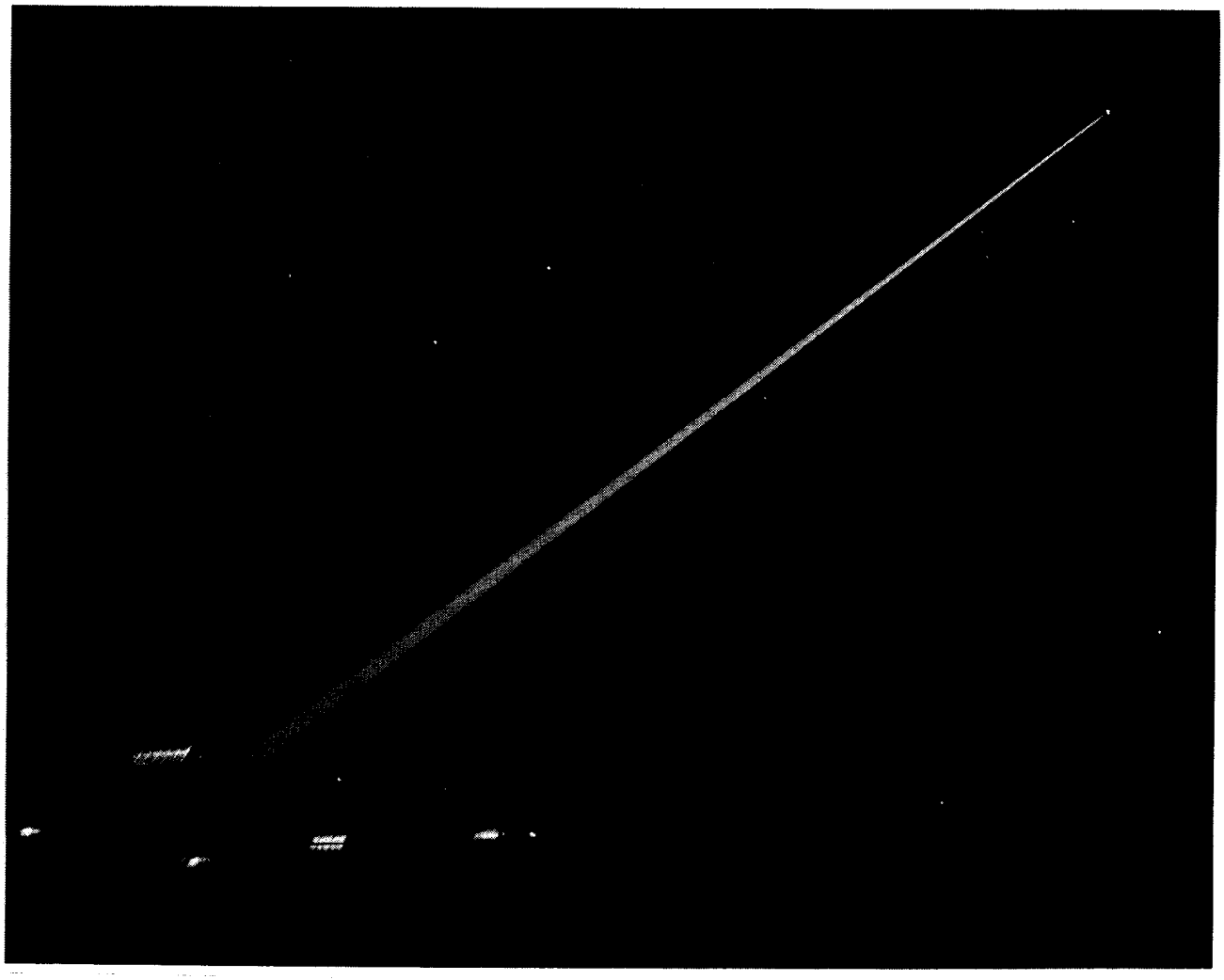

Figure 2. Laser Transmission from 1.5-meter telescope at SOR, Albuquerque, NM.

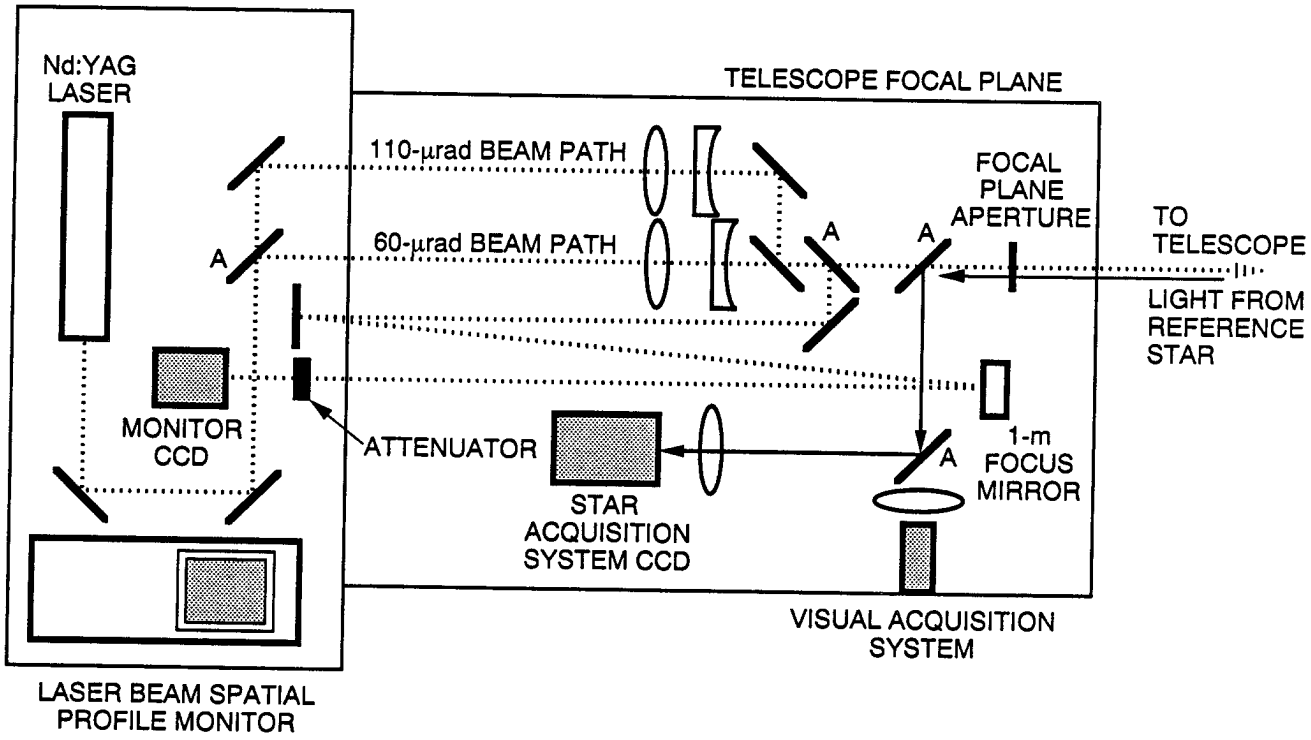

Figure 3. GOPEX optical train, at TMF. Relay mirrors (labeled "A" in the figure) are appropriately inserted into the optical train to obtain the required beam divergence.

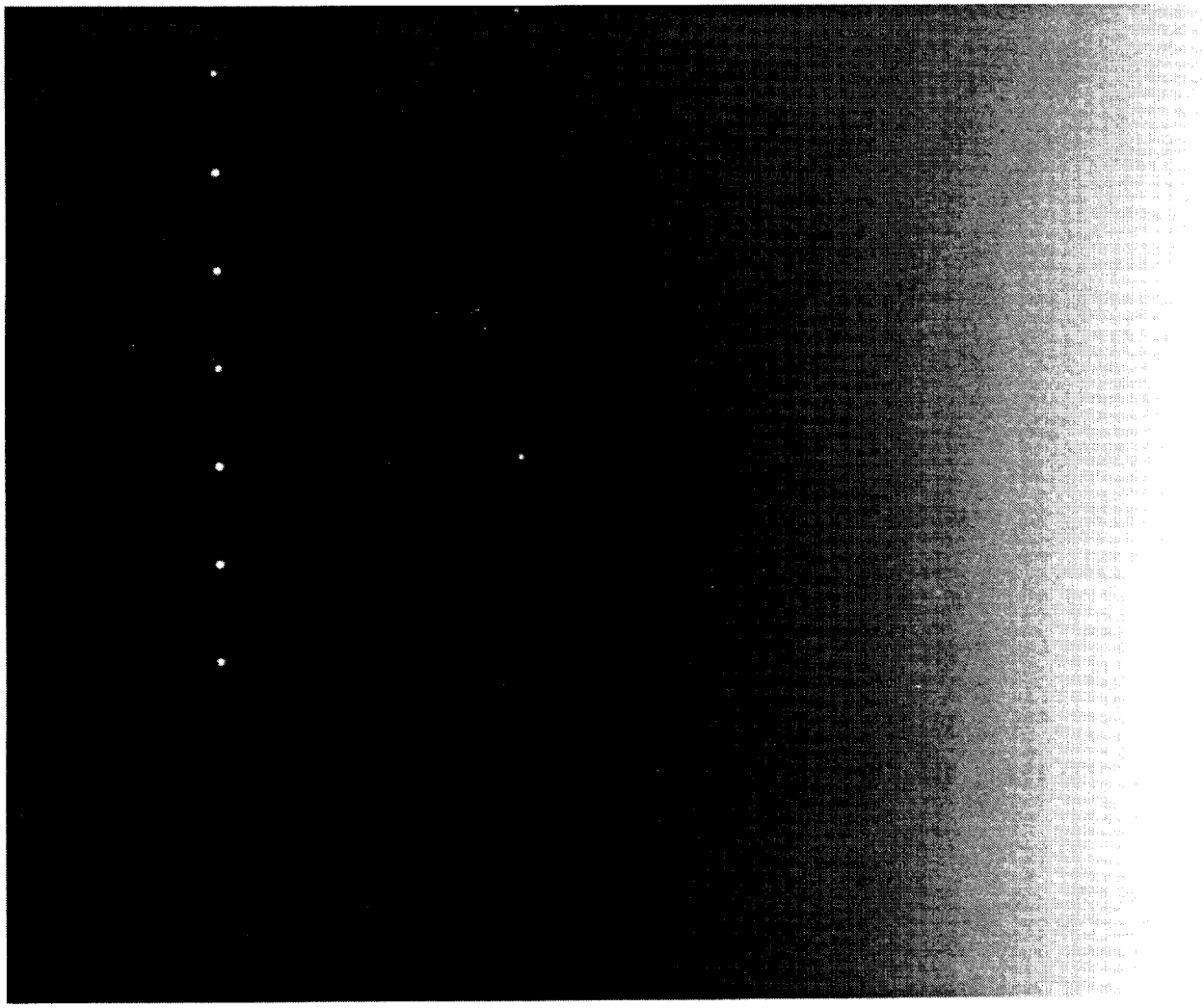

Figure 4. Camera image showing detected pulses from TMF and SOR. To the right of the figure is the blurred image of the portion of the Earth illuminated by sunlight. Detections of the TMF laser pulses are shown on the left and of SOR pulses closer to the right. The missing pulses are due to the spatial scanning of the SOR beam.

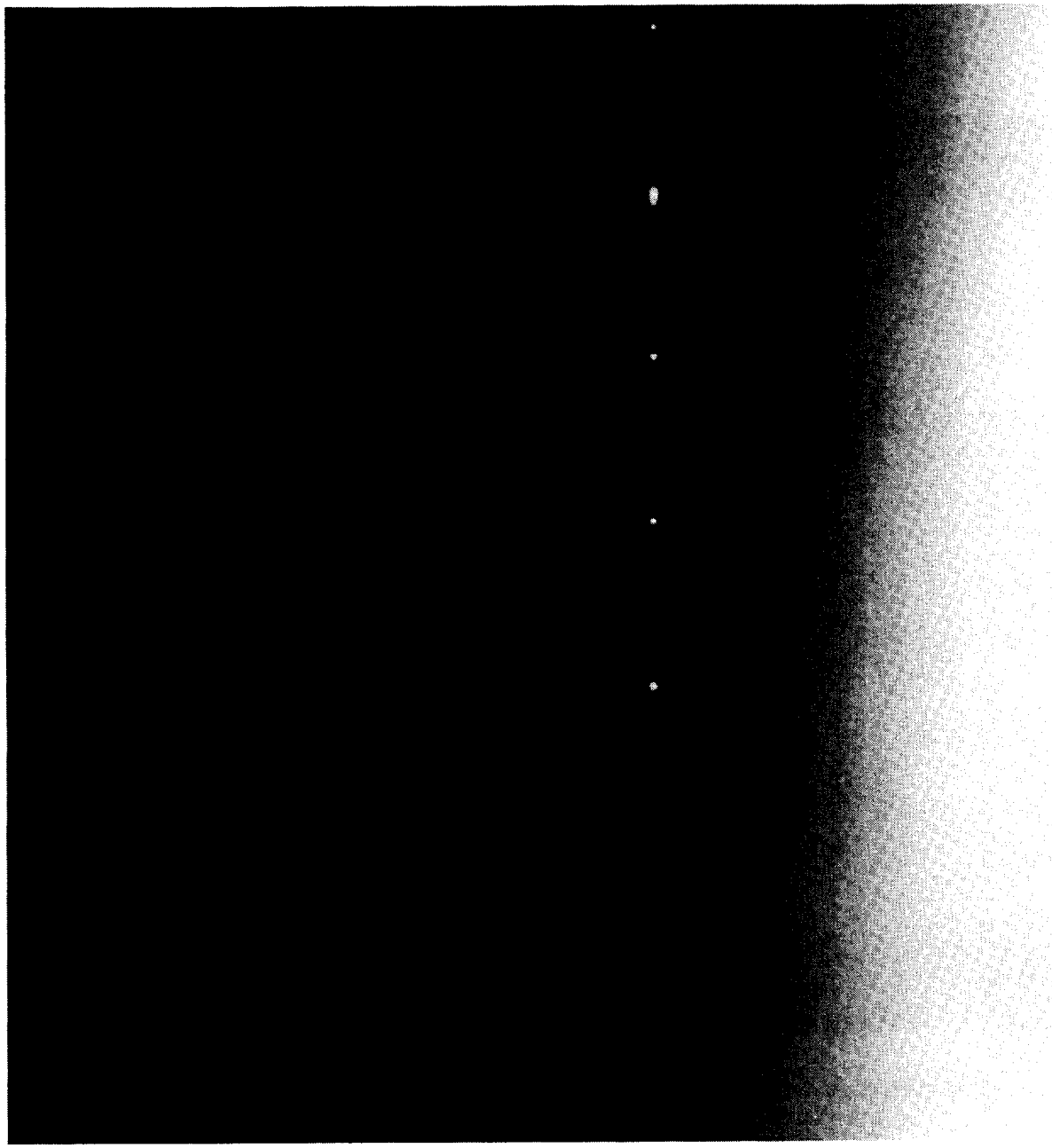

Figure 5. Camera image showing laser uplink detections from TMF (15-hertz repetition rate) and SOR (10-hertz repetition rate) on Day 2 of GOPEX. SOR scanning was off.

The XXIII International Physics Olympiad

Carwil James
A speech prepared for the National Society of Black Physicists Annual Meeting, Tallahassee, Florida

The XXIV International Physics Olympiad will be hosted this summer at the College of William and Mary in Williamsburg, Virginia. The U.S. is hosting this event on the heels of its successful competition at the XXIII Olympiad in Helsinki, Finland. That competition was both a proud achievement for the American Association of Physics Teachers and the many dedicated individuals involved with the United States Physics Team, and a rewarding, though challenging, experience for the five U.S. participants.

Last July, I had the privilege of representing, along with four other high school students, the United States of America at the XXIII International Physics Olympiad in Helsinki, Finland. The contest, which took place from July 5 to July 13, involved 178 participants and 99 team leaders and observers from 39 countries, and included ten hours of competition, was the largest ever International Physics Olympiad. For all of those people it marked the end of a very long process of competition, training, and other preparations.

The International Physics Olympiad is so named because the International Olympic Committee claims exclusive use of the term Olympics and the Olympic Rings. As an alternative, the U.S. Physics Olympiad uses a torch, but the International Organizers don't bother. The competition itself is a test of individual physics skill. While teams are created on the basis of nationality, the teams themselves do not compete, only individuals do. Of course, it isn't hard to add up the five scores of each team, but that's not what the competition is about. Rather, the competition is the meeting of physics students from around the world in both a competitive and a social setting. After my experiences in Helsinki, I truly wished for the opportunity to visit an Olympic village and see if the athletes developed the same international friendships. The competition part of the experience is divided into a theoretical competition with three problems and an experimental competition with two. Each of the five problems carries equal weight.

The theoretical competition consists of three questions (almost always multipart) in five hours. Very few people finish all the parts and a perfect score only occurs once every few years. Our questions dealt with: a rotating ferris wheel-type satellite in low earth orbit, satellites as blackbody radiators interacting with the sun, and the nature of straight chain molecules as masses connected by ideal springs with application to the radiation of CO_2 molecules. The experimental section provides much less information to the participants. As the key to the problem is devising an appropriate procedure for measurement, only the quantity to be measured and detailed descriptions of the equipment are provided. The first experiment we did was determining

the proportionality of spark gap potential to distance in air by the use of piezoelectric material as a voltage source. The second experiment was determining a variety of properties of some filters (including estimates of their frequency ranges) and the width of CD grooves, using a penlight, Duplo bricks, and a protractor.

The test is composed by the hosting nation and translated into both English and Russian. Team leaders then conduct debate in both languages about the merit of the questions, seeking to gain as much correspondence as possible between their team's knowledge and the topics on in the questions. After this process, each team leader translates from either English or Russian to his native language. Once, this process was put to democratic scrutiny, leading to hours of debate on translation. This has been replaced by the honor system, resulting in a good night's sleep for both the contestants and the coaches.

The questions in the Olympiad can deal with practically anything. In theory, the questions should involve problems from a specified list of topics. Also, Calculus should not be necessary for the problems. In reality the problems usual exceed these limits. As I was going through the backlog of problem sets, I found, as warned, that they became more and more difficult through the years. Every time students begin to approach the upper limit of scoring, the test is made more difficult the next year. After 23 years, the difference is extraordinary.

The selection of U.S. participants in the International Physics Olympiad is a three tiered process, each tier more involved than the last. During winter, the American Association of Physics Teachers (AAPT) sends out letter to numerous students and teachers, soliciting teachers to recommend their top physics students to take the preliminary exam and the students to try and take it. I received such a letter both years I was in high school, undoubtedly due my participation in a number of math contests in prior years. Whatever their source, I responded by taking the preliminary examination both years with the blessing of my physics teacher, Mr. Robert Shurtz. My first year, I was a student in AP Physics B, clearly unprepared to do very well in high level competition. Needless to say, I did not advance beyond this first phase of competition, which was a combination of a multiple choice test and a series of open response questions.

In my junior year, I was one of four students to take the exam at my school. I was joined by my friends and classmates, Omar Antar, Mike Antonelli, and Charlie Saulino. Omar, Mike and I all advanced to the second stage of competition, the Semi-Final exam. While Mike opted not to take the second exam, Omar and I went on to the Semi-Final exam with the aid of crash courses from Mr. Shurtz. This exam included two sections. The first had four challenging, but doable, open response questions in one hour. The second had two problems which we couldn't truly expect to fully complete within the allotted two hours. Omar and I both took the test, using our 15-minute intermission between the sections to see what we could of our high school talent show, and waited. Several weeks later, I found out I had been

selected along with nineteen other students to be on the 1992 United States Physics Team and was asked to attend training camp during my last week of classes in high school. I, of course, was more than happy to oblige.

When I arrived at Baltimore-Washington International Airport, there were no representatives of the United States Physics Team at the gate. Finding this surprising and unusual, I looked at my table of arrivals and went to the gate of the next person arriving. There still were no USPT representatives, but when the flight arrived I found someone else on the team, José Lorenzo who is from Miami. It was not even five minutes before we ran into Chris, who was to be one of our lab instructors at training camp. The people meeting us at the airport had been waiting for us at the entrance to the terminal.

From the time we checked into our rooms at the Adult Education Center at the University of Maryland, College Park campus, we had physics problems to work on. A typical day include a two hour theoretical test with two problems, a three hour lab, a three hour morning lecture, and some discussion of problems in the evening. Both the laboratory experiments and the theoretical problems got more and more difficult as the week went on, serving as both practice for us and selection criteria for our coaches. We did, once in a while, have designated free time at training camp, but mostly we used whatever time we could find. We were taught and encouraged and led by our two academic directors, Professor Larry Kirkpatrick of Montana State University and Dr. Avi Hauser of Bell Labs as well as Mr. Ted Vittitoe of Libertyville High School in Illinois and our academic advisor, Arthur Eisenkraft who was at the time working primarily on the 1993 Olympiad in Williamsburg. Everyday, a researcher came to speak to us about their work. Their speeches discussed things ranging from scanning tunneling microscopy to lasers to cosmic rays. While not directly applicable to the competition, these speeches did help broaden our knowledge of physics and prepared us for more diversity in Olympiad questions.

The U.S. Team was quite an interesting group of people. We had a veteran of the 1991 Olympiad, Eric Miller, who was always looking for links to things he had done before. There was my extremely inquisitive roommate, Dean Jens, the very verbose and confident Mikhail Sunitsky, the modest (in attitude, not ability) Victoria Yung, the insightful if a bit soft-spoken Szymon Rusinkiewicz, the most sociable Michael Schultz, and the extremely enthusiastic Mary Pat Campbell. I don't need to point out that all these people, and the other dozen as well, were very competent in the area of physics and each brought their own perspective to the problems we faced.

Aside from our daily academic routine, we took the time to visit Washington, DC for half a day during training camp. Our first stop was the Old Executive Office building, where we met with former-President Bush's Advisor for Science and Technology. The visit included a speech by the Advisor and a short photo-op. We then walked over to the National Science Foundation, where things began to get interesting. While the head of the Foundation was away at a meeting, we did get to talk to three officials who encouraged us to discuss the status of science education in the United States.

We were, they said, what was going right in science education, and hopefully we could tell them what needed to be done in science education today. The most striking thing about this conversation was that there was no program or policy that we could point to as our inspiration. We all noted the importance of contests such as the one we were representing to encourage students to try harder. Mostly though, we considered ourselves the result of the dedication of our families and of our teachers, as individuals not as part of some broader program.

At the Department of Education which, by the way, shares its building with NASA as a prominent symbol of its importance to the government, the discussion continued. Once again the aides to the Education Secretary, Lamar Alexander, were sent in to hear our comments. Mr. Alexander emerged only for the photo and quickly retreated. The workers in the Department are proud, I remember one woman there who was happy to inform me of the symbolism of the Department's seal. Her knowledge of that piece of information for some reason impressed me. During our discussion, we talked a lot about what could be improved in American education. Standard textbooks were debated, as was how much the Federal Government can help. On the vast majority of issues, though, we agreed: the fundamentals of science must be taught earlier, the middle school science curriculum should serve as a bridge from the experimenting and tinkering of elementary science class to the rule based systems of high school, elementary physics should be taught earlier, a bad book can teach little or disenchant, and above all, we have to change the system. One government initiative drew particular fire: the America 2000 plan. Not one of us expects the United States to be first in the world in science and math by the end of the millennium. While they argued we couldn't aim for second or third, we made it clear that without more reasonable goals, nothing would get done.

The last full day, the team members were announced in random order. They were Szymon Rusinkiewicz, Michael Schultz, Dean Jens, Eric Miller, and myself. The alternate, who had to study for a month like us, but without the promise of a trip, was Michael Agney. The six of us were, naturally, ecstatic and received the support of the other students immediately. I personally had expected to be in the second group of five people at the camp and so I was pleasantly surprised. Of course, none of us could have been truly crushed had we not been selected. It really is an honor just to be on the team whether or not you represent them in the Olympiad.

As team members, we were all benefactors of the support of a wide variety of corporations, foundations and other agencies. The U.S. effort was primarily supported by AT&T and IBM (Bell Labs' Dr. Hauser insisted on alphabetical order), but some of our more direct support was in the form of in-kind donations. We received a wide variety of textbooks both at training camp and afterwards. Even last December, I received a new graphing calculator form Texas Instruments.

From the last night at training camp, I was vividly aware that our interaction with others at IPhO would be in some way representative of the

United States. We had instantly acquired the need for diplomatic courtesy in all our dealings as participants. That night I made a mental note not to pack my Tienanmen Square T-shirt when I went to Finland. There were very few occasions when I felt constrained by this diplomatic courtesy, but they existed. The night before one of the competitions, the Romanian team went around offering samples of a folk drink from a wooden flask. We were warned by Eric and Mike to expect them. When they did visit us, we could not refuse, though rumor had it that the proof of the concoction had three digits. Nonetheless, we all had about half a mouthful. Our diplomacy cost merely a head rush thirty seconds later.

Between training camp and the actual competition, the real training took place. To train for a physics Olympiad is to enter into a degree of seclusion. Everyday included a five hour exam, checking your work, and about twice a week there was a lab experiment. I took the time to enjoy the festivities surrounding my semi-graduation, so I had all of the experience of training in less time. We were each given every problem from the previous twenty-two olympiads, each harder than the previous one. Each day, we were asked to visualize ourselves in the competition, going from problem to problem and succeeding. As verification we sent Arthur Eisenkraft a three sentence mantra on a postcard everyday. The third part of this training was completion of the freshman physics laboratory course at a local university. I performed this part of my training at Case Western Reserve University, where my high school physics teacher, Mr. Shurtz had enough authority to make it easy for me to get access to the laboratory program. This lab experiment included some truly interesting experiments including measuring the charge to mass ratio of an electron, something I think every physics student should see and do for him or herself.

The night before I left, I did not sleep at all in an effort to adjust to the time change. If it had gone as planned I would have slept on the flight and awoke at about 10 AM Finnish time. It didn't, and I ended up getting the first part of that sleep in the airport in New York, a few more hours on the plane and the remainder when I fell over on the bed in my hotel room.

We arrived on the third of July, two full days before the Olympiad convened in order to adjust to the time change and to experience a little bit of Helsinki for ourselves. After giving us time to settle into our rooms (or fall into them as the case may be), we were taken on a walk around Helsinki including a visit to the embassy district and the front of the U.S. embassy. We found out the location of the Independence Day festivities, which just happened to be on July 3rd, and left. We also visited a small snacks restaurant and saw a lot of the Baltic Sea before we headed back to our hotel, the Ramada Presidentii.

Our only celebration of Independence Day actually on July 4th was the lighting of a pyramid of matches in symbolic fireworks. Eric, perhaps remembering what we had just seen, insisted on having a full glass of water ready for the occasion. What we had just seen was one of the most unusual cartoons ever produced outside of Japan. The protagonist, who is in a dream

sequence, got cold in his house. So, naturally he built a fire on his coffee table. As his room fills with smoke, he goes outside to cut a hole in the roof. Now, unsatisfied by the heat generated, he proceeds to put his television in the flames and shortly thereafter, it explodes. I won't get into the ending, but it nearly as confusing as the Japanese film Akira.

We took the Helsinki street car to the Independence Day Celebration, meeting a group of Canadians living for two years as missionaries in Helsinki. We agreed to remain silent as to their nation of origin. We arrived late to the Seursaari Show Area, site of the festivities and missed the opening by the U.S. ambassador. On the other hand, we missed very little of the actual party. Surrounded by other Americans, we thoroughly enjoyed ourselves. We took part in the volleyball and other sports and took home a sizeable amount from the raffle.

The next day, we took the officially recommended walking tour of downtown Helsinki visiting sites such as the beautiful Upensky cathedral which along with another cathedral and the parliament building dominates the skyline. There are no sky scrapers in Helsinki, apparently under a six to eight story building limit which makes the vast majority of buildings of uniform height. In many ways, the design of the buildings and the streets resembles an eight-story Legoland town set up. If the streets were in an American city, we would find them impassibly narrow, but the Finns don't drive, they walk and take public transport and they have a great system with which to do that.

The contest itself took place in Espoo, rather than Helsinki proper. Espoo is Finland's second largest city, with a population of 175,000, and is just to the west of Helsinki. We stayed in the easternmost administrative district of Espoo, Otaniemi, home of the Helsinki University of Technology. So, the morning of the fifth we boarded a bus and moved to Espoo where we were to stay in the Summer Hotel Dipoli and our leaders in the actual Hotel Dipoli. Unfortunately, the Finnish government had other plans.

At the same time as the Olympiad, another gathering of many nations was taking place in the Helsinki metropolitan area, the Council on Security and Cooperation in Europe (CSCE). While I'm sure much was accomplished at that meeting (including the expulsion of Yugoslavia from the organization), the only thing we could see of the conference were the incredible number of police lines strung up all across the city which we passed at least daily. More directly affecting us, the CSCE preempted us from our original hotel. As a result the team leaders, who saw the questions in advance, were staying two floors above the team members, who hadn't. While not truly presenting a problem for anyone, it did create a certain degree of anxiety at times when we saw our coaches. For us to say anything more than 'hi' would have potentially aroused suspicion. Protocol was thus kept to a minimum.

In keeping with international tradition we brought gifts from our home cities and states and exchanged them with other teams. We each built up a sizeable collection of pins, boomerangs, maps and postcards from around

the world. To be honest, the boomerangs were only from Australia, but nearly everyone brought something. It all made the occasion very festive and added to experience of meeting people from other cultures.

The participants at Helsinki were clearly representatives of the post-cold war world. In the opening ceremonies, we sat next to Ukraine. Five other participating countries had been independent for less than three years. The members of these new teams were very open, warm and friendly people. By contrast, we were told of the Soviet teams from earlier years. They remained austere and extremely serious. Like us, they considered the competition important and strove to do as well as possible, but these cold war teams thought of, or were told to think of, more than that. They, like the Soviet bloc Olympic athletes contemporary to them, were representatives of a political and economic system on the world stage. Their performance was a triumph for their nation, an advance in the cold war. Now that the Soviet bloc has disappeared, the sole austere team was the People's Republic of China.

For the first few days, up until the competition was over, the Chinese team wore white dress shirts and black trousers to every meal. They were the picture of unity and, at least to me, unapproachable. This is no impeachment of their character: afterwards they were as friendly as any other team there, joining freely in the gift giving which so often marked our contact with those for whom the language barrier was too great. And notably, they gave us a slip of paper with their addresses, ages and other information.

Of the 178 participants, only four were female. For this ratio to exist in my major continually disappoints me. We must work to interest just as many young women as men in physics. Likewise, of the thirty-nations in attendance: twenty-four were European; three, North American; a pair, South American; and seven, Asian. Even granted the location was more convenient for the European teams, especially the eastern bloc nations for whom science is rapidly becoming an unaffordable luxury, the geographic distribution of teams is in need of improvement. I hope that the Olympiad in Williamsburg will include nations from six continents rather than five, all of the most populated nations, and will inspire students of all nations to educate themselves as a symbol of pride in their homelands.

The United States had the single largest contingent at Helsinki, participating both as representatives of a nation of 250 million and as the next hosts of the competition. Besides the five of us, there were our two coaches, Avi Hauser and Larry Kirkpatrick, textbook-writer Anthony P. French, AAPT representative Delores Mason, the coordinator of the XXIV Olympiad, Arthur Eisenkraft, a high school teacher, and two members of the press paid by the American Institute of Physics.

Helsinki is a city very familiar with foreigners, even somewhat shaped by their presence. The two official languages of Finland, Finnish and Swedish, are accompanied by English and German nearly everywhere in Helsinki, even on the public transit. Downtown Helsinki, which we took a walking tour of the first two days, is filled with governmental centers, commercial sites, and cultural landmarks integral to the heart of Finland. Nonetheless, I

didn't feel that I had seen real Finnish life until four of us visited our guide's home in northern Helsinki. Although, many residential districts sprawled out before us on the perspective map I purchased for seven dollars from the Finnish national tourism organization, the life of the Finns would have remained unknown to me had I not made this visit.

The experimental competition was conducted in two flights. The evening before the experimental competition, we learned that we would be in the A shift of the competition, scheduled for 8:00 AM to 1:00 PM. My roommates, Dean Jens and Szymon Rusinkiewicz took this news with some alarm, and as I showered that evening made preparation to go to sleep by 8:45. They would awake, they assured me, at 6:15 with plenty of time to shower and get ready for breakfast at 7. I remained awake that night until nearly ten, entering the Dreaming to the sound of Billy Joel's Vienna. The next morning at 6:45, I awoke and glanced at my watch. When I told my sleeping roommates what time it was, they were not pleased. Once the experimental session started (at least 30 minutes late), we were divided into two groups. Each group worked on one experiment at first and then we switched. This procedure was simple enough in principle but in practice was confused in at least two major ways. First, the descriptions of both were in our lab books allowing us extra time to prepare for the second experiment. Second, they decided, or were forced by procedural difficulties, to give us time to eat between experiments. Besides putting us further behind schedule, this gave us the opportunity to prepare for the 2nd experiment and for some teams to discuss that experiment.

Just as I felt less nervous about the experimental competition than my teammates did, I felt calm before theoretical competition. Once I had gathered the materials I needed for it (ruler, calculator, and writing utensils), I removed my yearbook from the Merimekko bag they had given each of us and turned up my Walkman, as I read through what my friends at school and from the U.S. Physics Team had written inside it. My thoughts of the conflict between my personal feelings and the chaos of getting ready for the competition which surrounded me are only in hindsight. Then, I thought of nothing but the goodwill scattered in the formerly blank pages and margins of my yearbook.

The relations between participants should not, in theory, reflect the political situation of their nations. After all, the purpose of international interaction at this level is to foster friendship and community. Nonetheless, one case where such harmony was not so easy quickly comes to mind. Among the gifts brought by the Cypriot team were pamphlets from their government, both advertising the island nation's tourism potential and condemning the 1974 Turkish invasion. While I recognize the imperative to make such statements as members of international society, it seemed that the presence of the Turkish team must have resulted in a little bit of trouble on both sides. I hoped they learned not to condemn each other for their governments.

As the week went along, I went to sleep progressively later and later, excepting the night before the experimental competition. One of the things that kept me awake so late was the card game, Bartog which is basically Uno played with real cards and with one twist. After each round, the winner gets to make up one rule. In a good game there is a fair mix between verbal rules and procedural rules and everyone is confused beyond belief, but someone always remembers a rule when you don't. We had one or two really good games with about five verbal rules which made each play of the cards into a speech.

One of the least interesting mandatory activities which we participated in was the visit to the Porvoo works of Neste Technology. No matter how science oriented a group of teenagers is, I doubt I could find a group of them who would revel in the opportunity to visit and industrial plant. When we first arrived, we saw a film designed to give an overview of Neste Corporation. Three economics students decide, in order to complete a project for class, to make an energy company based in Scandinavia. As they do more and more research they refine the idea; skimping on their social lives to design the perfect corporation. What they decided on, of course, was in fact what Neste sees itself as, a growing energy supplier in a strong market, branching out into other fields. As a corporation introducing itself, the film had merit; as entertainment it needed serious help. Bus and walking tours, and a very restful presentation on solar energy completed this excursion. The afternoon was to redeem our day.

That afternoon we visited Heureka, the Finnish Science Center located in Vantaa, a city just north of Helsinki and the third largest city in Finland. There was the typical conglomeration of hands-on science activities, Commodore Amiga and Macintosh terminals with educational programs, and short video presentations. In true form, nearly everything was translated into both Swedish and English. While the featured exhibit was a celebration of Finland's 75 years of independence, the things I found most interesting were elsewhere. There was an especially large area devoted to language. Finnish is a Finno-Ugric language similar to Hungarian and a distant relation of Korean. There was a huge globe with earphone jacks corresponding to various languages. While the U.S. speaker says "I speak English," the one from the United Kingdom says, "I speak British English."We spent 3 hours looking at computer simulations, examining World War I artifacts, having our names printed in Cuneiform, and searching for obscure Finnish coins.

During the walk on the first day I noticed the ships in the harbor which went back an forth to the various Baltic nations, serving a market that would not have existed a few years before. The Estonia New Line boat service advertised a one day visa-free trip to Talinn, Estonia which looked very promising. By the end of the week there was a troop of four of us willing to go, if we could. Eric Miller, myself and two members of another team all woke up at some insane hour and proceeded downtown. That morning, as the four of us walked to the offices of the Estonia New Line, I had a definite feeling that our trip to Talinn was not to be. Twenty minutes later, we found

out that no tickets remained for that day. Before heading back to Espoo, I purchased a breakfast of strawberries from one of the merchants at the Helsinki central market whose stand was less than fifty feet from police lines put up for a CSCE motorcade. The most enjoyable part of the experience was the contact with people from around the world, something no day excursion could match, although Estonia might have come close.

When we went downtown again, I spent all day walking around with Michael Schultz. The first place we went to was the Forum Mall. Finally having a chance to see the European Legos, we were duly impressed. As there was a conveniently available supply of technically minded people available at IPhO, we decided it would be a good idea to get a group of people and buy one of the larger sets of Technic Legos (formerly known as the Expert Builder sets), and assemble them as a group and raffle them off. Some of the more advanced models even included a programmable interface. Keeping this in mind we explored the city, hoping to run into people who would team up to buy with us and accept a lottery among the builders to decide who should keep it. While we did see a lot of Helsinki that day including, possibly, the Chinese restaurant with the worst quality to cost ratio on the planet. We only found two fellow participants. They were willing to buy into the idea, but not to pay a fourth of what could be up to $180. Taking a large risk, Mike bought a $150 set anyway, with his parents' credit card.

Starting that night at dinner, we lobbied for builders and for people willing to contribute 10 markka for a shot at winning the completed model. We easily found a group of about 15 builders willing to work on it. The number of people buying into the raffle lagged behind the number needed to break even, but we pressed forwards anyway. With so many people constructing the model, which was a working pneumatic bulldozer and backhoe, we always had about twice as many people as could successfully work together on something of that scale. But keeping about eight people working at a time wasn't a problem with lack of interest, overcrowding and the need for sleep. We completed the device that very night between 2:00 and 3:00 AM.

Regrettably, as a direct consequence, our team was less than fully prepared for the closing ceremonies the next morning. While we had known our awards from talking to our leaders the previous day, the experience of going down to the stage and receiving the awards was just as impressive. Eric and Szymon both received gold medals; Mike, a silver; and Dean and I each got honorable mention. The United States had done the best it had ever done in the International Physics Olympiad. We placed fifth among the nations participating based on both our average performance and our medal count. First was China whose team garnered five gold medals. Of course these team scores are unofficial, teams don't receive awards, only individuals do. Through the day, we got enough participants in the raffle to break even, at which point we stopped selling. Our last buyer was Arthur Eisenkraft who gave his ticket to our guide, Amy Wassenich upon realizing the potential problems if a U.S. team leader won. We scheduled the raffle and departed for

downtown Helsinki. That night, our coaches, and by extension all the organizations supporting us, treated the entire United States entourage to a very expensive dinner. While, I made sure not to convert back to dollars until I went home, I knew it was a lot. The meal, which averaged about $40 per person, was the best one we had in Helsinki and a great end to a great week.

We somehow managed to be only about 45 minutes late to the raffle and collected an audience. We gave a hotel employee the honor of selecting the winner. After looking up the name next to the number on the list, we found that the winner was in fact, Amy Wassenich. I'm sure Amy and her fianceé, who joined us at the closing ceremonies have already had hours of fun with their pneumatically powered bulldozer/backhoe Lego model. That night, I got as many people as I could to sign my yearbook and didn't get much sleep. My return trip was uneventful excepting the last twenty minutes on approach to New York. As the overhead monitor indicated the exact flight path of the plane, we all watched one of the best definitions of zig-zag take shape before our eyes. And then, triumphant, we were back in the United States.

Even as I finish talking about my experiences of last year, many of the dedicated people who made that U.S. a reality are working on hosting this year's Olympiad in Williamsburg, Virginia. With many other countries eager to host the contest, this may be the last chance to see and help out with such an event in America for a long time. I encourage all of you to get involved and to contribute to yet another rewarding experience for students from around the world.

Minority Owned High Technology Businesses - Techniques for Growing a Successful One

Donald Butler, BLES Scientific, Inc.,Thousand Oaks, CA

- There may be no such thing as minority business, however, the content of this presentation is focussed on the issues confronted by a minority member starting a business.

- The passion behind the need for this presentation is very much a minority issue.

A recent article in the Los Angeles Times stated that there are three ingredients needed for African-Americans to reach the middle class: competent school system, dedicated students and employment. The author stated that African-Americans have come through on the first two ingredients and that the United States has failed them on the third.

The Civil Rights Institute in Birmingham, Alabama has a display that memorializes the killing by racists of four young children in the bombing of the Sixteenth Street Baptist Church. Far more than four children have been killed by African-Americans in urban senseless killing sprees. Asked why, they say they have nothing to do, so they join gangs. When asked what they need to make other choices, they say they need jobs.

Starting a business in not the direct answer to this problem. However, I see a direct link to the despair I have seen in their eyes and the economic state of Africans in this country.

Thirty years ago, the push was for Black pride. No one stated this one step would solve all problems African-Americans have. However, that was a necessary part of our journey. I believe a consensus exists that African-American economy is the current issue to be taken on.

My passion for starting my business is partly personal - love of a challenge, desire to be special, blind faith in my capabilities. And partly political - our parents had a burden that was lifted, that is now not heavy enough to stop us. Now, we can pursue business activity with a reasonable chance to succeed. My political passion is that if one is capable of making a significant economic contribution to this cause, it is criminal not to.

PLANNING

- Inadequate planning is the primary reason for business failure. These failures often are described as "We ran out of money."

- Analogous to packing up your family and traveling through a remote region to get a "New Land"

    You have a general idea where you want to be, but you cannot verify location or if it really exists. Others tell you of reaching such a place but all the descriptions are different.

    Are you truly ready for the sacrifices needed to reach this new place? Is your family?

    Do you need a guide? Do you have all the needed skills for such a journey or should you get others to go with you?

    How much food and water should we take?

- Successful planning (within this analogy) requires you to:

    Specify the location of where you want to end up,
    Map your trip in spite of the uncertainties,
    Document all anticipated obstacles and unusual situations,
    Estimate the duration of the trip,
    Specify all required skills,
    Determine the minimum level of sustenance needed by the travelers to stay alive,
    Require revision of plans as new information is acquired.

- In a business setting, the above items are written in a business plan. Business plans are often described as something needed to get funding. This concept is misleading. A business plan is for YOU. You must complete this document before you start your business. The contents will have varying levels of confidence. Assign someone to monitor each low confidence item.

- The most difficult part of planning is accepting that it must be done in spite of great uncertainty and ignorance. The business plan is part of a "prediction/correction state estimation" scheme.

Choosing a Product or Service

- What your business offers must be required by your customer. That is the ONLY reason for a business to offer a product or service.

- Technology students and employees are taught to think value lies in the science or engineering embodied in a product or service. This kind of value is almost irrelevant to your customer. Your customer ONLY wants his or her problem solved.

- The uninitiated business person may think of something that is "neat", develop it, then run around telling everyone about it. They will usually expend a lot of dollars and time but ultimately have an unsuccessful product. A product can be better technologically and even advertized but fail.

- The services you provide to your employer or university may not be the services to build a business on. Your employer's customers are buying the whole company's capabilities. That customer may not buy your particular skills from you.

- Logic can fail you in selecting a product. Simply asking around can be infinitely more effective.

- The United States business arena has "money streams" that are already in place. One approach is to provide a product that makes that "stream" flow smoother.

I called a hardware vendor of a product we buy in volume and asked "What is the problem you are most frequently asked about by your customers?" They quickly told me since they would sell more hardware if I solved this problem.

BLES Scientific developed a product for the health care industry. In the process of producing it, two techniques were developed that could have general application. I called a vendor whose shortcoming we had overcome and asked "Could other software developers use our solution?" They said yes, FAXed us names of all the developers supporting their product, promised to advertize our product in their international news letter and offered us free space in their booth area at trade shows. Selling these offshoots will likely repay us the development cost of the entire medical product.

Licensee Questions

Do you see an immediate need in the market place or is market development required?

What do you estimate to be the size of the market?

Estimate the market duration.

What competition do you see?

Will you pursue foreign markets? If so, what is your experience in foreign markets? What experience do you have with export control regulations and for what countries?

What will be your marketing strategy?

What marketing expertise do you have for this product?

Will the product be distributed separately or bundled with another product?

When do you anticipate providing the product for sale?

What is your estimated pricing structure?

What maintenance agreements will you offer to your customers?

What kind of user support will you provide, such as training, newsletters user group meetings or hot lines?

What kind of license do you seek? (Exclusive, nonexclusive, area, use or hybrid.)

What royalty base do you have in mind?

Describe your current and future projects in this technology.

Financing

- Savings. The best source of financing since the discipline used to acquire the savings will help you make a successful business. I read of a simple vendor who saved $79,000 dollars in four years. His annual income was $22,000. I know a maid who has saved $350,000. She used $240,000 of it to buy a house. I know a mail carrier who saved $170,000 to buy a restaurant. I know a store owner who saved $15,000 and opened a store in a California coastal city. He later bought a $450,00 house for cash. All of these people are immigrants who felt forced to do this since they were not proficient in English. I feel African-Americans are in denial of our financial situation. Most of the money coming into our hands leaves.

- Your customer. When we get a software development contract, we specify in the contract that we will start when we receive one-third of the project's price. We receive one-third half way through and the remainder at finish.

- Your employees. Stock offering may make a better company since employees feel a sense of ownership.

- Joint Development. A customer, supplier or investor provides the funding, you product the product at cost and share ownership. Some customers only want a copy of what is developed and you retain ownership to sell again and again.

- Small Business Independent Research (SBIR). Various government agencies tell you what they want and will provide you up to $100,000 in Phase I and up to $750,000 in Phase II to develop it. You retain ownership and the government gets an unrestricted license to use it.

- Professional fund raisers. Once you have something to offer, there are people who use their contacts to raise money for you, retaining perhaps, 10% of the funds raised. You must investigate these people and be very wary of giving them money prior to funds being raised. An honest one can be very helpful in suggesting options you may have never thought of.

- Public stock offering. The Security Exchange Commission has recently provided easier rules for small fund raising (under $5 million).

Information on Business Funding
(from the Wall Street Journal, February 19, 1993)

American Bankers Association
800 872 7747

Business Consortium Fund
212 872 5590

National Association of Community Development Loan Funds
215 923 4754

National Association of Investment Companies
202 289 4336

National Association of Minority Contractors
202 347 8259

National Bankers Association
202 588 5432

National Business Incubator Association
614 593 4331

National Council of State Legislators
303 830 2200

National Federation of Independent Business
800 552 6342

National Minority Supplier Development Council
212 944 2430

National Small Business United
202 293 8830

Overseas Private Investment Corporation
202 336 8400

Small Business Legislative Council
202 639 8500

U.S. Office of Small and Disadvantaged Business/AID
703 875 1551

U.S. Small Business Administration
800 827 5722

Cash Flow

- Imagine you have started a business out of your house. You have developed a prototype of a device that costs you $1150.00 to make but you can feel you can sell each device for $2250.00. You finally get that "big break". You received an order for 5000 devices. They need them at a rate of 250 per month and you can invoice them after each month's delivery. They will pay the invoice for that months supply thirty days after they receive the invoice. You call your suppliers for pricing at that level of volume and determine your costs reduce to $750.00. You pull out your calculator and discover your profit will be $7.5 million on the deal!

- Is that what will really happen and should you accept the deal? The answer is you will not see $7.5 million and you may or may not be able to accept the offer even if you wanted to. The problem is cash flow.

Even without awareness of cash flow, you realize things will be more complicated. Up until now, you have been making them yourself and there is no way you could make 250 per month. You need an assembly line and assemblers. You even know this only has a chance if you contract a company that already has an assembly line to make them for you. You find a company that will charge you $22,000 per month for labor and $50,000 per month for your own assembly line.

- First the income: $562,500 per month for 20 months.

- Your monthly cost:

$187,500	for parts
72,000	for assembly

$259,500	total cost

This cost is a little high to you since you read your costs should be no more than 40% of revenue ($225,000). But why complain since...

- Net monthly pretax profit: $303,000

- Taxes: Quarterly estimated tax of $409,050. Yes, the federal and state tax collectors want their taxes paid every three months based on projections of annual sales. Federal, state and local taxes can total 45% of revenue.

- So what is the problem?

	Income	Payables	Cumulative Net
Month 1	$ 0	$259,500	$(259,500)
2	0	259,500	(519,000)
3	562,500	668,550	(625,050)
4	562,500	259,500	(322,050)
5	562,500	259,500	(19,050)
6	562,500	668,550	(125,100)
7	562,500	259,500	177,900
8	562,500	259,500	480,900
9	562,500	668,550	374,850
10	562,500	259,500	677,850
11	562,500	259,500	980,850
12	562,500	668,550	874,800

The cumulative net stays positive here after.

The problem is there are six months where payables exceed accumulated income. You will need $625,050 in cash prior to accepting the offer to survive to see the overall net profit.

- This an example that is simpler than real life. It is worth your while to purchase a spreadsheet program and have someone in your organization who makes cash flow projections.

- From Inc. Magazine, March 1993. The Zen of Cash Flow:

As it passes over a bridge exactly one mile long, your car travels the first half at 30 mph. How fast must you travel for the second half to average 60mph for the entire span? The answer is NOT 90 mph. You blew your minute traveling over the first half of the bridge.

The lesson to apply to a business setting is: even if the average income for a project is positive, if you spend all your money during the negative cash flow portion, you blew it for the entire contract.

Question - What would you do to make the above contract example easier to accept?

Marketing

- Your market is that portion of the population or of businesses that you are offering your product to. The function of marketing is to uncover the true purchaser of your goods and make them your market.

- Specify the characteristics of your typical customer in terms of its customer base, revenue and geographic location. This estimate should be included in your business plan. Your market description must be reviewed as new information is gathered.

- Ask the people you are approaching what they perceive as your company's value. Acknowledge them for whatever they say. In time, a pattern will arise. Go with what shows up. Including ...

- You may not have a market for your offerings. One should realize that as soon as possible and change your offering. My first contract led me to believe the customer was part of a sustainable market. They were not.

- Usually the entity raising the problem is a member of your market no matter where the solution is installed. For example, the largest number of units of our medical product will be in physician's offices. Initially, we considered physicians to be our market. However, the problem was presented to us by clinical laboratories and ultimately, we realized they comprise our market. Clinical laboratories and hospital based laboratories are interested in purchasing our product and providing them to physicians.

- A small business needs sales persons far more that marketing employees, but it is critical that thought is given to where your sales effort should be directed.

Promotion of your Business

- Advertising must have the highest priority in your business, higher than the development of your product.

- Promotion consists of public relations and advertising. Many companies opt to develop and execute their own promotion campaign. A PR firm will ask for a $10,000 to $30,000 retainer and also bill you for monthly expenses. These firms also require a training period to learn about your business. This is especially true in the high technology industry.

- Public relations can be established by:

  News releases
  Letters to editors of magazines
  Magazine and journal articles
  Join trade and community organizations
  Conducting open houses for youth organizations
  Donating equipment or service for use in highly public situations

- Advertising a high technology company may be done by:

  Direct mailing - letters, brochures
  Advertisement in trade journals or magazines
  Telephone calls
  Word of mouth. Ask you customers to tell others about you
  Trade shows (the ones your customers come to, not the ones only your competition attends)
  Company newsletters (you can buy news letters that are printed with your company's name on it)

  Some forms of advertising are inappropriate for high technology companies. For example,

  Don't use: Telephone directory advertisement
  Newspaper advertisements
  Television time
  or any ad media designed for impulse buying

Selling

- Your education, experience, staff office and product exist to perform this function.

- High technology companies make sales in two steps. 1) Find leads, 2) Close sale.

- Finding leads, i.e. potential customers

    Previous Customers - You would be amazed how these are forgotten.
    Trade magazines - Top 50 lists
    Commerce Business Daily Awarded Contract Section
    Chamber of Commerce
    Telephone Yellow Pages. Your library may have out of state books.
    Newspaper employment advertisements
    Professional Organization Membership Lists
    Word of Mouth
    Procurement Automated Source System (PASS)
    Rented Mailing Lists
    Your Suppliers. They may supply potential customers.
    Promotion

- Qualify the prospective customer.

    Some people are unwilling or unable to purchase or seal a contract.
    Don't give a lot of details about your service over the telephone.
    Ask them about what they do and what they need.
    Don't debate an objection. Tell the person you heard their concern.
    Ask prospects how they conduct your kind of purchases.
    Ask who you should be speaking to for these kinds of purchases.
    Ask if funding exists now to purchase your product or service.
    Ask them how they want you to respond if now is not a good time.
    Ask for an appointment to demonstrate your product.

- Listen to how people approach you over the telephone when they are selling to you. You will find there are a wide range of talents out there.

- Closing the sale

This is an interesting area that you should not be afraid of, but it may require some training for you to perform adequately. There are lots of books and seminars on this subject. A few tips:

Don't try to sell over the phone.

Get yourself into the prospect's office or get him into your office.

Ask the prospect what he or she wants. Listen to the issues raised and respond with answers to their concerns. You may be in the customer's office because of your technology, but you will get the order if the customer believes you will solve the problem.

After you have addressed the issues raised by the customer, ask them to purchase your product. For example, Should we start Monday or do you need us to start sooner.

If possible, have some kind of agreement typed that each of you can sign that indicates an agreement has been reached.

Telephone Survey Date: _____

STATUS:

Immediate Follow Up __ Appt Date: _____ Time:_____
Call Back __ on Date: _____ Time:_____
Not a Lead __

Prospect's Name _____
Phone Number _____

****

Hello. This is _____ of BLES Scientific. We are conducting a survey of manufacturing firms in this area and, if I could, I'd like to ask you a couple of questions. Do you have two minutes to answer these questions?

:if no; When would be a good time to call back?

1. What type of products do you manufacture at your facility?
Answer:_____

2. Are you currently using computers to assist you in your manufacturing efforts?

: if no; Let us send you a brochure that describes the benefits you can gain from our production support software. The information may help you when you configure your new system.

: if yes; What kind of hardware? _____
What kind of software? _____
Is your system meeting your needs? _____
_____

3. Are you thinking of getting/upgrading your software capability in: 0-3 months __
3-6 months __
6-12 months __

4. Thank you very much for your time. Good bye.

****

Immediate Impressions: Hot __
Possible __
Cold __

General Tips

- Set bold goals but derive conservative plans to reach them. This is my resolution to all the words I have heard and schemes I have tried.

Start your company with the least necessary facilities. Necessary is defined as what is the least a customer might expect you to have. There is a minimum level of presentation needed and everything above that is unnecessary. An example, printed stationary is needed before a customer will take you seriously if you approach them through the mail. One color flat printing is acceptable. Four color, raised lettering or 3-D logos are above the minimum and therefore unnecessary. Also, watch the love you may have for technology. Don't buy equipment because it would be nice to have or because it is the state of the art if you can do business without it.

Have plans for expanding your company in terms of office space, employees or inventory but DON'T implement the changes until a contract has been signed and the initiation check clears the bank. Companies sign contracts requiring they have facilities and employees in a town where they have nothing. After they get the contract, they fly out to rent office space and hire local employees.

Raise funds based on projected times to complete development or to reach positive cash flow, but don't spend the funds based on the projections. Once you have the funds, spend them as if they had to last until the end of time.

Understand that the lives of your family and the family of your employees depend on you. Your aggressive leadership and careful steps are for everyone's benefit.

- Remember your dreams belong to you only and may not be shared by your family. They will go along because they love you, not your business. Accept their concerns, worries and discouraging words as part of the price of doing business.

- Expect to be taken to court by someone eventually. Customers, employees, suppliers and the government will appear to want to dampen your spirits. This also part of the price of your choice.

- Business will test your persistence. Be open to reality, but otherwise be stubborn beyond reason. Our friend, H. Ross Perot says "Most people give up just when they're about to achieve success. They quit on the one yard line. They give up at the last minute of the game one foot from a winning touchdown."

Properties of the Solutions to the Time–Independent, Nonlinear Cubic, Schrödinger Equation

Ronald E. Mickens
Clark Atlanta University
Department of Physics
Atlanta, Georgia 30314, USA

Abstract

We study the mathematical properties of the time–independent, nonlinear cubic, Schrödinger equation. This ordinary differential equation has complex–valued solutions and corresponds to two coupled, second–order differential equations. Using a polar coordinate representation, we show that the radial equation reduces to a one–dimensional conservative classical problem for which the potential has all bound states. A knowledge of the radial function then allows the direct calculation of the phase function. Approximations to the solutions are obtained by means of a perturbation procedure.

I. Introduction

The time–dependent, nonlinear cubic Schrödinger equation (TDNSE)

$$\frac{\partial u}{i\partial t} = \frac{\partial^2 u}{\partial x^2} + |u|^2 u, \qquad u = u(x,t), \tag{1}$$

is ubiquitous in the sciences and engineering[1,2,3,4]. In particular, this equation provides a mathematical model for shallow water waves[2], the transport of vibrational energy along α–helix proteins through the formation of solitons[3], and nonlinear wave propagation in optical fibers.[4] Our purpose is to investigate the properties of the solutions to the time–independent, nonlinear cubic, Schrödinger equation

$$\frac{d^2 u}{dx^2} + |u|^2 u = 0, \qquad u = u(x). \tag{2}$$

For future references, Eq. (2) will be denoted as TINSE: the time–independent, nonlinear Schrödinger equation. While a great deal of information exists on the various solutions of Eq. (1), in particular its soliton solutions[1,2], little is known concerning the properties of the solutions to the TINSE.

Certain preliminary results on Eq. (2) have been obtained by D. Lockett and presented in his Master–of–Science thesis.[5] There, he used the method of harmonic balance[6] to calculate an analytic approximation to the general solution of Eq. (2). In this paper, we extend the investigations of Lockett and study the general mathematical properties of $u(x)$.

The next section provides certain background information needed for our analysis. Section III gives the polar representation of the solution and shows how exact first–integrals can be calculated. In Section IV, we give two special exact solutions to the TINSE. They follow from, respectively, requiring the amplitude and phase functions to be constant. Section V is devoted to a detailed study of the mathematical properties of the solutions to Eq. (2). We find that much can be learned about these solutions in spite of the fact that an explicit representation for them does not exist. In Section VI, we show that approximate solutions for the TINSE can be calculated using a perturbation procdure.

II. Preliminaries

Examination of Eq. (2) shows that, in general, $u(x)$ is a complex–valued function of the real variable x. The solutions to Eq. (2) can be written in either the cartesian or polar representations:

$$u(x) = X(x) + iY(x), \tag{3}$$

$$u(x) = R(x)e^{i\theta(x)}, \tag{4}$$

where X, Y, R and θ are real functions of x. Substitution of these results into Eq. (2) and setting the real and imaginary parts equal to zero gives

$$\begin{cases} X'' + (X^2 + Y^2)X = 0, \\ Y'' + (X^2 + Y^2)Y = 0, \end{cases} \tag{5}$$

and

$$\begin{cases} R'' - (\theta')^2 R + R^3) = 0, \\ R\theta'' + 2R'\theta' = 0, \end{cases} \tag{6}$$

where the prime ($'$) denotes taking the derivative with respect to x. These representations indicate that the TINSE is equivalent to two second–order, coupled differential equations. For the remainder of this paper only the polar forms given by Eqs. (4) and (6) will be considered. Also, with no loss of generality, the following initial conditions will be selected.

$$R(0) \neq 0, \qquad R'(0) = 0; \qquad \theta(0) = 0, \qquad \theta'(0) \neq 0. \tag{7}$$

III. Details of the Polar Representation

Equations (6) can be integrated once to obtain first–integrals. First, note that the second of Eqs. (6) can be integrated to give

$$R^2\theta' = A = [R(0)]^2\theta'(0), \tag{8}$$

where the integration constant A is expressible in terms of the initial conditions. Second, solving Eqs. (8) for θ' and substituting it into the first of Eqs. (6) gives

$$R'' - \frac{A^2}{R^3} + R^3 = 0. \tag{9}$$

This equation has the following first–integral

$$\frac{(R')^2}{2} + U(R) = E = \text{ constant } \geq 0, \tag{10}$$

where

$$U(R) \equiv \frac{A^2}{2R^2} + \frac{R^4}{4}. \tag{11}$$

Note that $R(x)$ can be considered to be the dependent variable describing a one–dimensional dynamic system having the convex potential energy function $U(R)$[7,8]; consequently, Eq. (10) is the energy integral. Since both terms on the left–side of Eq. (10) are non–negative, it follows that for $R > 0$, all the integral curves in the phase–plane (R, R') are closed.[7] Hence, $R(x)$ is a periodic function of x.

The following comments are in order at this point: (i) Examination of Eqs. (9), (10) and (11) show that the radial equation is equivalent to a one–dimensional classical

nonlinear oscillator problem. (ii) From the definition of the radial function $R(x)$, it follows that $R(x) > 0$. For the potential function $U(R)$, this condition is seen to hold for any finite energy $E > 0$. (iii) The potential function $U(R)$ has a single minimum located at

$$\bar{R} = |A|^{1/3}, \tag{12}$$

for which it has the value

$$U(\bar{R}) = \left(\frac{3}{4}\right)|A|^{4/3} > 0. \tag{13}$$

The phase function $\theta(x)$ can be determined once $R(x)$ is known. From Eq. (8), we have

$$\theta'(x) = \frac{A}{[R(x)]^2}. \tag{14}$$

The solution of this equation is

$$\theta(x) = A\int_0^x \frac{dt}{[R(t)]^2}. \tag{15}$$

In spite of the fact that $R(x)$ is periodic, i.e., the integral of a periodic function does not, in general, give a periodic function.

IV. Exact Solutions

Equations (6) have two special exact solutions. The first is obtained by requiring

$$R(x) = \text{ constant}. \tag{16}$$

The solution for this case is

$$u(x) = \bar{R}e^{i(\bar{R}x+\theta_0)}, \qquad \bar{R} = |A|^{1/3}, \tag{17}$$

and correspnds to the "motion" of the one–dimensional system being confined to the bottom of the potential well $U(R)$ at $R = \bar{R}$.

The second solution is gotten by requiring

$$\theta(x) = \theta_0 = \text{ constant}. \tag{18}$$

This condition gives

$$u(x) = e^{i\theta_0} R(0) c_n[R(0)x; 1/\sqrt{2}], \tag{19}$$

where $c_n[\cdots]$ is the Jacobi elliptic cosine function[8].

Both of these special solutions are periodic. In each case, the period depends on the initial conditions.[8] It is unlikely that other special exact solutions exist to the TINSE. In any case, the general solution cannot be expressed in terms of a finite combination of the elementary functions. In Section VI, we show how to determine approximations to the exact solutions of the TINSE for "motions" near the bottom of the potential well.

V. Mathematical Properties of $u(x)$

Theorem 1. $R(x) > 0$.

Proof. This follows directly from Eqs. (11) and (13).

Theorem 2. *$R(x)$ is periodic with period $\bar{x}$.*

Proof. See the arguments immediately following Eq. (11). Note that while the value of $\bar{x}$ is not known, we can be sure that it does exist.[7,8] (Section VI will provide a means to calculate its value using a perturbation procedure.)

Theorem 3. *$R(x)$ can be represented as a "cosine" Fourier series. This means that $R(x)$ is an even function, i.e.,*

$$R(-x) = R(x). \tag{20}$$

Proof. This result is a direct consequence of the selection of initial conditions for $R(x)$ as given in Eq. (7).

Theorem 4. *$\theta(x)$ is an odd function, i.e.,*

$$\theta(-x) = -\theta(x). \tag{21}$$

Proof. From Eq. (15), we have that

$$\theta(-x) = A\int_0^{-x} \frac{dt}{[R(t)]^2}. \tag{22}$$

Now let $z = -t$. Therefore,

$$\theta(-x) = A\int_0^{x} \frac{(-dz)}{[R(-z)]^2} = -A\int_0^{x} \frac{dz}{[R(z)]^2} = -\theta(x). \tag{23}$$

Theorem 5. $u(-x) = [u(x)]^*$.

Proof. The $(*)$ denotes complex–conjugation. From Eq. (4), it follows that

$$u(-x) = R(-x)e^{i\theta(-x)}. \tag{24}$$

However, Theorems 3 and 4 state that $R(x)$ is even and $\theta(x)$ is odd. Consequently, using these facts in Eq. (24) gives

$$u(-x) = R(x)e^{-i\theta(x)} = [u(x)]^*. \tag{25}$$

Theorem 6. *There exists a constant c_0 such that*

$$u(x + \bar{x}) = e^{ic_0\bar{x}}u(x). \tag{26}$$

Proof. As previously defined, $\bar{x}$ is the period of the periodic function $R(x)$, i.e., $R(x+\bar{x}) = R(x)$. Let

$$\omega = \frac{2\pi}{\bar{x}}. \tag{27}$$

Then from Theorem 3, it follows that $R(x)$ has the Fourier representation

$$R(x) = \frac{a_0}{2} + \sum_{k=1}^{\infty} a_k \cos(k\omega x). \tag{28}$$

Since $R(x) > 0$ (Theorem 1), there exists coefficients $\{d_k\}$ such that

$$\frac{1}{[R(x)]^2} = \frac{d_0}{2} + \sum_{k=1}^{\infty} d_k \cos(k\omega x). \tag{29}$$

Hence, from Eqs. (15), it follows that

$$\theta(x) = A\left[\frac{d_0 x}{2} + \sum_{i=1}^{\infty}\left(\frac{d_k}{d\omega}\right)\sin(k\omega x)\right] \equiv c_0 x + \theta_1(x), \tag{30}$$

where

$$c_0 = \frac{Ad_0}{2}, \tag{31}$$

$$\theta_1(x) = A\sum_{k=1}^{\infty}\left(\frac{d_k}{k\omega}\right)\sin(k\omega x), \tag{32}$$

and

$$\theta_1(x + \bar{x}) = \theta_1(x). \tag{33}$$

Consequently,

$$u(x) = R(x)e^{i\theta(x)} = R(x)e^{i[c_0 x + \theta_1(x)]}, \tag{34}$$

and

$$u(x + \bar{x}) = R(x + \bar{x})e^{i[c_0(x+\bar{x})+\theta_1(x+\bar{x})]} = R(x)e^{i\theta(x)}e^{ic_0\bar{x}} = e^{ic_0\bar{x}}u(x). \tag{35}$$

Theorem 7. *$u(x)$ has the representation*

$$u(x) = \Phi(x)e^{ic_0 x} \tag{36}$$

where

$$\Phi(x + \bar{x}) = \Phi(x). \tag{37}$$

Proof. This result follows from Theorem 6 where Eqs. (26) is treated as a finite difference equation.[9,10]

VI. An Approximate Solution

While Eq. (9) cannot, in general, be solved exactly, we can calculate good approximate solutions for motions near the bottom of the potential well at $R = \bar{R}$.

Define the parameter a to be

$$a = R(0) - \bar{R}, \qquad \bar{R} = |A|^{1/3}, \tag{38}$$

and the new variable $y(x)$ as

$$y(x) = R(x) - \bar{R}. \tag{39}$$

We assume that

$$|a| \ll \bar{R}. \tag{40}$$

From this it follows also that

$$|y(x)| \ll \bar{R}. \tag{41}$$

Substitution of Eq. (39) into Eq. (9) gives, after a large amount of algebraic manipulation, the result

$$y'' + [6|A|^{2/3}]y - [3|A|^{1/3}]y^2 + 11y^3 = 0, \tag{42}$$

where only terms through order y^3 have been retained. The initial conditions for $y(x)$ are

$$y(0) = a, \qquad y'(0) = 0. \tag{43}$$

Equations (42) and (43) are an example of a mixed-parity perturbation problem[11] and unless one is very careful difficulties can arise in the construction of a uniformly valid solution. In a recent paper, Mickens has shown how to resolve the various issues related to having the perturbation solution satisfy exactly the initial conditions of Eq. (43). Using these results of Mickens[11] the following perturbation solution is obtained for Eqs. (42) and (43):

$$\begin{aligned} R(x) = \bar{R} &+ a\cos(\omega x) \\ &- \left[\frac{a^2}{126\bar{R}}\right][-3 + 2\cos(\omega x) + \cos(3\omega x)] \\ &+ \left[\frac{a^3}{1323(\bar{R})^2}\right]\left[-1 - \left(\frac{43,311}{576}\right)\cos(\omega x) + \left(\frac{1}{3}\right)\cos(2\omega x)\right. \\ &\left. + \left(\frac{26,901}{352}\right)\cos(3\omega x)\right] + O(a^4), \end{aligned} \tag{44}$$

where the parameter a plays the role of the perturbation expansion parameter. The angular frequency is given by the expression

$$\omega = 1 + \left(\frac{14,533}{20,168}\right)\frac{a^2}{(\bar{R})^2} + O(a^4). \tag{45}$$

The phase function $\theta(x)$ can be calculated by direct substitution of Eq. (44) into the right–side of Eq. (15). We do not give this calculation, but, leave it as an exercise in Taylor series expansion and elementary integration for the reader to complete.

VII. Summary

We have shown that many of the important mathematical properties of the TINSE can be determined by use of a polar representation for the solution. The theorems of Section V summarize the results found to date.

Note that $u(x)$, in general, is not periodic. This follows from the relation given by Eqs. (36) and (37). There are two periodic behaviors associated with $u(x)$. The first is related to the fact that the radial function $R(x)$ can be considered as the solution to a one–dimensional classical nonlinear oscillator problem; this period $T_1 = \bar{x}$ and its value depends on the initial conditions. The second period is determined by

$$T_2 = \frac{2\pi}{c_0}. \tag{46}$$

If T_1/T_2 is a rational number, then $u(x)$ is periodic, otherwise, $u(x)$ is quasi–periodic or almost periodic. In general, for arbitrary initial conditions, we expect the latter situation to hold.

It is of interest to see what, if any, relationships exist between the solutions of the TDNSE (1) and the TINSE (2). We are currently investigating this issue.

Acknowledgements

The research reported in this paper has been supported in part by funds provided by ARO–ACEIS, NIH–MBRS and NSF–CTSPS.

References

1. G. L. Lamb, Jr., *Elements of Soliton Theory* (Wiley, New York, 1980).

2. R. K. Dodd et al., *Solitons and Nonlinear Wave Equations* (Academic Press, New York, 1982).

3. A. S. Davydov, *Solitons in Molecular Systems* (D. Reidel, Dordrecht, 1985).

4. M. J. Potasek and M. Tabor, Physics Letters **154A**, 449–452 (1991). "Exact solutions for an extended nonlinear Schrödinger equation."

5. D. Lockett, Master–of–Science Thesis (Clark Atlanta University, May 1992): "Construction of analytic approximations to the solution of the time–independent cubic nonlinear Schrödinger equation."

6. R. E. Mickens, Journal of Sound and Vibration **94**, 456–460 (1984). "Comments on the method of harmonic balance."

7. J. B. Marion, *Classical Dynamics of Particles and Systems* (Academic Press, New York, 2nd edition, 1970).

8. R. E. Mickens, *Nonlinear Oscillations* (Cambridge University Press, New York, 1981).

9. H. Levy and F. Lessman, *Finite Difference Equations* (Macmillan, New York, 1961).

10. R. E. Mickens, *Difference Equations: Theory and Applications* (Van Nostrand Reinhold, New York, 2nd edition, 1990).

11. R. E. Mickens, Journal of Sound and Vibration (1993): "Construction of a perturbation solution to a mixed parity system that satisfies the correct initial conditions." (Accepted for publication).

INTERDIFFUSION IN MULTILAYERED THIN FILM CMOS STRUCTURES

Principles, Effects, and Application

Donald G. Prier, II and B. Rambabu
Department of Physics
Southern University
Baton Rouge, Louisiana 70813

Integration of a large number of components on a single chip requires sophisticated interconnections to minimize signal delays and simultaneously optimize the packing density. Aluminum has been most widely used for contacts and interconnections in both bipolar and MOS integrated technology. Low temperature interdiffusion of aluminum and silicon[1] during contact sintering, passivation, or packaging of the device can result in gain degration and increased junction leakage. The use of Al films containing 1% to 2% Si has been proposed to minimize contact pitting,[2] but precipitation and solid-phase epitaxial growth of Al-doped Si in the contact window during the cooling cycle of a heat treatment[3] increases the contact resistance of small-area contacts drastically. Device reliability can be improved by interposing a barrier layer between the Al and the Si which reduces the mass transport in the contact structure during processing or operation of the device.

With the evolution of VLSI technology into the submicron dimension there is an increase in the proximity of layers of different materials and arguments the role of structural defects inherent in these layers. This increases the possibility of materials reactions in multilayer thin film assemblies. Therefore, a rapidly growing number of studies are devoted to the development of suitable barrier layers to reduce or prevent such materials reactions. In spite of these efforts, rules have not been foundto date which would permit to select a barraier layer material from first principles. However, general trends in the barrier properties of materials used in contact structures to silicon semiconductor devices become apparent. Similar trends can be attributed to materials belonging to the same materials class.[4-7]

REQUIRMENTS FOR BARRIER LAYERS

The general approach to form an electrical contact to a silicon semiconductor device is a multilayer thin film structure. It consists of a combination of different materials which are bound from each other by interfaces. In addition, the individual films contain structural defects, such as grain boundaries and dislocations. Unfortunately, such an assembly is rare in thermodynamic equilibrium. Therefore, atom migration will take place to establish equilibrium by lowering the total free energy of the assembly. The driving force for the atomic motion is the gradient of the chemical potential of the atoms in the assembly.

BARRIER FOR CHEMICAL INTERDIFFUSION

The net flow of atoms is commonly described as diffusion and characterized by a diffusion coefficient D. In a multi-layer thin film system the combined effect of

several diffusing species is expressed by a chemical interdiffusion coefficient

$$D = \sum_i x_i D_i$$

where x_i and D_i are the atomic fraction and diffusitivity, respectively, of the species i. It is D which is determined in an ordinary diffusion experiment. The temperature dependence of D is generally written in the form $D = D_0 \exp(-Ea/kT)$, which is known as the Arrhenius equation. Ea is the experimental activation energy and D_0 is the frequency factor. In the case of self-diffusion and diffusion in dilute substitutional solid solutions a specific meaning in terms of atomic processes can be attributed to the quantities Ea and D_0. However, in the general case of chemical interdiffusion the nature of the activation energy becomes complex.

Structural defects have a profound effect on the diffusion rate of atoms in thin films. From a large number of experimental measurements it is generally concluded that diffusion at free surfaces is the quickest. Diffusion along grain boundaries and dislocations is the intermediate, and diffusion in interior of crystals is the slowest process in thin film diffusion mechanisms. Each of these process have a different activation energy which results in different temperature behavior. In a polycrystalline, thin film lattice diffusion is dominant at high temperatures. The reason is that the total cross-sectional area of the grain boundaries is small compared to that of the grain boundaries, resulting in a small contributions of the grain boundaries to the overall diffusion mechanism. At low temperatures, however, processes of low activation energy become progressively important. Thus, grain boundary diffusion dominates at low temperature. In addition, the smaller the grain size, the greater the importance of boundaries in the diffusion process. The crossover of the dominant mechanism from lattice to grain boundary diffusion in metals occurs at about 1/1 to 3/4 of the melting point temperature.

Naturally, one would prefer a single crystal material as barrier layer against chemical interdiffusion, because lattice diffusion has the lowest diffusivity. But for device processing, single crystal or epitaxial layers are impractical, because they can rarely bef formed in a contact structure. Therefore, the next best choice for a diffusion barrier layer is a large-grained polycrystalline material. In addition, solutes segregated at the grain bondaries may decrease the grain boundary diffusivity. However, this is not a general rule, since it has been observed that the converse can also occur. [8] For this reason, the concept of segregating impurities or second phase particles at the grain boundaries of a polycrystalline barrier matterial, does not necessarily yield an efficient diffusion barrier.

Another class of possible diffusion barrier materials are amorphous thin-films. The diffusivity in these materials is intermediate between lattice and grain boundary diffusion. [9-10] However, due to the very limited data available, the diffusion mechanism in amorphous materials is poorly understood. More studies are needed to evaluate the usefulness of amorphous materials as diffusion barriers. It should be noted that diffusion barriers do not eliminate the driving force for

diffusion, also known as, the concentration gradient. They merely reduce mobility for atomic migration. The efficiency of a diffusion barrier material is thus determined by how well it diminishes mass transport through its diffusion paths present.

BARRIER FOR CHEMICAL INTERACTION

The total free energy barrier of a thin-film assembly can also be lowered by a chemical reaction resulting in the formation of a new phase. The interfacial reaction between two dissimilar materials generally requires mass transport across the intermatter of kinetics. The formation of a new phase is a matter of nucleation and growth. For a new phase to nucleate the free energy of an atom in the new phase must be lower than that in the inital phase.

A multilayer thin-film system is in stable chemical equilibrium as long as any change in temperature, concentration, or pressure does not decrease the total free energy of the system. If the total free energy is reduced, a spontaneous chemical reaction may occur. A thermodynamic criterion for a chemical reaction to take place at a given temperature is a negative Gibbs free energy change for the reaction $G = \Delta H - T\ \Delta S$, where H is the change in enthalpy and S is the change in enthropy. In many cases the contribution form S is small and the reaction is mainly determined by H. Thus, the main driving force for an interfacial reaction is a difference in chemical free energy.

Barrier layers can be used to reduce the total free energy of a thin-film system. Two thin-films A and B in contact with each other have a tendency to react and form a compound AB if the fee energy of the system compared to the A/B configuration. By the addition of the layer C, the system becomes more stable. The layer C has therefore been named reaction barrier.

In general, the barrier layer C does not establish chemical equilibrium in the system A/C/B. An interfacial reaction will therefore still occur, but at a reduced rate. This reaction consumes the layer C prevent reactions between the layers A and B. This situation is illustrated in Figure 2. Contact structure in Figure 2 consists of a silicide layer, a transition metal layer as reaction barrier, and the aluminum overlayer. An increase in temperature during processing or operation of the device will initiate interfacial reactions between the aluminum and the transition metal layer, and the transition metal and silicide layer. The reaction products are an aluminum intermetallic compound and a transition metal silicide. In many cases, the reaction rates can be measured experimentally. Provided that the reaction is laterally uniform, the point in time when they transition metal barrier layer is consumed by the interfacial reaction is then predictable for a given temperature.

Thus, a minimum barrier layer thickness can be found for any given time-temperature cycle. Upon consumption of the barrier layer, rapid interdiffusion generally causes a fast deterioration of the contact structure. This concept of a consumable barrier layer, which has been termed "sacrificial barrier" by Nicolet, [11, 12] can only be applied if atomic diffusion through the barrier layer is negligible.

RESISTIVITY AND ADHESION REQUIREMENTS

Barrier layers have to fulfill two other requirements for device application, namely, low contact resistance and good adhesion. It is clear that the barrier layer should have metallic properties. However, a low resistivity is generally not of primary concern. A typical thickness for barrier layers is 1000A. For a $1\mu\Omega\ cm^2$ contact area, a barrier layer material of $100\mu\Omega\ cm^2$ resistivity would only contribute $0.1\Omega cm^2$ to the total contact resistance. More important is a low contact resistivity when the barrier layer is used as an Ohmic contact to silicon. For shallow junction devices, contact resistivities in the 10^{-8} to low $10^{-7}\Omega cm^2$ range are required.

Barrier layer material should be compatible with device processes, such as patterning, passivation, multilevel metallization, and packaging. Good adhesion to insulators and corrosion resistance in various gas ambients may also be required.

ALUMINIUM-ALLOY METALIZATIONS:

Simple single layer aluminium metallizations are unstable even at moderate temperatures. Grain degradation or Junction shortening is a result of low temperature interdiffusion of Aluminium and Silicon during contact intering, passivation or packaging. The aluminum tends to mound up into hillocks during post disposition anneal cycles degrading the texture and reflectively of the films causing patterning problems. Grain growth at 400 degrees C is a result of the low melting point of aluminum and high solubility of silicon.

Reduction of interdiffusion of in the Contact System can be reduced by interposing a barrier layer in between the aluminum and the silicon.

An example of a "Barrier Metal" is titanium. The structures consisting of aluminum as an interconnect refractory metal, titanium as the diffusion barrier, and Silicon as the main contact material imporves the contact stability but only up to 400°C. At 400°C, aluminum and titanium start to react with each other. They form a new compound TiA13. As the temperature exceeds 400 degrees C, the aluminum will penetrate into the Silicon substrate. The end result of this is a binary and ternary compound. Figure I illustrates the effect of the phase transformations in the vicinity of the contact hole. First, the TiA13. As the temperature exceeds 400 degrees C, the aluminum will penetrate into the Silicon substrate. The end result of this is a binary and ternary compound. Figure I illustrates the effect of the phase transformations in the vicinity of the contact hole. First, the TiA13 formation begins to across the entire Ti layer. When all the Ti is consumed, Si begins to react with the TiA13 layer to produce the ternary phase. Si then migrates from the contact and diffuses into the A1 layer while A1 moves into the area of the removed silicon. The ternary layer then appears to extend beyond the contact window as the Si saturated Al provides Si to convert the Tia13. Titanium is a good diffusion barrier for Silicon as long as the titanium layer in not totally consumed, it is an effective barrier to A1Si interdiffusion. It has been found that stuffing the refractory metal titanium with oxygen or nitrogen is seen to greatly improve the barrier properties. Titanium nitride has been used as a

salicided CMOS technology. The A1 / TiN / TiSi2 / Si and A1 / TiN / Si systems are both stable up to annealing temperatures of 550°C for 30 min anneal. Significant interdiffusion occurs at 600°C. Therefore, interdiffusion of aluminum has become an intrinsic defect with the barrier and contact material in the salicided structures since processing temperatures range from 700° - 900°C.

As the device dimensions are scaled to the submicron regime, the reduction in the dimensions of metallization film, juction depth, and contact size affecting the electro and stress migrations leading junction leakage currents and increased contact resistance. Even at moderate current densities, the bulk self diffusivity of aluminum is sufficient to cause voids and open circuits. In an effort to improve the electro and stress migrations, several metals such as Cu, Si, Ti, Pd, etc have been added as impurites to pure aluminum. Allowing of aluminum decreases the grain boundary self diffusivity. The main conducting layer improves electromigration. Addition of cooper primarily reduces the number of hillocks, improves reflectively, increases hardening etc. It improves electromigration resistance by blocking grain boundary diffusion paths while Si addition eliminates A1 penetration into the Si substrate at the contact areas allowing to decrease contact resistance. At the present time, A1 alloys containing lwt% Si and .1 - .5wt% Cu are widely used in submicron CMOS technologies. The .5wt% of Cu addition improves the uniformity of the grain structure and further increase of Cu impurity content degrades electromigration strength. So it is important to understand the interfacial reactions of these layered structures while studying the effect of implanted aluminum alloy layers with underlying barrier and contact layers. The dopants As, P, or BF_2 distribute themselves in the shallow junctions during rapid thermal processing or rapid thermal nitridation and also believed to be interacting with the new intermetallic phases in the salicided structures effect the sheet resistance, reflectively, and microstructures of the film. So we present our results of our experiments on A1-Si- Cu / TiN / TiSi2 / Si and A1-Cu / Tin / TiSi2 / Si. Unlike the earlier studies, this work aims to understand how multilayered metallizations in salicides behave during heat treatments, and their impact in the submicron technology.

EXPERIMENTAL

Salicide films are formed on Silicon by ion implantation and subsequent annealing. Titanium nitride films were sputter deposited in the TiSi2. The thickness of the TiSi2 and TiN layer were 600°C each. A1-0.5wt%Cu - 1wt%Si film was subsequently sputter deposited on the top of the TiN layer. Since conventional techniques do not satisfy via filling requirements for submicorn devices. MX214IOE bias sputtering metallization techniques are used for filling and planarization of aluminum by taking advantage of low melting point of aluminum high target power, substrate bias and substrate temperature to enhance aluminum mobility, in order to achieve uniform grain size distribution. The samples were subsequently annealed in pure nitrogen for 30 minutes at temperatures of 400° to 550°C. The sheet resistance of the samples were measured with a PROMETRIX four point probe apparatus. SIMS depth profiles were obtained using a camera IMA-35 ion microanalyser. X-ray diffraction data were recorded using a Rigaku glancing angle X-ray diffractometer with a monochromatic Cu radiation. Cross sectional TEM

analysis were done using Phillips 120 keV transmission electromicrograph. Specimens for cross sectional TEM analysis were obtained by means of mechanical polishing and ion milling. The surface orphology was obtained using SEM and hillocks were counted per picture. In order to see the reflectively changes with respect to hillock formation, conventional optical microscopes were used. AES analysis was used to characterize the A1 alloy layer. Most of the experimental data were obtained from AT&T Bell Laboratories , Allentown, PA 18103.

RESULTS

We begin this section with our sheet resistance and reflectively measurements. Figures 2 and 3 show sheet resistance of the n-A1-Ca and n-A1-Si -Cu samples as a function of annealing temperatures. The sheet resistance of the samples annealed below 450°C is about 80% of that A1 deposited sample. The sheet resistance increases in between 400°C - 550°C. The increase of sheet resistance is significant at 525°C. Also, both n-A1-Cu and A1-Si-Cu show more increase in sheet resistance compared to P-A1-Cu and P- A1-Si-Cu. The reflectance is uniform up to 400°C anneal and decreases drastically. Also, the formations of hillocks has increased in temperatures between 400°C - 550°C which in turn affected the reflectance. Figure 3 shows the reflectance versus temperature plot of the samples. As the hillocks increased reflectively decreased in the temperature range of 400° - 550°C. Table 1 shows the number of hillocks formed during different heat treatments for the samples studied. Figure 4 shows the SIMS depth profiles of samples annealed at 400°C - 550°C. SIMS intensity of each element is correlated with the total ion density. At 550°C, the temperature at which the increase in sheet resistance is observed Ti and N move significantly in the A1 layer towards the surface A1 and Si move in the TiN layer. In addition to the TiN thickness, A1 moved in to Si substrate at the temperature 550°C. The TiA13 phase is not identified in the temperature 400°C since copper addition reduced the interdiffusion. However, at the temperature 550°C, weak X-ray Diffraction signal have been identified.

CONCLUSIONS

The interdiffusion of the A1 - .5wt% Cu - 1wt%Si/ TiN / TiSi2 / Si due to the different heat treatments at temperatures 400°C and 550°C in nitrogen was investigated using XRD, SIMS, AES, RBS and TEM. The inter-diffusion resulted in increase of sheet resistance, decrease of reflectively and increase of hillocks. Titanium started to diffuse into the A1 alloy layer at 400°C. However, the Ti reaction product could not be detected by the XRD and TEM at 400°C. Titanium on the otherhand, n diffused and reacted with A1 at 550°C. Copper segregation is more at the film surface or film substrate interface in n type material than the p+ type material. Also the increase of sheet resistance is more in n type samples than the p+ samples.

ACKNOWLEGEMENTS

Bobba Rambabu would like to thank Dr. Diola Bagayoko for his time and objectivity. Bobba Rambabu would also like to thank S. Chittipeddi for his creativity and AT&T Bell Laboratories for their funding.

Donald G. Prier, II would like to thank Bobba Rambabu for his patience and his time to direct and encourage effort toward researching this material.

REFERENCES:

1. S.P. Murarka, D.B. Fraser, A.K. Sinha, and H.J. Levinstein, "Refractory silicides of titanium and tantalum for low resistivity gates and interconnects", IEEE Trans. Electron Devices, vol. Ed-27, pp 1409-1417, Aug. 1980.

2. S.P. Murarka, J. VAC. Sci. Tech., Vol 17, pp 775-780 (1980).

3. K.C. Sarswat, D.L. Brors, J.A. Fair, K.A. Monning and R. Beyers, IEEE Trans. Electron Devices, vol. Ed-30, No 11, pp 1497-1505.

4. C.Y. Ting, F.M. D'Heurle, S.S. Iyer, and P.M. Fryer., J. Electrochem. Soc., vol. 133, No 12 pp 2621-2625, 1986.

5. Bill Cochran, Semiconductor International, pp 146-148 May 1991.

6. M.A. Nicolet, Thin Solid Films 64, 17 (1979).

7. J.K. Howard, J.F. White, and P.S. Ho, J. Applied Phys. 49, 4083 (1978).

8. W.J. Garceau, P.R. Fournier, and G.K. Herb, Thin Solid Films 60 (1979).

9. N. Cheung, H. von Scofeld, and M.A. Nicolet, in Proceeding of the Symopsium on Thin-Films Interfaces and Interactions, Los Angeles, 1979.

10. M. Wittmer, Appl. Phys. Lett 36, 456 (1980).

11. B. Rambabu*, s. Chittipeddi, V.V. Kannan, M.J. Kelly, W.T. Cochran.

12. Technical Memo, Doc. No 52814-911608-01TM, Sept 1991. AT&T Bell Laboratories.

Classical and Quantum Statistical Physics: An Exact Approach

U. F. Edgal and D. L. Huber

Department of Physics

University of Wisconsin-Madison

Madison, Wisconsin 53706

A scheme analogous to that developed for 'efficiently' and 'exactly' determining the free energy of classical fluids with realistic many-body interaction potentials at arbitrary densities and temperatures has been evolved for quantum systems. We present in this paper, a brief outline of the scheme. The case for classical systems which was recently published is readily shown to be a limiting case obtainable from the more general quantum treatment.

I. INTRODUCTION

The free energy of equilibrium systems is said to be characterized by the dimensionless parameter ϵ. By employing an exact integral recursion relation for the partition function, a highly nonlinear 'differential algebraic equation' [1] governing ϵ is formulated. An important parameter governing the nonlinear equation involves the function termed the 'general point process nearest neighbor probability density function'(NNPDF)[2]. NNPDF's are used to replace radial distribution functions (and more generally, n-body correlation functions) for describing the microstructure

of equilibrium systems. They may also be exactly formulated in terms of the ϵ parameter. In quantum systems, the analogue of the NNPDF is the QNNPDF (Q standing for Quantum). ϵ is determined from the governing differential algebraic equation via an iterative scheme. The case for classical systems presented in detail elsewhere[2] is shown to result from the present quantum treatment as a limiting case.

II. SUMMARY OF RESULTS

The summary given in this section is elaborately presented in a paper[3] presently under preparation for submission (for publication). The canonical partition function of a system of N identical classical or quantum (fermi or bose) particles in a volume V may be written without loss of generality as:

$$Z(N,V) = (\epsilon\Omega V)^N/N! \tag{1}$$

where ΩV may be seen as a 'one particle phase space'. Ω is connected with the volume in 'internal coordinate' space of the particles. For particles with no internal structure, $\Omega = \lambda^{-3}$ where λ is the thermal wavelength $(\beta h^2/2\pi m)^{1/2}; \beta = 1/k_B T$, T is temperature, k_B is Boltzmann constant, h is planck's constant and m is mass of a particle. The following relation is found to hold for Z(N,V):

$$Z(N,V) = \int_0^V Z(N-1,V_1) P\Omega dV_1 \tag{2}$$

where for quantum systems:

$$P = \int \cdots \int \frac{W_{n+1}(\vec{X}_1', \vec{X}_1, ..., \vec{X}_n)}{W_n(\vec{X}_1, ..., \vec{X}_n)} g^Q_{1,...,n}(\vec{X}_1, ..., \vec{X}_n) \Pi_{i=1}^n d\vec{X}_i \qquad (n \gtrsim 10) \tag{3}$$

$W_{n+1}(\vec{X}_1', \vec{X}_1, ..., \vec{X}_n)$ is the 'slater sum'[4] for n+1 particles located at $\vec{X}_1', \vec{X}_1, ..., \vec{X}_n$. The coordinate $\vec{X}_1'$ is situated on the boundary of volume V_1 and is taken as the origin (The boundary of volume V_1 may usually be assumed to be locally flat 'almost

always'). $\vec{X}_i$ is the coordinate (relative to the origin) of the i-th nearest neighbor to the origin. $g^Q_{1,...,n}(\vec{X}_1,...,\vec{X}_n)$ is the general point process QNNPDF describing the probability that the first nearest neighbor to the origin is located (relative to the origin) at $\vec{X}_1$, the second nearest neighbor to the origin is located (relative to the origin) at $\vec{X}_2$ etc. The term general point process implying a particle is not necessarily situated at the origin. We may write:

$$g^Q_{1,...,n}(\vec{X}_1,...,\vec{X}_n) = h_n exp(-\frac{2}{3}\pi r_n^3 \beta P') W_n(\vec{X}_1,...,\vec{X}_n) \qquad (n \gtrsim 10) \qquad (4)$$

where r_n is the radial part of $\vec{X}_n$ and P' is the system's pressure. h_n is a normalization constant. Eqns.(1)-(4) are exact relations which have couterparts for classical systems. In the classical limit where the average distance between particles is $\gg \lambda$ (usually applicable under weakly degenerate conditions[4]), $W_n(\vec{X}_1,...,\vec{X}_n) \rightarrow e^{-\beta U_n}$ where U_n is the potential energy of the n particles at $\vec{X}_1,...,\vec{X}_n$. With this, Eqns.(3) and (4) are easily shown to reduce to their classical counterparts[2]. The validity of Eqns.(2) to (4) as 'exact' equations for the 'exact' determination of ϵ is made possible by the fact that the slater sum possesses a 'product property' which is a generalization of that usually stated in the literature[4]; ie: If we may write $W_n = e^{w_n}$, then it is true that:

$W_N = e^{w_{N_1}} e^{w_{N_2}} e^f$

where $\mid w_{N_1} \mid, \mid w_{N_2} \mid \gg \mid f \mid; N_1, N_2 \gg 1$ and $N_1 + N_2 = N$ (It is assumed we have two 'clusters' of N_1, N_2 coordinates). We may employ (1) and (2) (after differentiation) to arrive at the differential algebraic equation (assuming T constant):

$$\epsilon(1 - \frac{\rho}{\epsilon}\frac{\partial \epsilon}{\partial \rho}) = P exp(-\frac{\rho}{\epsilon}\frac{\partial \epsilon}{\partial \rho}) \qquad (5)$$

ρ is the particle number density N/V. The equation of state of the system is easily obtained as:

$$\phi = \rho(1 - \frac{\rho}{\epsilon}\frac{\partial \epsilon}{\partial \rho}) \tag{6}$$

where $\phi = \beta P'$. In the full version of this paper[3], we briefly describe how (5) and (6) may be solved iteratively. The efficiency of computation depends mainly on how accurately the slater sum may be evaluated. The slater sum (the diagonal matrix element of the Boltzmann operator in coordinate representation) may be written (after employing a complete set of states) as:

$$W_n(X) = \sum_m \sum_{m'} < X \mid m >< m' \mid X >< m \mid e^{-\beta \hat{H}_n} \mid m' > \tag{7}$$

X stands for the coordinates $\vec{X}_1, ..., \vec{X}_n$; m and m' stand for occupation numbers of a set of basis states. In second quantized formalism, $\hat{H}_n$ may be written as sums or integrals (with infinite limits) over terms involving creation and annihilation operators. We may readily show that the Boltzmann operator may be accurately written as $\sum_{i=0}^{k}(-\beta \hat{H}_n)^i/i!$ (for arbitrary temperatures), where k is some finite number which may always be chosen large enough. Also, it may be shown[3] that the limits of the sums in (7) (including the limits of the sums or integrals introduced by expressing $\hat{H}_n$ in second quantized formalism) may be chosen to be finite without limiting the accuracy in the evaluation of (7). Hence we may expect that given a sufficiently powerful computing environment, (7) may always be accurately evaluated for a variety of configurations X at reasonable 'computing cost'.

III. REMARKS

We observe that our above scheme first reduces a many problem to a 'few body' problem involving computations with n $\sim$ 10 particles; the method of second quantization (which may be said to be well adapted for accurately handling few body problems) is then employed in the computation of W_n (which provides probably the most computationally intensive aspect of our scheme). In which case, the "power" of

second quantization as a computational tool[4] (book-keeping device) is fully realized when used in conjuction with our scheme. It is interesting to note that NNPDF's and QNNPDF's provide fundamental ways alternative to 'n-body correlation functions' for describing microstructure. Presently the above scheme is being applied to the ideal fermi and bose systems at all densities and temperatures. Also, multicomponent systems are under development and these are found to have the same general mathematical structure as that for single component systems. Additionally, the simulation method required to realize our scheme is under development. We hope by the above that various properties of material systems (including liquid He^4, high T_c superconductors etc.) may be investigated with renewed vigor.

REFERENCES

[1] Zwillinger D., *Handbook Of Differential Equations* (2nd edition) Academic Press: Boston (1992)

[2] Edgal U. F., J. Chem. Phys., 94,8179(1991); ibid, 94, 8191(1991)

[3] Edgal U. F. and Huber D. L., 'Quantum Statistical Physics: An Exact Approach' (1993)–Unpublished

[4] Huang K., *StatisticalMechanics* (2nd edition) John Wiley: New York (1987); Negele J. W. and Orland H., *QuantumManyParticleSystems*, Addison-Wesley: Redwood City, California (1988)

Characterization of short pulse laser-produced plasmas at the Lawrence Livermore National Laboratory Ultra short-Pulse Laser+

Ronnie Shephard, Dwight Price, Bill White, Susana Gordan++, Albert Osterheld, Rosemary Walling, William Goldstein, and Richard Stewart

Lawrence Livermore National Laboratory
P.O. Box 808
Livermore, CA 94550.

Ultra-short pulse (USP) laser-produced plasmas have opened a new, exciting regime in plasma physics [1-3]. The USP experiments at LLNL have focused on the study of high energy-density matter. The K-shell emission from porous aluminum targets is used to infer the density and temperature of plasmas created with 800 nm and 400 nm, 140 fs laser light. The laser beam is focused to a minimum spot size of 5 μm with 800 nm light and 3 μm with 400 nm light, producing a normal incidence peak intensity of $\approx 10^{18}$ Watts/cm^2. A new 800 fs x-ray streak camera is used to study the broadband x-ray emission. The time resolved and time integrated x-ray emission implies substantial differences between the porous target and the flat target temperature.

1. J.A Cobble, et al., Phys. Rev. A. **39**, 454 (1989).
2. M.M. Murname, H. Kapteyn, and R. Falcone, Phys. Rev. Lett. **62**, 155 (1989).
3. H.M. Milchberg, R.R. Freeman, S.C. Davey, and R.M. More, Phys. Rev. Lett. **61**,2364 (1988).

+Lawrence Livermore National Laboratory under contract number W-7405-ENG- 48.
++Physics Department, University of California, Berkeley.

Why the Speed of Light is Reduced In a Linear Dielectric Medium

Mary B. James

Department of Physics
Reed College
Portland, Oregon

Maxwell's electrodynamic theory predicts that the speed of a plane wave in a linear dielectric medium is reduced from its speed in vacuum by a factor of n, the index of refraction of the medium, which is closely related to the material's electric susceptibility. While Maxwell's description of this phenomenon is straightforward, it does little to illuminate the mechanism responsible for the reduced speed of propagation. I describe a mechanistic model in which the main molecular dipoles induced in the material by a plane wave travelling at speed c "conspire" to produce a single plane wave travelling through the medium at the reduced speed, c/n.

Recent Results of Research on 1.3 GHz Annular Electron Beam Powered Multi-Gigawatt Microwave Amplifier

Walter R. Fayne, Kyle J. Hendricks, Michael D. Haworth[+], Robert C. Platt[+], James Wells[+], Thomas A. Sperncer, Lester A. Bowers, Moe J. Arman[X], Raymond W. Lemke[*], Michael Mazarakis[*], M. Collins Clark[*]

Electromagnetic Sources Division (PL/WSR)
Phillips Laboratory
Kirkland AFB, NM 87117-6008

Recent experimental and computer simulation results of our annular electron beam amplifier will be presented. Our research includes the generation of a annular electron beam using the IMP pulser (500 KV, 5 Ω, 300 ns), the modulation of this beam by a two cavity relativistic Klystron amplifier, and the radiation of the microwave power. Our work also includes the measurements of power used to modulate the electron beam, the resulting modulating voltage, the resulting electron beam modulation, and the excitation of the idler (second) cavity. Included in our work is the design and construction of a 1.5 Tesla pulsed magnet to constrict the beam, and the recently revised design of a more efficient cathode. We will also present comparisons of our experimental results with the computer simulated results from the 2 1/2-D code **MAGIC** and the 1-D code **RKA.**

[+]SAIC, Albuquerque, New Mexico
[X]National Research Council Senior Fellow
[*]Sandia National Laboratory, Albuquerque, New Mexico

Soft X-Ray Lithography and Nanostructures Program

Keith H. Jackson

Center for X-ray Optics
Lawrence Berkeley Laboratory
Berkeley, CA

As the semiconductor industry begins to consider the challenge of lithography and pattern transfer at critical dimensions below 0.25 μm, it is becoming increasingly clear that the development of ultra high precision x-ray optical elements will be essential. The fabrication issue for diffraction limited imaging optics at a wavelength of 130 Å can be generalized with the following statement, "If the optical figure can be measured the optic can be fabricated." This requires a technique that can measure the surface figure of complex aspheric optics with a precision better than a tenth of a wavelength, i.e., less than one nanometer (10 Å). The most powerful optical testing tool of surface figure is interferometry. The scale of precision in interferometry is determined by the wavelength of the source. The need to perform these measurements at soft x-ray wavelengths is clear. The Advanced Light Source (ALS) finishing completion at LBL is the ideal source for interferometric measurements. The low emittance, relativistic electron beam in the ALS storage ring will provide partially coherent radiation at soft x-ray wavelengths. Undulators, periodic magnetic structures, will increase the intensity of the radiation and narrow the bandwidth, providing soft x-ray source of extraordinary brilliance.

The Center for X-ray Optics at the Lawrence Berkeley Laboratory is currently constructing two x-ray beamlines at the ALS that are dedicated to optical metrology, and a Nanostructures fabrication laboratory. The processing lab will include a direct write e-beam lithography system, a Nanowriter, that will allow the fabrication of reflective masks, zone plates, and device structures with feature sizes as small as 0.05 μm over an 8" wafer. This development of soft x-ray optical metrology, advanced e-beam writing, and processing technology will allow soft x-ray projection lithography, for pattern transfer in the 0.1 μm range and beyond.

Semianalytic Methods for Slater-Type Orbitals

Andrew Jackson, Jay Jackson, Babak Etemadi and Herbert Jones

Department of Physics
Florida A&M University
Tallahassee, FL 32307

It would be desirable to use Slater-type orbitals (STOs), characterized by $\exp(-x)$, rather than Gaussian-type orbitals (GTOs), characterized by $\exp(-x^2)$, as basis sets in all calculations involving molecules and their interactions. This is because STOs represent electron clouds surrounding nuclei with greater fidelity.

The difficulty with STOs are computational: when molecular integrals are derived as formulas, they are subject to enormous cancellation errors; when they are set up with Fourier transforms for numerical integration, pathologies and singularities often appear.

Our approach uses computer algebra to generate a C matrix for use in the Lowdin alpha-function method, and then performs a Gauss-Legendre numerical quadrature. This semi-analytic method is being initiated by finding overlap integrals over s orbitals with an application to the hydrogen molecular ion, H_2^+

Diamond/Diamond-Like Thin Film Growth and the Alkanes: Methane, Ethane, and Butane

Elvira Williams, Johnnie Richardson Jr., Donald Anderson, and Kristen M. Starkey

Department of Physics
North Carolina Agricultural and Technical State University
Greensboro, North Carolina 27411

Abstract

Determination of synthesis conditions for diamond (and diamond-like) thin films from various hydrocarbon plasmas is an important aspect of Plasma Enhanced Chemical Vapor Deposition (PECVD) research. In the current work, PECVD synthesis of diamond was investigated in radio frequency (Rf) generated plasmas of alkane and atomic hydrogen mixtures. The alkanes, methane (CH_4), ethane (C_2H_6) and butane (C_4H_{10}) were used.

Some experimental results related to the study of diamond/diamond-like thin films on unheated, unetched p-type silicon (100) substrates produced in different alkane plasmas are reported. The relationships between film index of refraction, Rf power, density, molecular mass, hydrocarbon structure, hydrocarbon flow rate and hydrogen flow rate were determined. Index of refraction, measured with an ellipsometer was used to characterize the films

Diamond Thin Films Synthesis in a Non-Hydrogenated Methane Plasma on Unheated, Unetched Si(100) N-type Substrates

Elvira Williams, Johnnie Richardson Jr., Donald Anderson and Bryan Brown

Department of Physics
North Carolina Agricultural and Technical State University
Greensboro, North Carolina 27411

Abstract

The growth of diamond thin films on various substrates by a variety of methods is an important part of diamond thin film research. Both scientific and practical application are almost limitless.

Successful diamond growth experiments typically employ a hydrogen-hydrocarbon gas mixture.It is widely accepted by researchers in the diamond thin film field that such films can be grown in hydrogenated methane plasmas. The objective of this work, however, is to explore the possibility of growing diamond films using the hydrocarbon, methane, in the absence of atomic hydrogen.

Diamond thin films were synthesized in a non-hydrogenated methane plasma using the technique of Plasma Enhanced Chemical Vapor Deposition (PECVD). A series of experiments were performed to characterize the film. Measurements of index of refraction, composition, thickness and mass were made for these films.

A Study of Butane-Hydrogen Plasma Enhanced Chemical Vapor Deposition of DiamonThinFilms on Unheated, Unetched Silicon Substrates

Elvira Williams, Johnnie S. Richardson, Jr., Donald Anderson, Vernon Simmons

Department of Physics
North Carolina Agricultural and Technical State University
Greensboro, North Carolina 27411

ABSTRACT

Plasma Enhanced Chemical Vapor Deposition (PECVD) diamond-growing techniques have been used to grow very thin diamond films on materials since the early 1950's. However, the matter gained little attention for the next thirty years. The primary reason was that it was thought to have little commercial potential due to the extremely slow growth rate. In the past few years, increasing attentionn has been drawn to the special form of carbon. In 1990, diamond was named "Molecule of the Year" by Science magazine. The thin films have been named i-carbon, diamond-like, hard carbon or a-C. Some of the methods used to produce the film are evaporation, sputtering, ion beam and plasma deposition. Ion beams and plasma deposition produce films whose properties resemble those of diamond. If made under apprpriate deposition conditions, the films are extremely hard and electrically insulating.

Very important aspects of diamond deposition research involves investigating diamond films characterization and deposition on various substrates. The tremendous excitement of growing diamond is largely generated by the wide variety of applications. A thin coating could be placed on a materials which would enhance their longevity; anything from tools and lenses to turbine blades could be coated. In these experiments, the Si (100) substrate was unheated and unetched.

Not heating the substrate allows the coating of all materials which remain stable at room temperature. The growth process is more convenient when the surface of the substrate is unetched. Experiments under these conditions were used to investigate the growth of diamond in a very low frequency using butane (C_4H_{10}) as the reactant gas in the presence of hydrogen.

A series of experiments were performed in which film index of refraction, film thickness, and mass were measured as functions of radio frequency (Rf) power and butane flow rate. The hydrogen flow rate remained constant throughout the series of experiments. Index of refraction, measured with an ellipsometer, was used to characterize the films.

A Study of Plasma Enhanced Chemical Vapor Deposition of Diamond Thin Films on Unetched, Unheated Aluminum Substrates

Elvira Williams, Johnnie S. Richardson, Jr., Donald Anderson, John M. Brown, Jr.

Department of Physics
North Carolina Agricultural and Technical State University
Greensboro, North Carolina 27411

ABSTRACT

Diamond thin films offer a wide variety of unique thermal, chemical, electrical, and optical properties. These diamond thin films have properties similar to bulk diamond: high thermal conductivity, high electrical resistivity, extreme hardness, radiation resistance, large index of refraction, and ultraviolet to infrared transparency. In the past few years, interest in diamond research has gained much momentum due to the potential applications of diamond films.

There are many methods and techniques to produce diamond thin films. Some of the methods are evaporation, sputtering, ion beams, and plasma deposition. Of these, the plasma and ion beam methods produce diamond thin films with properties most resembling those of bulk diamond.

The primary objective of the current investigation is to deposit from a hydrogen-methane plasma, uniform layers of diamond on unetched, unheated aluminum (metal) substrates using PECVD techniques.

A series of experiments were conducted in which the film thickness, film mass, and film index of refraction were measured as a function of the Rf power. The methane and hydrogen flow rates, substrate chamber position, and the deposition times were kept constant throughout this series of experiments. Index of refraction was used to characterize the films.

The Effects of Variation in Methane Flow Rates on the Index Of Refraction of Diamond Thin Films on Unetched and Unheated Silicon Substrates

Dr. Elvira Williams
Dr. Johnnie S. Richardson Jr.
Donald Anderson
Stacey Barrett
L'Tonya Jefferson

Department of Physics
North Carolina Agricultural and Technical State University
Greensboro, NC

ABSTRACT

Diamond and diamond-like films were produced from methane and hydrogen mixture by a capacitively coupled radio frequency (R.f.) reactive plasma deposition process under particular deposition conditions. The index of refraction, mass, and thickness were determined. Variations in the index of refraction could be correlated with the methane flow rate. Characterization of the diamond films were done by the technique of ellipsometry. The deposition of diamond and diamond-like thin films on variety of substrates can be studied by varying the processing parameters and using different reaction gases. Thin films with material properties similar to diamond or graphite can be deposited using the technique of Plasma Enhanced Chemical Vapor Deposition (PECVD). Diamond is most noted for it's extreme hardness and high thermal conductivity. In addition, diamond has excellent electrical properties such as it's large dielectric constant and its high resistivity which are important in some of today's emerging technologies. The unique structure of diamond has the potential of providing improved arc resistance and dielctric breakdown strength, which are critical properties. Furthermore, chemical vapor deposition techniques offer the possibility of developing conductive n and p-type diamond films which would be enabling materials for these new technologies. The chemical vapor deposition technique uses hydrocarbon gases as the carbon source. The general reaction is that these hydrocarbon gases react via the supplied Rf energy to produce solid reactants products and gaseous by-products. Methane and hydrogen were heated with Rf energy to produce diamond and some gaseous by-product. Rf plasma deposition is a technique for the controlled hetergeneous polymerization of thin films from active species produced in an Rf generated glow discharge. The index of refraction and the amount of deposited mass decreased rapidly while the film thickness increased, rapidly as the flow rate of methane gas was increased from 22.1 to 22.9 SCCM.

Deposition of Diamond/Diamond-Like Carbon Films on Unetched, Unheated Silicon (100) Substrates produced in an Ethane Plasma

Dr. Elvira Williams
Dr. Johnnie S. Richardson Jr.
Donald Anderson
Katina Wilson

Department of Physics
North Carolina Agricultural and Technical State University
Greensboro, NC

ABSTRACT

Diamond and diamond-like films were produced from ethane and hydrogen mixture by a capacitively coupled radio frequency (R.f.) reactive plasma deposition process. The films were deposited at room temperature on unetched p-type silicon (1OO) substrates. The films were characterized by ellipsometer measurements of index of refraction. The Department of Physics at North Carolina Agricultural and Technical (A&T) State University is currently engaged in research to study the deposition of diamond and diamond-like thin films on variety of substrates. By varying the processing parameters, thin films with material properties similar to diamond or graphite can be deposited using Plasma Enhanced Chemical Vapor Deposition (PECVD). Diamond is most noted for it's extreme hardness and high thermal conductivity. In addition, diamond has excellent electrical properties such as it's large dielectric constant and its high resistivity which are important in some of today's emerging technologies. The unique structure of diamond has the potential of providing improved arc resistance and dielctric breakdown strength, which are critical properties. Furthermore, chemical vapor deposition techniques offer the possibility of developing conductive n and p-type diamond films which would be enabling materials for these new technologies. The chemical vapor deposition technique uses hydrocarbon gases as the carbon source. The general reaction is that these hydrocarbon gases react via the supplied Rf energy to produce solid reactants products and gaseous by-products. Specifically in this experiment, ethane and hydrogen are heated with Rf energy to produce diamond and some gaseous by-product. Rf plasma deposition is a technique for the controlled hetergeneous polymerization of thin films from active species produced in an Rf generated glow discharge. The index of refraction decreased, the film thickness increased, and the amount of deposited mass increased as the flow rate of ethane gas was increased from 19 to 23 SCCM.

PROGRAM

of the

16th Annual Meeting

of

The National Society of Black Physicists

and

The XX Day of Scientific Lectures

Tallahassee, Florida

Wednesday, April 21, 1993

5-8 pm — Registration at Radisson Tallahassee Hotel

7-8 pm — Reception at Radisson

(Hospitality room provided at hotel.)

Thursday, April 22, 1993

Scientific Sessions I and II will be held at Florida A. & M. University (FAMU).

7:00-8:30 am — *Breakfast at Radisson\hotel*

8:40 am — Buses leave Radisson Hotel going to FAMU

9:00-9:30 am — *Welcome*

Dr. Charles A. Weatherford
Chairman, Department of Physics
Florida A. & M. University

Greetings

Dr. Richard A. Hogg
Provost
Florida A. & M. University

Dr. Aubrey M. Perry
Dean, College of Arts and Sciences
Florida A. & M. University

Session I — Moderator: Dr. Mogus Mochena
Santa Monica College / University of California, Riverside

9:30-10:00 am **"Characterization of short pulsed laser-produced plasmas at the LLNLUltra short-pulse Laser"**

Dr. Ronnie Shepard
Lawrence Livermore National Laboratory
Livermore, California

10:00-10:30 am **"Why the speed of light is reduced in a transparent Medium"**

Dr. Mary B. James
Department of Physics
Reed College
Portland, Oregon

10:30-11:00 am *Coffee Break*

11:00-11:30 am **"Recent Results of Research on a 1.3 GHz Annular Electron Beam Powered Multi-Gigawat Microwave Amplifier"**

Mr. Walter Fayne
Phillips Laboratory
Albuquerque, New Mexico

11:30-12:00 pm **"Oscillations of the volcano function: new max-min quantization procedure"**

Dr. Carlos Handy
Department of Physics
Clark Atlanta University
Atlanta, Georgia

12:00-1:30 pm *Lunch at FAMU*

Session II — Moderator: Dr. Kennedy Reed
Lawrence Livermore National Laboratory

1:30-2:00 pm **"Turbulent Behavior of the Second Viscosity"**

Mr. Jean Orou Chabi
Institut de Mathematique et de Sciences Physiques
Universite' Nationale du Benin
Cotonou, Benin

2:00-2:30 pm **"Addition Theorem for Coulomb Sturmians in Coordinate and Momentum Space"**

Dr. Charles Weatherford
Department of Physics
Florida A. & M. University
Tallahassee, Florida

2:30-3:00 pm **"A Calculation of the Magnetic Moment of the D^{++}"**

Dr. Milton Slaughter
Department of Physics
University of New Orleans
New Orleans, Louisiana

3:00-3:30 pm *Coffee Break*

3:30-4:00 pm **"Spectra of He-like Krypton from TFTR Plasmas A potential Ti diagnostic for ITER"**

Dr. Augustine Smith
Department of Physics
Lock Haven University
Lock Haven, Pennsylvania

4:00-4:30 pm **"Progress in Multicenter Molecular Intergrals Over Slater-Type Orbitals"**

Dr. Herbert Jones
Department of Physics
Florida A&M University
Tallahassee, FL

5:00 pm Buses leave FAMU going to Radisson Hotel

7:00-9:00PM Poster Session at Radisson Hotel

(Hospitality room provided at hotel.)

Friday, April 23, 1993

Scientific Sessions III and IV will be held at the Radisson Tallahassee Hotel.

7:30-9:00 pm *Breakfast at Radisson Hotel*

Session III Moderator: Dr. Mary B. James
Reed College

9:00-9:30 am **"Search for the Top Quark"**

Dr. Larry Gladney
Department of Physics
Univ. of Pennsylvania
Philadelphia, Pennsylvania

9:30-10:00 am **"Deep Space Optical Communications Research at JPL: Results of the GOPEX uplink to Galileo"**

Dr. Keith Wilson
Jet Propulsion Laboratory
Pasadena, California

10:00-10:30 am **"International Physics Olympiad"**

Mr. Carwil James
Department of Physics
Northwestern University
Evanston, Illinois

10:30-11:00 am *Coffee Break*

11:00AM-12:30 pm **Theme Panel:**
Physics, Techonology and Business

"Minority owed high technology busineses - techniques for growing a successful one"

Featuring: Dr. Donald Butler
BLES Scientific, Inc.
Thousand Oaks, California

12:30-2:00 pm *Lunch at Radisson*

Speaker: Dr. Sekazi Mtingwa
Department of Physics
North Carolina A& T State University
Greensboro, NC

Session IV Moderator: Dr. Ronnie Shepard, LLNL
Lawrence Livermore National Laboratory

2:00-2:30 pm **"Properties of the Solutions to the Time-Independent, Nonlinear Cubic, Schroedinger Equation"**

Dr. Ron Mickens
Department of Physics
Clark Atlanta University
Atlanta, Georgia

2:30-3:00 pm **"Soft-X-ray Lithography and Nanostructures Program"**

Dr. Keith Jackson
Center for X-Ray Optics
Lawrence Berkeley Laboratory
Berkeley, California

3:00-3:30 pm *Coffee Break*

3:00-5:00 pm *Business Meeting*

6:15 pm *No Host Beverages at Radisson Hotel Lounge*

6:40 pm Board Buses at Radisson Hotel going to Governors Club

7:00-9:00 pm ***Banquet at Governors Club***

Keynote Speaker:

Professor James H. Stith
Department of Physics
United States Military Academy
West Point, New York

9:00 pm Board Buses at Governors Club going to Radisson Hotel

(Hospitality room provided at hotel.)

Saturday, April 24, 1993

Scientific Session V will be held at the Radisson Tallahassee Hotel

8:30-9:30 am *Continental Breakfast at Radisson Hotel*

Session V Moderator: Mr. Aric Gardner, FAMU
Florida A. & M. University

9:30-10:20 am **Student Seminars**

10:20-10:40 am *Coffee Break*

10:40-11:40 am **Student Seminars**

11:40 am Adjourn

11:20-11:40AM Student Speaker

12:15PM Board buses for tours of attractions in the Tallahassee Area
(Please preregister for tours at the conference registration desk before Saturday.)

(Hospitality room provided at hotel.)

Conference Participants

Sulaimon Adeogun
Louis Adolph
Hilary C. Akpati
Edsel A. Ammons
David Beam
Quincy Bell
Roderick Bethly
Patricia Brow
Willie D. Brown
Bryan W. Brown
John Brown
Donald Butler
Jean Chabi
Benny Cox II
Tyrone Clinton
Corey Echols
Uduzei F. Edgal
Mario Encinosa
Walter Fayne
Kristen M. Flackey
Anita Foster
Dionne M. Franklin
Kaiana Franklin
Alexander B. Gardner
Aric Gardner
S. James Gates, Jr.
Larry Gladney
Ali P. Gordon
Juliette D. Griggs
Carlos Handy
Terry Harrington
Nancy Hayes
Irvin Heard Jr.
Michael B. Hedge
Maleika Holder
Keith Jackson
Monica Jackson
Carwil James
Mary B. James
L'Tonya Jefferson
Thulani Jili
Al C. Johnson
Joseph Johnson
Lynette Johnson
Herbert W. Jones
George King III
Elaine Lalanne
Lonzy J. Lewis
Alan Mackellar
Latikka S. Magee
Talib-vd-Din Mahmoud
Charles H. McGruder
Cynthia McIntyre
Ron Mickens
Mogus Mochena
Carlyle E. Moore
Daryl L. Moore
Dwight Mosby
Sekazi Mtingwa
Fuad Muhammad
Romain Murenzi
Kale Oyedeji
Edward Patterson II
Alfred Phillips, Jr.
Antwan Pinckney
Donald Prier II
Stephen Pullen
Aki Radhuthi
Kennedy Reed
Aaron Richard
Monica D. Roberson
Tommy Rockward
Ronnie Shepherd
Wilson J. Sheppard
Vernon Simmons
Milton D. Slaughter

Augustine Smith
Victor L. Smith
Kwame A. Smith
Kristen M. Starkey
Dawn Stephens
James H. Stith
Tamra Thomas
Christopher A. Trammell
William P. Tucker
Neil D. Tyson
Demetrius D. Venable
Watasha Wade
Marlon L. Walker
Valencia L.Walker
Charles Weatherford
Michael D. Williams
Elvira Williams
Kema Williams
Ronald Williams
Roselyn Williams
Katina M. Wilson
Larice L. Wilson
Keith Wilson
Tessema G. X.
Ben Zeidman

OFFICE OF THE UNDER SECRETARY OF DEFENSE (ACQUISITION)
DEFENSE TECHNICAL INFORMATION CENTER
CAMERON STATION
ALEXANDRIA, VIRGINIA 22304-6145

IN REPLY REFER TO DTIC-OCC

SUBJECT: Distribution Statements on Technical Documents

TO: ONR/CODE 22
~~ATTN: AL DUMAS~~
ARLINGTON, VA 22217-5000

1995 1031 043

1. Reference: DoD Directive 5230.24, Distribution Statements on Technical Documents, 18 Mar 87.

2. The Defense Technical Information Center received the enclosed report (referenced below) which is not marked in accordance with the above reference.

"PROCEEDINGS OF THE 16th ANNUAL MEETING AND THE 20th DAY OF SCIENTIFIC LECTURES OF THE NATIONAL SOCIETY OF BLACK PHYSICISTS"

N00014-94-I-0309

3. We request the appropriate distribution statement be assigned and the report returned to DTIC within 5 working days.

4. Approved distribution statements are listed on the reverse of this letter. If you have any questions regarding these statements, call DTIC's Cataloging Branch, (703) 274-6837.

FOR THE ADMINISTRATOR:

1 Encl

for Norman Dalton
GOPALAKRISHNAN NAIR
Chief, Cataloging Branch

FL-171
Jul 93

DISTRIBUTION STATEMENT A:

APPROVED FOR PUBLIC RELEASE: DISTRIBUTION IS UNLIMITED

DISTRIBUTION STATEMENT B:

DISTRIBUTION AUTHORIZED TO U.S. GOVERNMENT AGENCIES ONLY; (Indicate Reason and Date Below). OTHER REQUESTS FOR THIS DOCUMENT SHALL BE REFERRED TO (Indicate Controlling DoD Office Below).

DISTRIBUTION STATEMENT C:

DISTRIBUTION AUTHORIZED TO U.S. GOVERNMENT AGENCIES AND THEIR CONTRACTORS; (Indicate Reason and Date Below). OTHER REQUESTS FOR THIS DOCUMENT SHALL BE REFERRED TO (Indicate Controlling DoD Office Below).

DISTRIBUTION STATEMENT D:

DISTRIBUTION AUTHORIZED TO DOD AND U.S. DOD CONTRACTORS ONLY; (Indicate Reason and Date Below). OTHER REQUESTS SHALL BE REFERRED TO (Indicate Controlling DoD Office Below).

DISTRIBUTION STATEMENT E:

DISTRIBUTION AUTHORIZED TO DOD COMPONENTS ONLY; (Indicate Reason and Date Below). OTHER REQUESTS SHALL BE REFERRED TO (Indicate Controlling DoD Office Below).

DISTRIBUTION STATEMENT F:

FURTHER DISSEMINATION ONLY AS DIRECTED BY (Indicate Controlling DoD Office and Date Below) or HIGHER DOD AUTHORITY.

DISTRIBUTION STATEMENT X:

DISTRIBUTION AUTHORIZED TO U.S. GOVERNMENT AGENCIES AND PRIVATE INDIVIDUALS OR ENTERPRISES ELIGIBLE TO OBTAIN EXPORT-CONTROLLED TECHNICAL DATA IN ACCORDANCE WITH DOD DIRECTIVE 5230.25, WITHHOLDING OF UNCLASSIFIED TECHNICAL DATA FROM PUBLIC DISCLOSURE, 6 Nov 1984 (Indicate date of determination). CONTROLLING DOD OFFICE IS (Indicate Controlling DoD Office).

The cited documents has been reviewed by competent authority and the following distribution statement is hereby authorized.

A

(Statement)

OFFICE OF NAVAL RESEARCH
CORPORATE PROGRAMS DIVISION
ONR 353
800 NORTH QUINCY STREET
ARLINGTON, VA 22217-5660

(Controlling DoD Office Name)

(Reason)

(Controlling DoD Office Address, City, State, Zip)

DEBRA T. HUGHES
DEPUTY DIRECTOR
CORPORATE PROGRAMS OFFICE

(Signature & Typed Name)

(Assigning Office)

25 SEP 1995

(Date Statement Assigned)